Regulation of Deoxy-Sphingolipids and Their Role in Disease

Dissertation

zur

Erlangung der naturwissenschaftlichen Doktorwürde

(Dr. sc. nat.)

vorgelegt der

Mathematisch-naturwissenschaftlichen Fakultät

der

Universität Zürich

von

Daniela Ernst

aus

Deutschland

Promotionskomitee

Prof. Dr. Arnold von Eckardstein (Vorsitz, Leitung der Dissertation)

PD Dr. Thorsten Hornemann

Prof. Dr. Howard Riezman

Prof. Dr. Thierry Hennet

Dr. Sabrina Sonda

Zürich, 2013

Table of contents

Abstract

1-Deoxy-sphingolipds (dSL) are atypical and neurotoxic sphingolipids which are formed by the enzyme serine palmitoyltransferase (SPT) due to a promiscuous use of L-alanine over its canonical substrate L-serine. Pathologically elevated dSL levels are a hallmark for the rare hereditary sensory neuropathy type I (HSAN I) - which is caused by several missense mutations in SPT. Significantly elevated dSL levels were also found in patients with Metabolic Syndrome (MetS) or diabetes type 2 (T2DM) as demonstrated in various clinical studies. The mechanisms which underlie this increased dSL formation in metabolic disorders is not understood.

Here, we report two novel HSAN I causing mutations in the SPTLC2 subunit of SPT. The A182P variant was found in two members of a single family and the S384F variant in members of two unrelated families. We showed detailed clinical and neurological assessments, confirming the association of these mutations with HSAN I. All affected patients had elevated plasma dSL levels that were comparable to patients with other previously described HSAN I mutations, further supporting the concept that elevated plasma dSLs are a hallmark for HSAN I. The ectopic expression of the A182P and S384F mutants in HEK293 cells increased dSL formation.

Interestingly, the S384F mutation resides at a putative phosphorylation site of SPTLC2. Therefore we investigated the influence of this site on SPT activity and substrate specificity by creating a set of constitutively phosphorylated and non-phosphorylated SPTLC2 mutants. We demonstrated that the phosphorylation mimicking mutant S384D leads to increased dSL generation in isolated proteins and in intact cells. This was not observed for the S384A mutant where the phospho-site was knocked-out. Increasing L-alanine concentrations in the culture media elevated dSL generation in cells expressing the SPTLC2 S384D mutant but not in cells expressing wt SPTLC2. We therefore suggest that phosphorylation of S384 can act as a molecular switch to shift between the two amino acid substrates. A molecular mechanism to regulate the dSL formation also argues for a physiological function of these lipids.

Comparing several cell lines, we found high endogenous dSL levels in RAW macrophages but not in monocyte cell lines like THP or HL60. We showed that THP1 monocytes generate dSLs during their PMA induced differentiation into macrophages

and confirmed this effect in primary human monocytes. The dSL formation correlated with changes of intracellular L-alanine levels. Whether dSL formation has a physiological relevance during macrophage maturation is not clear yet.

In conclusion we propose that dSL generation in the SPT wt enzyme is partly depending on intracellular alanine levels but needs additional factors to switch between the use of L-serine and L-alanine as substrates. This substrate shift might be regulated by a phosphorylation of SPTLC2 at position S384.

Zusammenfassung

Deoxy-Sphingolipide (DSL) sind untypische neurotoxische Sphingolipide, die von dem Enzym Serine Palmitoyltransferase (SPT) aufgrund einer Substratverschiebung von L-Serin zu L-Alanin gebildet werden. Pathologisch erhöhte Deoxy-sphingolipid-Blutwerte sind ein Kennzeichen der seltenen vererbbaren peripheren Neuropathie HSAN I, die durch unterschiedliche Mutationen in den beiden Untereinheiten der SPT verursacht wird. Wie in vielen klinischen Studien gezeigt wurde, sind DSL-Blutwerte ebenfalls signifikant erhöht in Patienten, die an dem metabolischen Syndrom oder Diabetes Typ 2 leiden. Es ist nicht bekannt welche Mechanismen zu den erhöhten DSL Werten in diesen metabolischen Stoffwechselstörungen beitragen. Hier berichten wir von zwei neuen Mutationen in der SPTLC2 Untereinheit, welche HSAN I verursachen. Die A182P Mutation wurde in zwei Mitgliedern einer Familie und die S384F Variante in Mitgliedern von zwei unterschiedlichen Familien gefunden. Durch klinische und neurologische Untersuchungen konnten wir einen Zusammenhang zwischen HSAN I und den, in den Patienten gefunden Mutationen bestätigen. Alle betroffenen Patienten zeigten erhöhte DSL-Blutwerte, die vergleichbar sind mit DSL Blutwerten bei bereits charakterisierten HSAN I Mutationen. Dies unterstreicht weiterhin den Zusammenhang von erhöhten DSL-Blutwerten mit dem HSAN I Phenotyp. Die vermehrte Bildung von DSL konnte auch in HEK293 Zellen gezeigt werden, welche die Mutationen im *SPTLC2* Gen trugen.

Beim Versuch, unbekannte Phosphorylierungsstellen im Hela Proteom zu identifizieren, wurden zwei potentielle Phosphorylierungssstellen in der SPTLC2 Unterheit identifiziert. Diese gaben jedoch keinen direkten Hinweis auf eine abgeänderte Funktion der SPTLC2 Untereinheit. Eine der beiden potentiellen Phosphorylierungsstellen befindet sich an der gleichen Stelle wie die hier charakterisierte neu entdeckte HSAN I-S384F Mutation.

Wir untersuchten daraufhin den Einfluss dieser Phosphorylierungsstelle auf die Aktivität und Substratspezifität der SPT indem wir eine permanente Phosphorylierung (S384D) sowie De-Phosphorylierung (S384A) and dieser Stelle simulierten.

Untersuchung der SPT Aktivität in isolierten Proteinen und in intakten Zellen ergab, dass eine simulierte Phosphorylierung (S384D) zu einer erhöhten DSL Bildung führt. Die Mutante mit permanent de-phosphorylierter SPT (S384A) zeigte keine erhöhte DSL Synthese. Ansteigende L-Alanin Konzentrationen, die dem Kulturmedium

zugegeben wurden, führten zu einer erhöhten DSL Bildung in HEK Zellen mit simulierter Phosphorylierung (S384D), allerdings nicht in HEK Wildtyp Zellen. Basierend auf diesen Ergebnissen, schlagen wir ein Model vor, in dem die Phosphorylierung an der Stelle S384 in der SPTLC2 Untereinheit, die Funktion eines molekularen Schalters besitzt, der es erlaubt, zwischen den beiden Substraten L-Alanin und L-Serin zu wechseln. Das Vorhandensein eines solchen molekularen Mechanismus, zur Regulierung der DSL Bildung, lässt darauf schliessen, dass diese Lipide eine physiologische Relevanz haben. Der Vergleich verschiedener Zelllinien ergab, dass RAW Makrophagen nicht aber die Monozyten Zelllinien (THP1, HL60) hohe endogene Mengen an DLS aufweisen. Wir konnten zeigen, dass während einer PMA stimulierten Differenzierung von THP1 Monozyten zu Makrophagen, sowie in primären humanen Monozyten, die Synthese von DSL ansteigt. Hierbei korrelierte der Anstieg an DSL mit den intrazellulären L-Alanin Konzentrationen. Eine physiologische Relevanz von DSL während der Differenzierung gilt es weiter aufzuklären. Zusammenfassend schlagen wir ein Model vor, in dem die DSL Bildung durch die wildtyp SPT teilweise von der intrazellulären L-Alanin Konzentration abhängt, aber zusätzlich auf Faktoren angewiesen ist, die den Substratwechsel zwischen L-Serin und L-Alanin regulieren. Dieser Substratwechsel könnte durch eine Phosphorylierung von Serin an der Stelle 384 in der SPTLC2 reguliert werden.

General Introduction

I. Sphingolipid *de novo* synthesis and degradation pathway

Serine palmitoyltransferase (SPT) catalyzes the first step in the sphingolipid *de novo* synthesis[1] by metabolizing L-serine together with palmitoyl-CoA. The product 3-keto-sphinganine is rapidly reduced to sphinganine (SA) by the 3-keto-sphinganine reductase. Subsequently sphinganine is N-acylated to dihydro-ceramide, a reaction that is catalyzed by one of several isoforms of ceramide synthases[2]. Next, a desaturase introduces a trans double bond between the C4 and C5 in the sphingoid base backbone which results in ceramides[3, 4]. The 4,5 double-bond is only inserted into the dihydro-ceramide but not into SA directly[5]. The ceramides serve as a hub for the generation of complex sphingolipids, like glycosphingolipids, ceramide-1-phosphate and sphingomyelin[6-8]. Despite being metabolized to complex sphingolipids, ceramide can also be de-acylated to form sphingosine (SO) - a reaction that is catalyzed by various ceramidases[9] (all steps are illustrated in Figure 1).

Sphingolipid degradation

During the degradation of complex sphingolipids, mostly lysosomal enzymes (sphingomyelinases, glucocerebrosidases, ceramidases) are involved which leads eventually to the formation of ceramide and SO. In the salvage pathway SO can be re-acylated by CerS to form again ceramides[10]. It was suggested that ceramides that are generated through the salvage pathway cause different biological responses (growth arrest[11], apoptosis[12], cellular signaling[13] and trafficking[14]) compared to *de novo* generated ceramides. At the end of the sphingolipid degradation process, SO is phosphorylated to SO-1-phosphate (S1P) by SO-1-kinase. S1P can again be dephosphorylated by certain lipid phosphatases or irreversibly degraded by sphingosine-1-phosphate-lyase, a PLP-dependent enzyme that catalyzes the cleavage to phospho-ethanolamine and trans-hexadecenal[15] (Figure 1). Trans-hexadecenal was shown to cause cytoskeletal reorganization, detachment and apoptosis[16]. Moreover it has been shown to form adducts with DNA thereby potentially causing cancer[17].

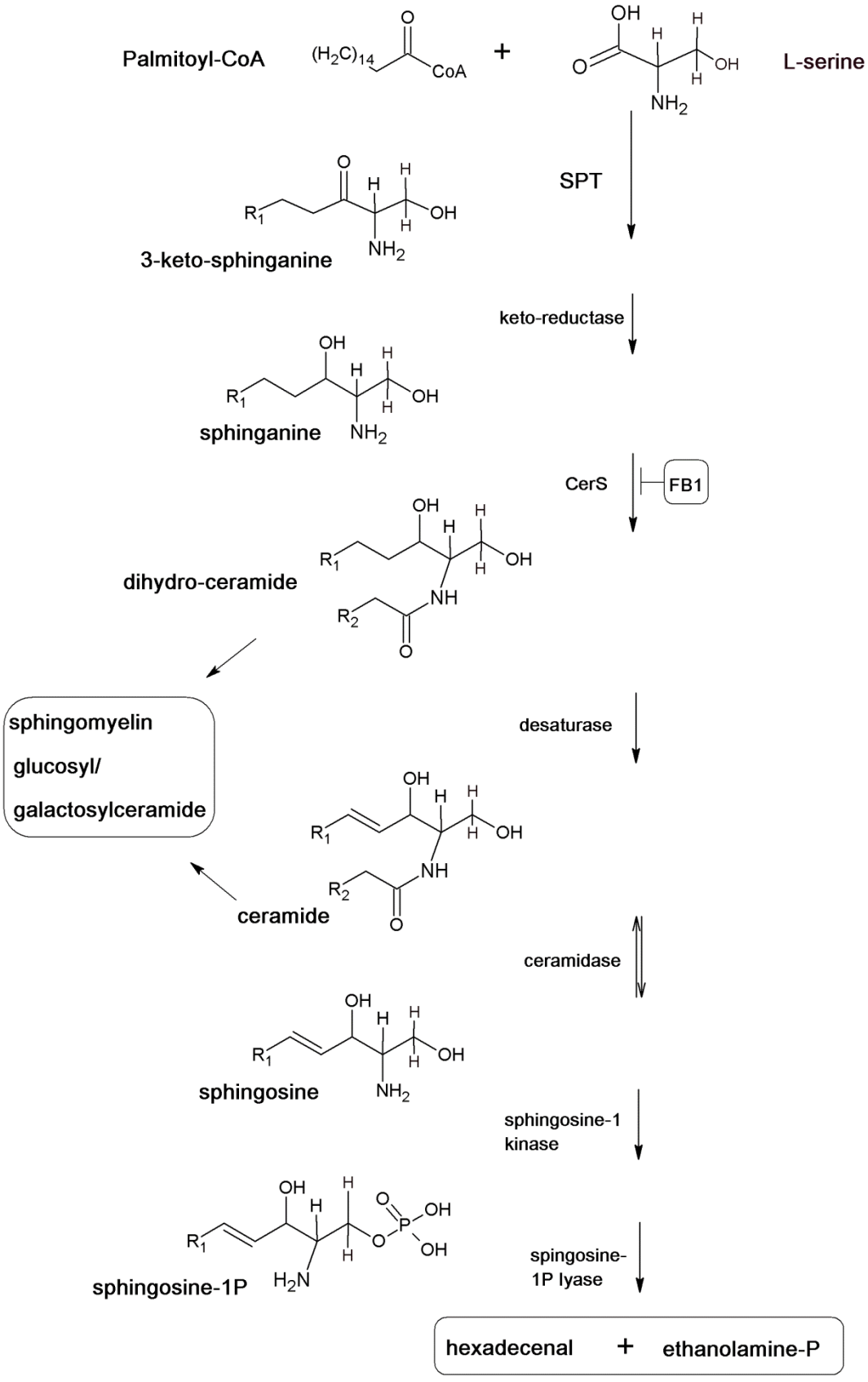

FIGURE 1: **Sphingolipid *de novo* synthesis and degradation pathway**

Sphingolipid de novo synthesis and degradation pathways are spatially separated

The steps of the sphingolipid *de novo* synthesis that lead to the formation of ceramide take place at the cytosolic leaflet of the ER. Ceramide, either bound to the CER transfer protein (CERT) or integrated into vesicles, is transported to the Golgi where it is converted to glycosphingolipids and sphingomyelin that are transported to the plasma-membrane by vesicular transport[1, 10]. Two sphingomyelinases were reported, one located in the Golgi and one at the plasma-membrane (PM)[18]. The phosphorylation of ceramide was reported to happen at the PM, Golgi and in the cytoplasm[19, 20]. De-acylation of ceramide by ceramidases results in the release of sphingosine and a free fatty acid which can occur at neutral, alkaline or acidic pH. Neutral ceramidase is located at the PM[21], acid ceramidase is lysosomal[22] and alkaline ceramidase is located at the ER/Golgi complex[23] (all illustrated in Figure 2).

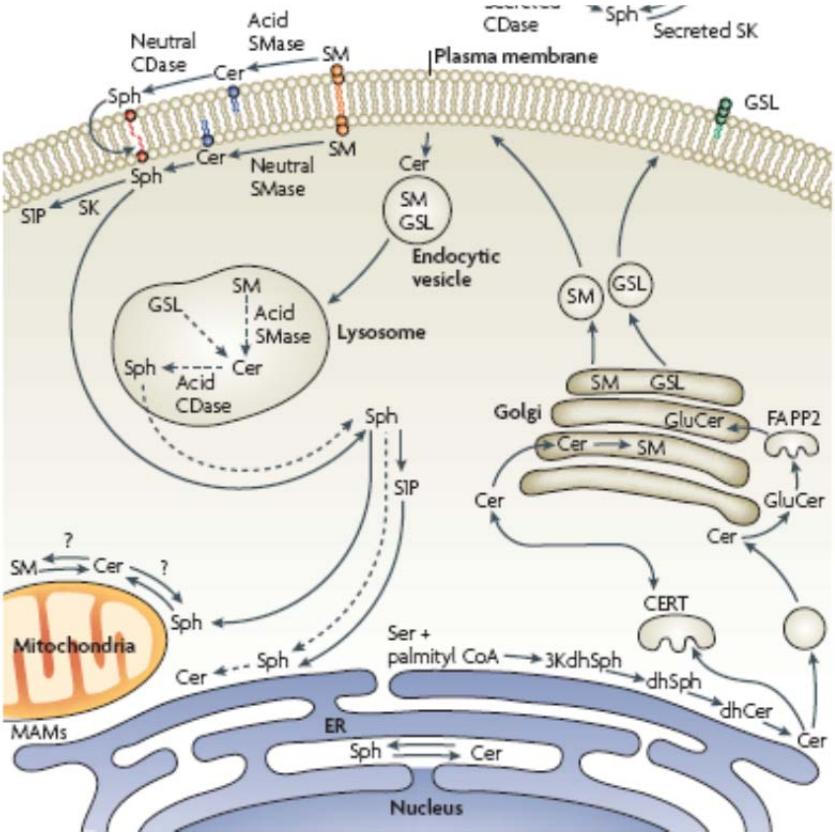

FIGURE 2: **Compartmentalization of the sphingolipid pathway**
(Picture taken from Hannun and Obeid *et al.*[24])

II. Key enzymes involved in ceramide *de novo* synthesis

1. Serine palmitoyltransferase (SPT)

SPT mRNA expression and enzymatic activity were shown to be influenced by many factors including UV radiation[25], endotoxins[26-28], cytokines[27], phorbol-ester[29], daunorubicin[30], magnesium defiency[31], nicotinamide[32], hypoxia[33] and others . Many of these stimuli are inflammatory, toxic or induce some other forms of cell stress. Furthermore, SPT activity was shown to be highly dependent on the supply of its substrates, L-serine and palmitate[34]. Other stimuli like retinoic acid[35], cannabinoids[36] and etoposide[37] have been reported to influence SPT activity without changing mRNA or protein levels which argues for posttranslational regulation. Several microRNAs were reported to negatively regulate SPTLC1 (miR-137/-181c) and SPTLC2 (miR-9/-29a/b-1) expression levels[38]. The loss of these micro RNAs increased SPT activity which resulted in higher ceramide levels and increased amyloid β formation in sporadic Alzheimer`s disease. Furthermore, two phosphorylation sites (S384, Y387) in the SPTLC2 subunit were found in an unbiased global proteomic approach to analyze the phospho-proteom in HeLa cells after EGF stimulation. The observed phosphorylation of SPTLC2 was independent of the EGF stimulus and the reported sequence motif was linked to casein kinase 1[39]. The effect on SPT activity or the context in which the phosphorylation occurs has not been investigated and is addressed in this report.

2. Ceramide synthases (CerS)

Ceramide synthases are catalyzing the N-acylation of sphinganine to form dihydo-ceramides. Six CerS isoforms are known[40] and expressed in a unique tissue distribution. The individual CerS isoforms show a special preference for a certain fatty-acid - CoA substrate. The N-acylation of a selection of various fatty acids results in a broad variety of formed ceramide species as reviewed by Hannun[41]. In detail, CerS1 uses mostly C18-CoA[42], CerS4 C18- and C20-CoAs[43], CerS5 and CerS6 mainly C16-CoAs[43, 44] and CerS3 is most specific for very long chain acyl-CoAs like C26 and higher ones[45]. CerS2 in contrast has a rather broad specificity and metabolizes typically C22 to C24-CoAs[46]. Not much is known about the regulation and interaction of the various CerS isoforms. Ectopic expression of CerS1 and CerS5

have been shown to sensitize cells to various drugs whereby CerS1 showed the broadest spectrum for the tested drugs (cisplatin, doxorubicin, carboplatin, vincristine)[47]. CerS1 protein levels were shown to be down-regulated due to stress stimuli like cisplatin or UV light. This turnover is regulated via phosphorylation by the opposing functions of p38MAP kinase (positive regulation) and PKC (negative regulation) where an activated PKC was associated with increased phosphorylation of CerS1 and reduced turnover[48]. Phosphorylation sites were also found in CerS5[39] and CerS2 [39, 49-52] whereas Cers2 was also shown to be glycosylated[53]. No functional consequence has been linked to these regulatory sites so far. A recent report described the modulation of CerS activity by dimer formation[54]. Ceramide synthase activity was shown to increase by dimerization of certain CerS isoforms, enabling the cell to respond rapidly to changing physiological conditions.

3. Dihydro-ceramide desaturase (DES)

Two dihydro-ceramide desaturases have been reported - DES1 and DES2. DES1 was shown to have high dihydro-ceramide Δ^4-desaturase and very low C-4 hydroxylase activities, whereas the ortholog DES2 exhibits a bifunctional sphingolipid C-4 hydroxylase and Δ^4-desaturase activity[55]. DES1 expression is ubiquitous whereas DES2 is most strongly expressed in skin, intestines and kidney, thereby leading to the higher levels of phyto-sphingolipids in these tissues[56]. Recently, DES1 was also identified as a retinol isomerase in a proposed alternative visual cycle for regenerating opsins in daylight[57]. As DES1 is the only known source of 9-cis-retinoic acid in vertebrates, the same group suggested that DES1 is an isomerase-2 which plays a role in other, nonvisual processes that are linked to 9-cis-retinoic acid like cell growth, differentiation or malignant transformation. The activity of DES1 increases upon attachment of myristate to the N-terminal glycine of the eukaryotic enzyme[58, 59]. Furthermore, N-myristoylation was shown to influence the cellular localization of DES1, targeting the enzyme to mitochondria where, due to the higher DES activity, increased levels of ceramides lead to apoptosis[59]. Besides, the length of the N-acyl chains influenced DES 1 activity as longer chains were associated with a lower *in vitro* DES 1 activity in liver microsomes[5]. As an exception it was shown that C14 is a better substrate over C18, C10, C6 or C2[60]. Moreover, DES1 was shown to be inhibited by increased ROS species[61] as well as by changes in the cellular redox state

(like treatment with antioxidants[62]) that was monitored via the cellular levels of thiols[5]. Both events were associated with increased dihydro-ceramide levels without affecting ceramide levels. Furthermore, hypoxia directly and reversibly inhibited dihydro-ceramide desaturase in a manner that was independent of hypoxia inducible factor (HIF1a) activation[63]. DES1 activity was found to be decreased in confluent cell layers compared to cells at low-density. Specifically, DES1 activity in cells at low-density could be decreased by adding conditioned media from confluent cultures and also by adding a reducing agent like DTT or L-cysteine[64] which confirms the role of free thiols as inhibitors of DES1.

III. Characterization of mammalian SPT

SPT belongs to the family of α-oxoamine synthases (POAS) [65, 66] which in addition to SPT includes three other members - the 8-amino-7-oxononanoate synthase (AONS, biotin synthesis)[67, 68], 5-aminolevulinate synthase (ALAS, heme biosynthesis)[69], and 2-amino-oxobutyrate CoA ligase (KBL, threonine degradation)[70]. They all catalyse a pyridoxal-5-phosphate (PLP) -dependent condensation of an amino acid and an acyl-CoA. All members of the POAS family, except the mammalian SPT, are soluble homodimers with two active sites which are positioned at the monomer-monomer interface. The x-ray structure of the mammalian SPT is not re-solved yet but the structure for the prokaryotic SPT was re-solved from two sphingolipid generating bacteria, *Sphingomonas paucimobilis* and *Sphingobacterium multivorum*[71, 72]. In contrast to the mammalian SPT which is a membrane bound heteromer, the prokaryotic form is a homodimer - either soluble (*S. paucimobilis*) or loosely attached to the inner cell membrane (*S. multivorum*)[73]. All POAS members contain a conserved PLP binding motif (T[FL][GTS]**K**[SAG][FLV]G) that stretches around the lysine residue which forms a Schiff's base together with PLP [1].

SPT subunits and complex composition

The mammalian SPT consists of three subunits SPTLC1 (Swiss-prot: O15269), SPTLC2 (Swiss-prot: O15270) and SPTLC3 (Swiss-prot: Q9NUV7)[1,74,75]. All three isoforms contain a putative transmembrane domain, but only SPTLC2 and SPTLC3 contain a PLP-binding motif characterizing them as the catalytically active subunits[1,

[76]. SPTLC2 and SPTLC3 show significant sequence similarities (approximately 70%) whereas SPTLC1 shows a mutual similarity of approximately 20% to SPTLC2 and SPTLC3[74]. The SPTLC1 and SPTLC2 subunits are ubiquitously expressed whereas SPTLC3 expression is restricted to certain tissue like placenta, liver and skin[75]. The structural composition of the active SPT enzyme is not completely understood. At least a heterodimer between SPTLC1 and SPTLC2 or SPTLC1 and SPTLC3 is needed for enzymatic activity[1, 77]. Results of biochemical analysis suggest that SPT is a heteromeric enzyme with a functional molecular weight of 460-480kD. This indicates that SPT is organized as a higher-order, probably octameric complex which can be composed of all three subunits[77]. The stoichiometry between SPTLC2 and SPTLC3 within the complex probably depends on their relative expression levels. The proposed SPT dimer and higher organized complex is shown in Figure 3.

A: B:

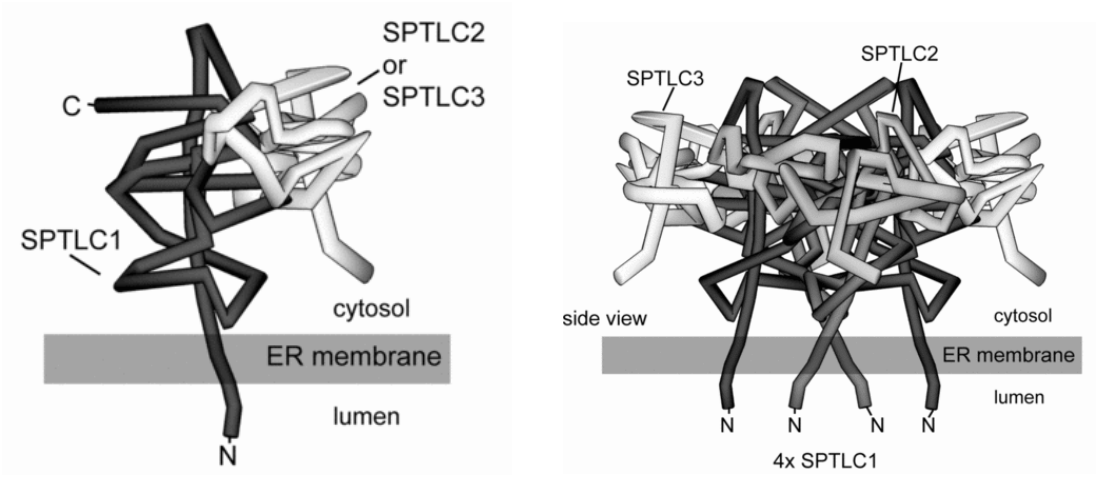

FIGURE 3: **Proposed structure of the mammalian SPT complex**[77]
A: Functional heterodimer composed of SPTLC1 with either SPTLC2 or SPTLC3
B: Proposed organization of functional units in a multi-subunit complex

Functionally it was shown that the carbon chain profile of the sphingoid bases in cells and tissue is defined by the relative expression of SPTLC2 and SPTLC3 subunit. Whereas SPTLC2 has a relatively defined specificity for palmitoyl (C16) CoA SPTLC3 is metabolizing a rather broad spectrum of acyl-CoAs in the range between C14 and C18. In SPTLC3 rich tissues like placenta and trophoblast-derived cell lines (JEG 3, JAR) but also in SPTLC3 transfected HEK cells, SPTLC3 expression levels correlated closely with the cellular levels of C16 sphingoid bases[76]. The biophysical

properties and physiological relevance of sphingoid bases with different chain lengths was not investigated in detail yet. However, it is reasonable to assume that differences in the biophysical properties like a lower hydrophobicity, shorter length, and altered lipid-lipid interaction will have some impact on various cellular processes like vesicular trafficking, ER-stress, membrane dynamics or the formation of stable membrane domains ("rafts")[78]. It should be noted that sphingoid bases with a C16 and C14 carbon chain are the most abundant sphingoid bases in insects[79]. Also about 10-15% of the sphingolipidome in human plasma consists of sphingoid bases with a carbon chain length other than C18[80].

SPT splice variants

In gene databases alternative splice-forms of SPT are postulated. Two SPTLC1 transcripts (Swiss-prot: O15269-1; -2) correlating to 53 and 16 kDa as well as two SPTLC3 variants with a putative size of 62 and 19.7kDa (Swiss-prot: Q9NUV7-1;-2) can be found. An additional SPTLC1 isoform was described by Wei *et al.* Here the first 32 nucleotides from exon 15 are missing which causes a frame-shift and skipping of the original stop codon. This results in a longer transcript (57kD - referred to SPTLC1L) which could also be detected on protein level[81]. However, a systematic database screen, revealed additional splice variants for SPTLC1 and SPTLC2. One additional variant was found for SPTLC1 which contained the first 143 amino acids of the N-terminal part (hSPTLC1-N143). For SPTLC2 three splice variants were identified; hSPTLC2-N162, containing the first 162 N-terminal amino acids, hSTPLC2-N204, comprising the first 204 N-terminal amino acids and hSPTLC2-C293, exhibiting the last 293 amino acids of the C-terminal end including the PLP binding motif (Figure 4).

The mRNA transcripts of these variants were expressed in a tissue specific manner and were also detected on protein level. However, overexpression of these variants in HEK293 cells had no obvious effect on SPT activity, sphingolipid profile or cell growth (unpublished data).

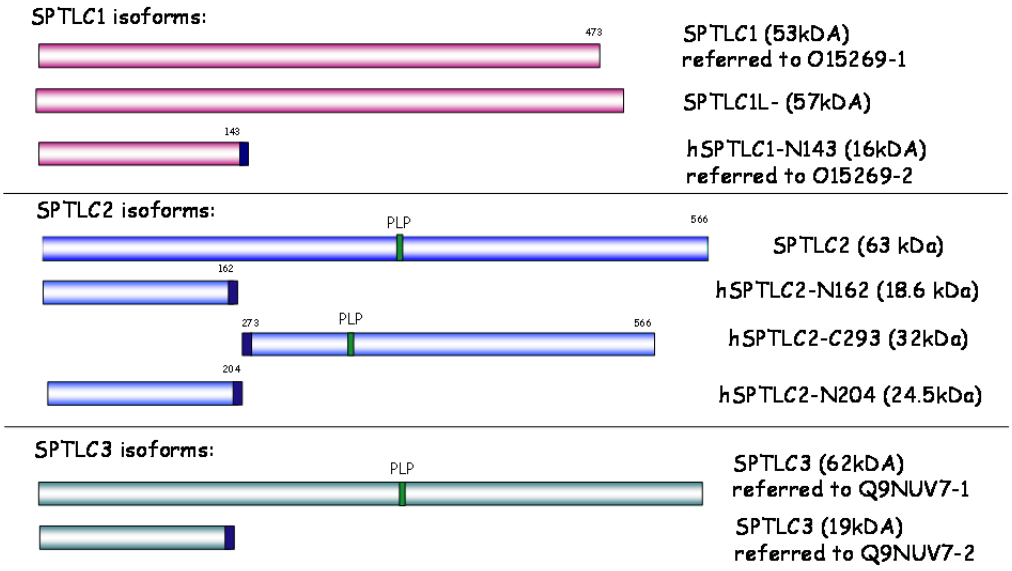

FIGURE 4: **Schematic illustration of proposed SPT isoforms**
SPTLC1L described by Wei[81], the three SPTLC2 splice variants (-N162, C293 and N204) were found by expressed sequence tag (EST) searches (unpublished data).

Orm proteins negatively regulate yeast and mammalian SPT

In addition to the three main subunits (SPTLC1-3) other proteins have been reported to interact with SPT. The ORM proteins have been shown to regulate SPT activity by a metabolic feedback mechanism to maintain sphingolipid homeostasis and to prevent the harmful overproduction of ceramides by the *de novo* synthesis pathway. The ORM family consists of two members in yeast (Orm1/2) and three members in mammalians (ORMDL1/2/3)[82].

It has been shown in yeast that non-phosphorylated Orm1/2 proteins bind to SPT thereby inhibiting its activity and sphingolipid *de novo* synthesis. If cells are in need of sphingolipid *de novo* formation, Orm proteins get successively phosphorylated and dissociate from the SPT complex thereby releasing SPT activity. In yeast, phosphorylation of the Orm1/2 proteins is catalyzed by Ypk1 via a TORC2 – dependent pathway [83]. When sphingolipid levels are restored, Orm1/2 proteins are de-phosphorylated by Sac1 phosphatase which leads to inhibition of SPT activity[84]. In yeast, a multisubunit complex called "SPOTS" was described that consists of Lcb1/Lcb2/Tsc3, Orm1/2 and the phosphoinositide phosphatase Sac1[84, 85].

The role of the ORM proteins in yeast was put forward by Sun *et al.*[86] who demonstrated that Orm phosphorylation is triggered by the heat stress induced depletion of sphingolipids, via the Pkh-Ypk pathway. Upon heat stress the Pkh-

TORC2-Ypk cascade is quickly activated which leads to rapid phosphorylation of the Orm proteins and the activation of sphingolipid *de novo* synthesis. The accumulation of intermediate metabolites of the sphingolipid synthesis pathway promotes a metabolic feedback mechanism that leads to de-phosphorylation of Orm proteins which in turn inhibits SPT. The de-phosphorylation of the ORM proteins was shown to be either due to inhibition of the Pkh-Ypk kinase [87] or by activation of Cdc55-PPA phosphatase [86]. The activation of Ypk1 by heat stress was proposed to be mediated via Slm1/2 that act as a sensor for the rigidity and dynamics of the plasma membrane. The release of Pkh kinase and Slm1/2 from eisosomes, activate TORC2 and trigger Ypk activation[86]. Since in yeast ORM2 is 10-fold higher expressed than Orm1, the authors speculated that this mechanism is primarily mediated by ORM2.

However, Liu and colleagues[88] proposed that Orm1 and Orm2 regulate sphingolipid synthesis by different mechanisms. They reported that Orm1 phosphorylation is increased upon supplementation of rapamycin to the growth media whereas Orm2 phosphorylation was not affected. Moreover, they found Orm1 phosphorylation partly mediated by protein kinase Npr1 and to be dependent on the Tap42-Sit4 protein phosphatase complex that acts downstream of TORC1. Thereby, the cell is able to respond to environmental stimuli like nutritional signals. Furthermore, they described a compensatory link between the two Orm proteins: Orm1 phosphorylation is altered in response to a loss or increased Orm2 expression. They demonstrated that Orm1 phosphorylation is increased (to activate SPT) when Orm2 is overexpressed, and that Orm1 is dephosphorylated (to inhibit SPT) when Orm2 is absent. This could be a compensatory response to balance SPT activity since Orm2 levels increase upon ER stress [85] whereas Orm1 is phosphorylated upon ER stress [88]. In addition an interaction of Orm1 and Orm2 with the ceramide synthase subunit, Lac1 was reported which was independent from the phosphorylation status of both Orm proteins[88].

Besides their role in regulating sphingolipid synthesis, overexpression of Orm2 (and to a lower extent of Orm1) was associated with resistance to high iron concentrations in yeast[89]. High iron concentrations increased sphingolipid levels which activate the Pkh/Ypk cascade leading to phosphorylation and inactivation of the Orm proteins. Over-expression of Orm2 is inhibiting this response and reduces Ypk phosphorylation thereby maintaining balanced sphingolipid levels[89].

In mammalians three ubiquitously expressed ORMDL isoforms are known: ORMDL1 (Swiss-prot: Q9P0S3), ORMDL2 (Swiss-prot: Q53FV1) and two variants of ORMDL3[90] (Swiss-prot: Q9P0S3-1 and -4). The three isoforms are highly identical in their protein sequences (81-84%) and were found to be extremely conserved between vertebrate species. All ORMDL isoforms co-localized with ER markers[82] and ORMDL3 was found to physically interact with the SPTLC1 subunit[84]. The silencing of all three ORMDL isoforms resulted in increased *de novo* formation of ceramides[84, 91] indicating that ORMDL proteins are also negative regulators of the mammalian SPT. Moreover, it was shown that ORMDL proteins suppress SPT activity under normal growth conditions and that the presence of serum in the growth media has an additional non-ORMDL mediated inhibitory effect on ceramide synthesis[91]. The authors showed that ORMDL proteins affect solely SPT activity and had no effect on ceramide synthases[91].

In contrast to yeast it is not known how the ORMDL proteins inhibit SPT, since the mammalian ORMDL proteins are N-terminally truncated in comparison to their yeast homologs and lack the serine residues that are phosphorylated by Ypk1 in yeast[82, 84]. The mammalian ORMDL proteins also lack the canonical phosphorylation motif for the mammalian Ypk-homolog - the serum and glucocorticoid-induced kinase (SGK). This leaves the question open whether ORMDL proteins in the mammalian system act in the same way as it is described in yeast.

Furthermore, the mechanism how the cell senses the ceramide status is not understood. It has been suggested that a downstream metabolite of the synthesis pathway like ceramide or even higher complexity substitute (e.g. sphingomyelin or glycosphingolipids) could drive this mechanism, since the sphingosine induced inhibition of SPT was lost when cells were co-stimulated with FB1 which prevents the conversion of the added sphingosine to complex sphingolipid-species[91].

ORMDL3 has been identified as a significant risk factor for early childhood asthma in several genome-wide association studies[92-95]. This can be linked to the recent finding that ORMDL3 expression is induced in the lung epithelium by allergens and cytokines (IL-4 or IL-13)[96]. ORMDL3 mRNA expression is strongly dependent on STAT-6 and the expression of ORMDL3 in lung epithelium cells induced metalloproteases, chemokines as well as oligo-adenylate synthetases genes and triggered the unfolded protein response (UPR) via activation of ATF6. Jin and colleagues found higher ORMDL3 mRNA expression in the peripheral blood of

patients experiencing wheezing compared to healthy controls. A specific analysis of the ORMDL3 promoter indicated the involvement of the transcription factors Ets-1, p300 and CREB to control ORMDL3 expression[97]. All three transcription factors are involved in regulating inflammatory processes underlying the association of elevated ORMDL3 levels with asthma or inflammatory diseases.

ORMDL3 was also found to bind to the sarco-endoplasmatic reticulum calcium pump (SERCA) thereby inhibiting the transport of calcium from the cytosol to the ER which leads to a reduced ER calcium content. This results in a UPR response which mediates NFκB- and JNK-activation and leads to a pro inflammatory response[98, 99]. Furthermore, an increased ORMDL3 mRNA expression was associated with decreased T-lymphocyte activation which provides a further functional link between the genetic association of ORMDL3 and inflammatory diseases[100]. Last but not least a reduced expression of ORMDL1 (also called Adoplin-1) was found to be associated with mutations in presenilin which is part of the γ-secretase complex that mediates the cleavage of amyloid precursor protein (APP)[101]. A knock-down of ORMDL1 led to a reduced γ-secretase activity indicating that ORMDL1 could also be a therapeutic target for treating Alzheimer's disease[101].

Small SPT subunits activate SPT activity and affect acyl-CoA specificity

A group of small proteins, designated as "small subunits SPT a and b"(ssSPTa/b) were shown to interact with SPTLC1/ SPTLC2 and SPTLC1/SPTLC3 heterodimers thereby generally increasing SPT activity and influencing acyl-CoA specificity[102]. A homologous protein (Tsc3) was found earlier in yeast[103]. In detail, co-expression of mammalian ssSPTa and ssSPTb in combination with either SPTLC1+SPTLC2 or SPTLC1+SPTLC3 in a yeast strain which lacks the endogenous SPT expression resulted in a significant increase of overall SPT activity. The activity increase was more pronounced upon co-expression of ssSPTa than of ssSPTb. It was shown that both small subunits interact directly with the SPTLC1 subunit. Moreover, it was demonstrated that co-expression of ssSPTa and b with the individual SPTLC subunits alter the preference of the enzyme for acyl-CoAs with different carbon chain lengths. A complex consisting of SPTLC1/SPTLC2/ssSPTa showed a higher preference for C16-CoA resulting in C18-derived sphingoid bases whereas a complex of SPTLC1/SPTLC3/ssSPTa preferentially used C14-CoAs forming C16-based

sphingoid bases. This is in line with previous findings that the SPTLC3 subunit has a higher specificity towards shorter acyl-CoAs like myristoyl- and lauryl-CoA whereas the SPTLC2 subunit preferentially uses palmitoyl C16-CoA[76]. The ssSPTb subunit modulates the preference of SPT for longer acyl-CoAs like stearyl C18-CoA which results in the generation of C20-derived sphingoid bases. Long chain acyl-CoAs were mostly generated by the combination SPTLC1/SPTLC2/ssSPTb whereas a SPTLC1/SPTLC3/ssSPTb constellation metabolized a broad range of acyl-CoAs without any apparent preference[102]. Based on this report small SPT subunits modulate overall SPT activity but also the generation of specific sphingolipid-species.

Other known and proposed binding partners of SPT

In addition to the ORMDL and ssSPTa/b regulators other proteins have been described to be associated with the SPT subunits. Inuzuka *et al.* described a novel class of endoplasmatic proteins, named Serine Incorporator (Serinc1-5) in yeast and mammalian cells that can increase the synthesis of phosphatidylserine and sphingolipids[104]. Yeast-two hybrid experiments revealed a potential binding of Serinc1 to SPTLC1 (LCB1) as well as to PGDH (yeast: SER3), an enzyme that catalyzes the first and rate-limiting step in serine synthesis. Overexpression of Serinc1 doubled SPT activity in COS cells. The authors speculate that Serinc could act as a platform to facilitate the interaction of the soluble L-serine with the membrane bound SPT [104]. Several regulatory sites have been identified in Serinc1 including-phosphorylation[39, 50], myristoylation[105] and glycosylation[53] sites, but no functions were connected to them yet.

Large-scale proteomic screens aiming to identify protein-protein interactions revealed several further potential binding partners for SPTLC2 in *S. cerevisiae* (LCB2)[106]. The identified proteins (Bmh1,2; Crm1; Ecm29; Fks1; Gea2; Gfa1; Kap104; Kap123; Lcb1; Lcb2; Lys12; Mir1; Sam1,2; YHR020W) are involved in growth regulation, protein transport and nuclear import and export, amongst others. Moreover, a genome-wide yeast two hybrid analysis suggested 13 potential binding partners for SPTLC2 in drosophila (lace2)[107]. Among these potential binding partners for lace2 (Hsc70-4; CG4287; RpS27A; CG5802; CG6126; Vha13; CG6453; CG9986; CG4162; RPL31; CG32758; CG4046; CG4193) are ribosomal proteins, heat shock proteins, thioredoxin and transmembrane transporters.

SPTLC1 has also been proposed to act via its PDZ binding motif with several other proteins including Par3, ABCA1, FRMPD4 and PTPN13[108, 109]. SPTLC1 was shown to interact with ABCA1 in THP1 monocyte-derived macrophages and in mouse liver. It has been proposed that the binding of ABCA1 to SPTLC1 inhibits the cholesterol efflux activity thereby maximizing the cellular cholesterol in cells with a high demand for membrane synthesis[109]. Moreover Par3, a scaffolding factor that recruits signaling molecules into multiprotein complexes, was identified to bind SPTLC1 in THP1-derived macrophages and in mouse liver. Knocking-down Par3 or SPTLC1 decreased both, SPT activity and chemotaxis induced migration of THP1 monocytes[108]. This suggests that the migration in monocytes involves sphingolipids and depends on the recruitment of SPTLC1 by the scaffolding factor Par3.

Serine palmitoyltransferase and hereditary sensory neuropathy type I

Several missense mutations in the SPTLC1 and SPTLC2 gene were associated with hereditary sensory and autonomous neuropathy type I (HSAN I)[110-117]. HSAN I is an autosomal dominantly inherited peripheral neuropathy with a primarily sensory (heat, pain, vibration) and a variable motor component. The disease is characterized by a length dependent axonal loss with a typically late onset in the second or third decade of life[114]. Due to the sensory loss, patients suffer from painless injuries, chronic skin ulcers and Charcot joints frequently requiring amputations. The variable motor component is characterized by variable muscle wasting primarily in the extremities and the need for orthopedic aids at later stages.

An increasing number of point mutations in the *SPTLC1* and *SPTLC2* genes were associated with HSAN I. They include mutations in SPTLC1 (C133W[110-112], C133Y[112], V144D[112] , G387A[118], S331F and A352V[119], C133R - personal communication) and in the SPTLC2 subunit (V359M, G382V, I504F[116] and T409M-unpublished). No HSAN I causing mutation was found in the *SPTLC3* yet. All confirmed HSAN I mutations resulted in decreased activity with L-serine in isolated proteins although this reduced activity does not transform into reduced total sphingolipid levels in mutant expressing cells or plasma of HSAN I patients [116, 120].

Interestingly, besides the reduction of canonical activity, the HSAN I mutations induce a shift in the amino acid substrate, leading to the metabolism of L-alanine and to a certain extent L-glycine as alternative substrates. This results in the formation of atypical 1-deoxy-sphingolipids (dSLs) which lack the C1-hydroxyl-group of normal

ceramides[114, 118, 119]. The dSLs are therefore not converted to complex sphingolipids. Also degradation by the canonical pathway is hampered, since the formation of sphingosine-1-phosphate as a catabolic intermediate is not possible. Elevated dSL levels were found in plasma and peripheral nerve tissue (PNS) of transgenic HSAN I mice[121] and in the plasma of HSAN I-patients[116, 120]. Deoxy-sphingolipids were shown to be neurotoxic in cultured DRG neurons by affecting number and length of neurite outgrowth[120]. The dSL formation could be suppressed in HSAN I mutant cells and transgenic HSAN I-mice[121] by supplementation with L-serine. Upon L-serine supplementation, plasma dSL levels normalized and the HSAN I transgenic mice did not develop any neurological defects up to an age of 20 month. The dSL-lowering effect in plasma due to oral L-serine supplementation was confirmed in a 10 week pilot study with 20 HSAN I patients. Improvements in the neuropathy were not addressed in that study. A comprehensive clinical trial over a period of 24 months is currently planned and will start in late spring 2013.

Other factors that contribute to deoxy-sphingolipid generation

Deoxy-sphingolipids can also be formed in the absence of mutations in SPT. Low but detectable dSL levels are generally found in plasma - also of healthy individuals. However, patients with metabolic syndrome or diabetes type 2 have significantly elevated plasma dSL levels[122, 123]. This shows that not only the mutant but also the wildtype SPT is capable of producing dSLs under certain conditions. The addition of Fumonisin B1 (FB1) - an inhibitor of Ceramide Synthase (CerS) – was shown to significantly stimulate dSL formation in cultured cells[124]. Also culturing cells at a high density for a prolonged time increases dSL formation[124]. Whether dSLs have a physiological role in lipid metabolism is not clear yet. Recently, deoxy-ceramides were identified as scaffold lipids facilitating lipid antigen presentation and suggesting a role in the innate immunity[125]. Another report showed that dSLs accumulate together with ceramides upon TNFa stimulation[126]. However, the observation that wt SPT forms dSL only under certain, not yet well defined conditions, argues for a regulatory mechanism allowing SPT to shift between L-serine and L-alanine as substrates.

Aim of the thesis

The aim of this thesis was to identify and characterize regulatory mechanisms that underlie the change in amino acid substrate specificity and dSL formation of wild type and mutated SPT.

References

1. Hanada K. Serine palmitoyltransferase, a key enzyme of sphingolipid metabolism. Biochimica et Biophysica Acta (BBA) - Molecular and Cell Biology of Lipids 2003;1632:16-30.
2. Pewzner-Jung Y, Ben-Dor S, Futerman AH. When Do Lasses (Longevity Assurance Genes) Become CerS (Ceramide Synthases)?: INSIGHTS INTO THE REGULATION OF CERAMIDE SYNTHESIS. Journal of Biological Chemistry 2006;281:25001-25005.
3. Causeret C, Geeraert L, Hoeven G, Mannaerts G, Veldhoven P. Further characterization of rat dihydroceramide desaturase: Tissue distribution, subcellular localization, and substrate specificity. Lipids 2000;35:1117-1125.
4. Michel C, van Echten-Deckert G. Conversion of dihydroceramide to ceramide occurs at the cytosolic face of the endoplasmic reticulum. FEBS Letters 1997;416:153-155.
5. Michel C, van Echten-Deckert G, Rother J, Sandhoff K, Wang E, Merrill AH. Characterization of Ceramide Synthesis: A DIHYDROCERAMIDE DESATURASE INTRODUCES THE 4,5-TRANS-DOUBLE BOND OF SPHINGOSINE AT THE LEVEL OF DIHYDROCERAMIDE. Journal of Biological Chemistry 1997;272:22432-22437.
6. Arana L, Gangoiti P, Ouro A, Trueba M, Gomez-Munoz A. Ceramide and ceramide 1-phosphate in health and disease. Lipids in Health and Disease 2010;9:15.
7. Milhas D, Clarke CJ, Hannun YA. Sphingomyelin metabolism at the plasma membrane: Implications for bioactive sphingolipids. FEBS Letters 2010;584:1887-1894.
8. Tafesse FG, Ternes P, Holthuis JCM. The Multigenic Sphingomyelin Synthase Family. Journal of Biological Chemistry 2006;281:29421-29425.
9. Xu R, Jin J, Hu W, et al. Golgi alkaline ceramidase regulates cell proliferation and survival by controlling levels of sphingosine and S1P. The FASEB Journal 2006;20:1813-1825.
10. Kitatani K, Idkowiak-Baldys J, Hannun YA. The sphingolipid salvage pathway in ceramide metabolism and signaling. Cellular Signalling 2008;20:1010-1018.
11. Ogretmen B, Pettus BJ, Rossi MJ, et al. Biochemical Mechanisms of the Generation of Endogenous Long Chain Ceramide in Response to Exogenous Short Chain Ceramide in the A549 Human Lung Adenocarcinoma Cell Line: ROLE FOR ENDOGENOUS CERAMIDE IN MEDIATING THE ACTION OF EXOGENOUS CERAMIDE. Journal of Biological Chemistry 2002;277:12960-12969.
12. Takeda S, Mitsutake S, Tsuji K, Igarashi Y. Apoptosis Occurs via the Ceramide Recycling Pathway in Human HaCaT Keratinocytes. Journal of Biochemistry 2006;139:255-262.
13. Kitatani K, Idkowiak-Baldys J, Bielawski J, et al. Protein Kinase C-induced Activation of a Ceramide/Protein Phosphatase 1 Pathway Leading to Dephosphorylation of p38 MAPK. Journal of Biological Chemistry 2006;281:36793-36802.
14. Becker KP, Kitatani K, Idkowiak-Baldys J, Bielawski J, Hannun YA. Selective Inhibition of Juxtanuclear Translocation of Protein Kinase C βII by a Negative Feedback Mechanism Involving Ceramide Formed from the Salvage Pathway. Journal of Biological Chemistry 2005;280:2606-2612.
15. Fyrst H, Saba JD. Sphingosine-1-phosphate lyase in development and disease: Sphingolipid metabolism takes flight. Biochimica et Biophysica Acta (BBA) - Molecular and Cell Biology of Lipids 2008;1781:448-458.
16. Kumar A, Byun H-S, Bittman R, Saba JD. The sphingolipid degradation product trans-2-hexadecenal induces cytoskeletal reorganization and apoptosis in a JNK-dependent manner. Cellular Signalling 2011;23:1144-1152.
17. Upadhyaya P, Kumar A, Byun H-S, Bittman R, Saba JD, Hecht SS. The sphingolipid degradation product trans-2-hexadecenal forms adducts with DNA. Biochemical and Biophysical Research Communications 2012;424:18-21.
18. Huitema K. Identification of a family of animal sphingomyelin synthases. In: The EMBO Journal 2004: 33–44.
19. Carré A, Graf C, Stora S, et al. Ceramide kinase targeting and activity determined by its N-terminal pleckstrin homology domain. Biochemical and Biophysical Research Communications 2004;324:1215-1219.
20. Van Overloop H, Gijsbers, Sofie, Van Veldhoven PP. Further characterization of mammalian ceramide kinase: substrate delivery and (stereo)specificity, tissue distribution, and subcellular localization studies. Journal of Lipid Research 2006;47:268-283.

21. Hwang Y-h, Tani M, Nakagawa T, Okino N, Ito M. Subcellular localization of human neutral ceramidase expressed in HEK293 cells. Biochemical and Biophysical Research Communications 2005;331:37-42.
22. Bernardo K, Hurwitz R, Zenk T, et al. Purification, characterization, and biosynthesis of human acid ceramidase. Journal of Biological Chemistry 1995;270:11098-11102.
23. Mao C, Xu R, Szulc ZM, Bielawska A, Galadari SH, Obeid LM. Cloning and Characterization of a Novel Human Alkaline Ceramidase: A MAMMALIAN ENZYME THAT HYDROLYZES PHYTOCERAMIDE. Journal of Biological Chemistry 2001;276:26577-26588.
24. Hannun YA, Obeid LM. Principles of bioactive lipid signalling: lessons from sphingolipids. Nat Rev Mol Cell Biol 2008;9:139-150.
25. Farrell AM, Uchida Y, Nagiec MM, et al. UVB irradiation up-regulates serine palmitoyltransferase in cultured human keratinocytes. Journal of Lipid Research 1998;39:2031-2038.
26. Chang Z-Q, Lee S-Y, Kim H-J, et al. Endotoxin activates de novo sphingolipid biosynthesis via nuclear factor kappa B-mediated upregulation of Sptlc2. Prostaglandins & Other Lipid Mediators 2011;94:44-52.
27. Memon RA, Holleran WM, Moser AH, et al. Endotoxin and Cytokines Increase Hepatic Sphingolipid Biosynthesis and Produce Lipoproteins Enriched in Ceramides and Sphingomyelin. Arteriosclerosis, Thrombosis, and Vascular Biology 1998;18:1257-1265.
28. Memon RA, Holleran WM, Uchida Y, Moser AH, Grunfeld C, Feingold KR. Regulation of sphingolipid and glycosphingolipid metabolism in extrahepatic tissues by endotoxin. Journal of Lipid Research 2001;42:452-459.
29. Garzotto M, White-Jones M, Jiang Y, et al. 12-O-Tetradecanoylphorbol-13-acetate-induced Apoptosis in LNCaP Cells Is Mediated through Ceramide Synthase. Cancer Research 1998;58:2260-2264.
30. Bose R, Verheij M, Haimovitz-Friedman A, Scotto K, Fuks Z, Kolesnick R. Ceramide synthase mediates daunorubicin-induced apoptosis: An alternative mechanism for generating death signals. Cell 1995;82:405-414.
31. Altura BM, Shah NC, Li Z, Jiang X-C, Perez-Albela JL, Altura BT. Magnesium deficiency upregulates serine palmitoyl transferase (SPT 1 and SPT 2) in cardiovascular tissues: relationship to serum ionized Mg and cytochrome c. American Journal of Physiology - Heart and Circulatory Physiology 2010;299:H932-H938.
32. Tanno O, Ota Y, Kitamura N, Katsube T, Inoue S. Nicotinamide increases biosynthesis of ceramides as well as other stratum corneum lipids to improve the epidermal permeability barrier. British Journal of Dermatology 2000;143:524-531.
33. Kang MS, Ahn KH, Kim SK, et al. Hypoxia-induced neuronal apoptosis is mediated by de novo synthesis of ceramide through activation of serine palmitoyltransferase. Cellular Signalling 2010;22:610-618.
34. Smith ER, Merrill AH. Differential Roles of de Novo Sphingolipid Biosynthesis and Turnover in the Burst of Free Sphingosine and Sphinganine, and Their 1-Phosphates and N-Acyl-Derivatives, That Occurs upon Changing the Medium of Cells in Culture. Journal of Biological Chemistry 1995;270:18749-18758.
35. Herget T, Esdar C, Oehrlein SA, et al. Production of Ceramides Causes Apoptosis during Early Neural Differentiation in Vitro. Journal of Biological Chemistry 2000;275:30344-30354.
36. Gómez del Pulgar T, Velasco G, Sánchez C, Haro A, Guzmán M. De novo-synthesized ceramide is involved in cannabinoid-induced apoptosis. Biochem J 2002;363:183-188.
37. Perry DK, Carton J, Shah AK, Meredith F, Uhlinger DJ, Hannun YA. Serine Palmitoyltransferase Regulates de NovoCeramide Generation during Etoposide-induced Apoptosis. Journal of Biological Chemistry 2000;275:9078-9084.
38. Geekiyanage H, Chan C. MicroRNA-137/181c Regulates Serine Palmitoyltransferase and In Turn Amyloid β, Novel Targets in Sporadic Alzheimer's Disease. The Journal of Neuroscience 2011;31:14820-14830.
39. Olsen JV, Blagoev B, Gnad F, et al. Global, In Vivo, and Site-Specific Phosphorylation Dynamics in Signaling Networks. Cell 2006;127:635-648.
40. Pewzner-Jung Y, Park H, Laviad EL, et al. A Critical Role for Ceramide Synthase 2 in Liver Homeostasis: I. ALTERATIONS IN LIPID METABOLIC PATHWAYS. Journal of Biological Chemistry 2010;285:10902-10910.
41. Hannun YA, Obeid LM. Many Ceramides. Journal of Biological Chemistry 2011;286:27855-27862.
42. Venkataraman K, Riebeling C, Bodennec J, et al. Upstream of Growth and Differentiation Factor 1 (uog1), a Mammalian Homolog of the Yeast Longevity Assurance Gene 1 (LAG1),

RegulatesN-Stearoyl-sphinganine (C18-(Dihydro)ceramide) Synthesis in a Fumonisin B1-independent Manner in Mammalian Cells. Journal of Biological Chemistry 2002;277:35642-35649.
43. Riebeling C, Allegood JC, Wang E, Merrill AH, Futerman AH. Two Mammalian Longevity Assurance Gene (LAG1) Family Members, trh1 and trh4, Regulate Dihydroceramide Synthesis Using Different Fatty Acyl-CoA Donors. Journal of Biological Chemistry 2003;278:43452-43459.
44. Mizutani Y, Kihara A, Igarashi Y. Mammalian Lass6 and its related family members regulate synthesis of specific ceramides. Biochem J 2005;390:263-271.
45. Mizutani Y, Kihara A, Igarashi Y. LASS3 (longevity assurance homologue 3) is a mainly testis-specific (dihydro)ceramide synthase with relatively broad substrate specificity. Biochem J 2006;398:531-538.
46. Laviad EL, Albee L, Pankova-Kholmyansky I, et al. Characterization of Ceramide Synthase 2: TISSUE DISTRIBUTION, SUBSTRATE SPECIFICITY, AND INHIBITION BY SPHINGOSINE 1-PHOSPHATE. Journal of Biological Chemistry 2008;283:5677-5684.
47. Min J, Mesika A, Sivaguru M, et al. (Dihydro)ceramide Synthase 1–Regulated Sensitivity to Cisplatin Is Associated with the Activation of p38 Mitogen-Activated Protein Kinase and Is Abrogated by Sphingosine Kinase 1. Molecular Cancer Research 2007;5:801-812.
48. Sridevi P, Alexander H, Laviad EL, et al. Ceramide synthase 1 is regulated by proteasomal mediated turnover. Biochimica et Biophysica Acta (BBA) - Molecular Cell Research 2009;1793:1218-1227.
49. Daub H, Olsen JV, Bairlein M, et al. Kinase-Selective Enrichment Enables Quantitative Phosphoproteomics of the Kinome across the Cell Cycle. Molecular Cell 2008;31:438-448.
50. Dephoure N, Zhou C, Villén J, et al. A quantitative atlas of mitotic phosphorylation. Proceedings of the National Academy of Sciences 2008;105:10762-10767.
51. Han G, Ye M, Zhou H, et al. Large-scale phosphoproteome analysis of human liver tissue by enrichment and fractionation of phosphopeptides with strong anion exchange chromatography. PROTEOMICS 2008;8:1346-1361.
52. Zahedi RP, Lewandrowski U, Wiesner J, et al. Phosphoproteome of Resting Human Platelets. Journal of Proteome Research 2007;7:526-534.
53. Chen R, Jiang X, Sun D, et al. Glycoproteomics Analysis of Human Liver Tissue by Combination of Multiple Enzyme Digestion and Hydrazide Chemistry. Journal of Proteome Research 2009;8:651-661.
54. Laviad EL, Kelly S, Merrill AH, Futerman AH. Modulation of Ceramide Synthase Activity via Dimerization. Journal of Biological Chemistry 2012;287:21025-21033.
55. Ternes P, Franke S, Zähringer U, Sperling P, Heinz E. Identification and Characterization of a Sphingolipid Δ4-Desaturase Family. Journal of Biological Chemistry 2002;277:25512-25518.
56. Fabrias G, Muñoz-Olaya J, Cingolani F, et al. Dihydroceramide desaturase and dihydrosphingolipids: Debutant players in the sphingolipid arena. Progress in Lipid Research 2012;51:82-94.
57. Kaylor JJ, Yuan Q, Cook J, et al. Identification of DES1 as a vitamin A isomerase in Müller glial cells of the retina. Nat Chem Biol 2013;9:30-36.
58. Beauchamp E, Goenaga D, Le Bloc'h J, Catheline D, Legrand P, Rioux V. Myristic acid increases the activity of dihydroceramide Δ4-desaturase 1 through its N-terminal myristoylation. Biochimie 2007;89:1553-1561.
59. Beauchamp E, Tekpli X, Marteil G, Lagadic-Gossmann D, Legrand P, Rioux V. N-Myristoylation targets dihydroceramide Δ4-desaturase 1 to mitochondria: Partial involvement in the apoptotic effect of myristic acid. Biochimie 2009;91:1411-1419.
60. Schulze H, Michel C, van Echten-Deckert G. [4] Dihydroceramide desaturase. In: Alfred H. Merrill JYAH, ed. Methods in Enzymology: Academic Press, 2000: 22-30.
61. Idkowiak‐Baldys J, Apraiz A, Li L, et al. Dihydroceramide desaturase activity is modulated by oxidative stress. Biochemical Journal 2010;427:265-274.
62. Signorelli P, Munoz-Olaya JM, Gagliostro V, Casas J, Ghidoni R, Fabriàs G. Dihydroceramide intracellular increase in response to resveratrol treatment mediates autophagy in gastric cancer cells. Cancer Letters 2009;282:238-243.
63. Devlin CM, Lahm T, Hubbard WC, et al. Dihydroceramide-based Response to Hypoxia. Journal of Biological Chemistry 2011;286:38069-38078.
64. Spassieva SD, Rahmaniyan M, Bielawski J, Clarke CJ, Kraveka JM, Obeid LM. Cell density-dependent reduction of dihydroceramide desaturase activity in neuroblastoma cells. Journal of Lipid Research 2012;53:918-928.
65. Eliot AC, Kirsch JF. PYRIDOXAL PHOSPHATE ENZYMES: Mechanistic, Structural, and Evolutionary Considerations. Annual Review of Biochemistry 2004;73:383-415.

66. Kerbarh O, Campopiano DJ, Baxter RL. Mechanism of [small alpha]-oxoamine synthases: identification of the intermediate Claisen product in the 8-amino-7-oxononanoate synthase reaction. Chemical Communications 2006;0:60-62.
67. Alexeev D, Alexeeva M, Baxter RL, Campopiano DJ, Webster SP, Sawyer L. The crystal structure of 8-amino-7-oxononanoate synthase: a bacterial PLP-dependent, acyl-CoA-condensing enzyme. Journal of Molecular Biology 1998;284:401-419.
68. Webster SP, Campopiano DJ, Alexeev D, et al. Characterisation of 8-amino-7-oxononanoate synthase. a bacterial PLP-dependent, acyl CoA condensing enzyme 1998;26:S268.
69. Hunter GA, Ferreira GC. 5-aminolevulinate synthase: catalysis of the first step of heme biosynthesis. Cellular and molecular biology (Noisy-le-Grand, France) 2009;55:102-110.
70. Schmidt A, Sivaraman J, Li Y, et al. Three-Dimensional Structure of 2-Amino-3-ketobutyrate CoA Ligase from Escherichia coli Complexed with a PLP−Substrate Intermediate: Inferred Reaction Mechanism. Biochemistry 2001;40:5151-5160.
71. Ikushiro H, Islam MM, Okamoto A, et al. Structural Insights into the Enzymatic Mechanism of Serine Palmitoyltransferase from Sphingobacterium multivorum. Journal of Biochemistry 2009;146:549-562.
72. Yard BA, Carter LG, Johnson KA, et al. The Structure of Serine Palmitoyltransferase; Gateway to Sphingolipid Biosynthesis. Journal of Molecular Biology 2007;370:870-886.
73. Ikushiro H, Islam MM, Tojo H, Hayashi H. Molecular Characterization of Membrane-Associated Soluble Serine Palmitoyltransferases from Sphingobacterium multivorum and Bdellovibrio stolpii. Journal of Bacteriology 2007;189:5749-5761.
74. Bertram Weiss WS. Human and Murine Serine-Palmitoyl-CoA Transferase. European Journal of Biochemistry 1997;249:239-247.
75. Hornemann T, Richard S, Rutti MF, Wei Y, von Eckardstein A. Mammalian serine-palmitoyltransferase - cloning and initial characterisation of a new subunit. J Biol Chem 2006:M608066200.
76. Hornemann T, Richard S, Rütti MF, Wei Y, von Eckardstein A. Cloning and Initial Characterization of a New Subunit for Mammalian Serine-palmitoyltransferase. Journal of Biological Chemistry 2006;281:37275-37281.
77. Hornemann T, Wei Y, von eckardstein A. Is the mammalian serine palmitoyltransferase a high-molecular-mass complex? Biochem J 2007;405:157-164.
78. Maula T, Artetxe I, Grandell P-M, Slotte JP. Importance of the Sphingoid Base Length for the Membrane Properties of Ceramides. Biophysical Journal 2012;103:1870-1879.
79. Fyrst H, Herr DR, Harris GL, Saba JD. Characterization of free endogenous C14 and C16 sphingoid bases from Drosophila melanogaster. Journal of Lipid Research 2004;45:54-62.
80. Quehenberger O, Armando AM, Brown AH, et al. Lipidomics reveals a remarkable diversity of lipids in human plasma. Journal of Lipid Research 2010;51:3299-3305.
81. Wei J. Study of Serine Palmitoyltransferase and de novo synthesis of sphingolipids: Georgia Institute of Technology
2009.
82. Hjelmqvist L, Tuson M, Marfany G, Herrero E, Balcells S, Gonzalez-Duarte R. ORMDL proteins are a conserved new family of endoplasmic reticulum membrane proteins. Genome Biology 2002;3:research0027.0021 - research0027.0016.
83. Roelants FM, Breslow DK, Muir A, Weissman JS, Thorner J. Protein kinase Ypk1 phosphorylates regulatory proteins Orm1 and Orm2 to control sphingolipid homeostasis in Saccharomyces cerevisiae. Proceedings of the National Academy of Sciences 2011;108:19222-19227.
84. Breslow DK, Collins SR, Bodenmiller B, et al. Orm family proteins mediate sphingolipid homeostasis. Nature 2010;463:1048-1053.
85. Han S, Lone MA, Schneiter R, Chang A. Orm1 and Orm2 are conserved endoplasmic reticulum membrane proteins regulating lipid homeostasis and protein quality control. Proceedings of the National Academy of Sciences 2010;107:5851-5856.
86. Sun Y, Miao Y, Yamane Y, et al. Orm protein phosphoregulation mediates transient sphingolipid biosynthesis response to heat stress via the Pkh-Ypk and Cdc55-PP2A pathways. Molecular Biology of the Cell 2012;23:2388-2398.
87. Friant S, Lombardi R, Schmelzle T, Hall MN, Riezman H. Sphingoid base signaling via Pkh kinases is required for endocytosis in yeast. EMBO J 2001;20:6783-6792.
88. Liu M, Huang C, Polu SR, Schneiter R, Chang A. Regulation of sphingolipid synthesis through Orm1 and Orm2 in yeast. Journal of Cell Science 2012;125:2428-2435.
89. Lee Y-J, Huang X, Kropat J, et al. Sphingolipid Signaling Mediates Iron Toxicity. Cell Metabolism 2012;16:90-96.

90. Jin R, Yuan W-X, Xu H-G, Ren W, Zhuang L-L, Zhou G-P. Characterization of a novel isoform of the human ORMDL3 gene. Cell Tissue Res 2011;346:203-208.
91. Siow DL, Wattenberg BW. Mammalian ORMDL Proteins Mediate the Feedback Response in Ceramide Biosynthesis. Journal of Biological Chemistry 2012.
92. Moffatt MF, Kabesch M, Liang L, et al. Genetic variants regulating ORMDL3 expression contribute to the risk of childhood asthma. Nature 2007;448:470-473.
93. Bouzigon E, Corda E, Aschard H, et al. Effect of 17q21 Variants and Smoking Exposure in Early-Onset Asthma. New England Journal of Medicine 2008;359:1985-1994.
94. Galanter J, Choudhry S, Eng C, et al. ORMDL3 Gene Is Associated with Asthma in Three Ethnically Diverse Populations. American Journal of Respiratory and Critical Care Medicine 2008;177:1194-1200.
95. Moffatt MF, Gut IG, Demenais F, et al. A Large-Scale, Consortium-Based Genomewide Association Study of Asthma. New England Journal of Medicine 2010;363:1211-1221.
96. Miller M, Tam AB, Cho JY, et al. ORMDL3 is an inducible lung epithelial gene regulating metalloproteases, chemokines, OAS, and ATF6. Proceedings of the National Academy of Sciences 2012;109:16648-16653.
97. Jin R, Xu H-G, Yuan W-X, et al. Mechanisms elevating ORMDL3 expression in recurrent wheeze patients: Role of Ets-1, p300 and CREB. The International Journal of Biochemistry & Cell Biology 2012;44:1174-1183.
98. Cantero-Recasens G, Fandos C, Rubio-Moscardo F, Valverde MA, Vicente R. The asthma-associated ORMDL3 gene product regulates endoplasmic reticulum-mediated calcium signaling and cellular stress. Human Molecular Genetics 2010;19:111-121.
99. Zhang K, Kaufman RJ. From endoplasmic-reticulum stress to the inflammatory response. Nature 2008;454:455-462.
100. Carreras-Sureda A, Cantero-Recasens G, Rubio-Moscardo F, et al. ORMDL3 modulates store-operated calcium entry and lymphocyte activation. Human Molecular Genetics 2013;22:519-530.
101. Araki W, Takahashi-Sasaki N, Chui D-H, et al. A family of membrane proteins associated with presenilin expression and γ-secretase function. The FASEB Journal 2008;22:819-827.
102. Han G, Gupta SD, Gable K, et al. Identification of small subunits of mammalian serine palmitoyltransferase that confer distinct acyl-CoA substrate specificities. Proceedings of the National Academy of Sciences 2009;106:8186-8191.
103. Gable K, Slife H, Bacikova D, Monaghan E, Dunn TM. Tsc3p Is an 80-Amino Acid Protein Associated with Serine Palmitoyltransferase and Required for Optimal Enzyme Activity. Journal of Biological Chemistry 2000;275:7597-7603.
104. Inuzuka M, Hayakawa M, Ingi T. Serinc, an Activity-regulated Protein Family, Incorporates Serine into Membrane Lipid Synthesis. Journal of Biological Chemistry 2005;280:35776-35783.
105. Suzuki T, Moriya K, Nagatoshi K, et al. Strategy for comprehensive identification of human N-myristoylated proteins using an insect cell-free protein synthesis system. PROTEOMICS 2010;10:1780-1793.
106. Gavin A-C, Bosche M, Krause R, et al. Functional organization of the yeast proteome by systematic analysis of protein complexes. Nature 2002;415:141-147.
107. Giot L, Bader JS, Brouwer C, et al. A Protein Interaction Map of Drosophila melanogaster. Science 2003;302:1727-1736.
108. Tamehiro N, Mujawar Z, Zhou S, et al. Cell Polarity Factor Par3 Binds SPTLC1 and Modulates Monocyte Serine Palmitoyltransferase Activity and Chemotaxis. Journal of Biological Chemistry 2009;284:24881-24890.
109. Tamehiro N, Zhou S, Okuhira K, et al. SPTLC1 Binds ABCA1 To Negatively Regulate Trafficking and Cholesterol Efflux Activity of the Transporter†. Biochemistry 2008;47:6138-6147.
110. Bejaoui K, Wu C, Scheffler MD, et al. SPTLC1 is mutated in hereditary sensory neuropathy, type 1. Nat Genet 2001;27:261-262.
111. Bi H, Gao Y, Yao S, Dong M, Headley AP, Yuan Y. Hereditary sensory and autonomic neuropathy type I in a Chinese family: British C133W mutation exists in the Chinese. Neuropathology 2007;27:429-433.
112. Dawkins JL, Hulme DJ, Brahmbhatt SB, Auer-Grumbach M, Nicholson GA. Mutations in SPTLC1, encoding serine palmitoyltransferase, long chain base subunit-1, cause hereditary sensory neuropathy type I. Nat Genet 2001;27:309-312.
113. Geraldes R, de Carvalho M, Santos-Bento M, Nicholson G. Hereditary sensory neuropathy type 1 in a Portuguese family—electrodiagnostic and autonomic nervous system studies. Journal of the Neurological Sciences 2004;227:35-38.

114. Houlden H, King R, Blake J, et al. Clinical, pathological and genetic characterization of hereditary sensory and autonomic neuropathy type 1 (HSAN I). Brain 2006;129:411-425.
115. Klein CJ, Wu Y, Kruckeberg KE, et al. SPTLC1 and RAB7 mutation analysis in dominantly inherited and idiopathic sensory neuropathies. Journal of Neurology, Neurosurgery & Psychiatry 2005;76:1022-1024.
116. Rotthier A, Auer-Grumbach M, Janssens K, et al. Mutations in the SPTLC2 Subunit of Serine Palmitoyltransferase Cause Hereditary Sensory and Autonomic Neuropathy Type I. The American Journal of Human Genetics 2010;87:513-522.
117. Rotthier A, Baets J, Vriendt ED, et al. Genes for hereditary sensory and autonomic neuropathies: a genotype–phenotype correlation. Brain 2009;132:2699-2711.
118. Verhoeven K, Coen K, De Vriendt E, et al. SPTLC1 mutation in twin sisters with hereditary sensory neuropathy type I. Neurology 2004;62:1001-1002.
119. Rotthier A, Penno A, Rautenstrauss B, et al. Characterization of two mutations in the SPTLC1 subunit of serine palmitoyltransferase associated with hereditary sensory and autonomic neuropathy type I. Human Mutation 2011;32:E2211-E2225.
120. Penno A, Reilly MM, Houlden H, et al. Hereditary Sensory Neuropathy Type 1 Is Caused by the Accumulation of Two Neurotoxic Sphingolipids. Journal of Biological Chemistry 2010;285:11178-11187.
121. Garofalo K, Penno A, Schmidt BP, et al. Oral l-serine supplementation reduces production of neurotoxic deoxysphingolipids in mice and humans with hereditary sensory autonomic neuropathy type 1. The Journal of Clinical Investigation 2011;121:4735-4745.
122. Bertea M, Rutti M, Othman A, et al. Deoxysphingoid bases as plasma markers in Diabetes mellitus. Lipids in Health and Disease 2010;9:84.
123. Othman A, Rütti M, Ernst D, et al. Plasma deoxysphingolipids: a novel class of biomarkers for the metabolic syndrome? Diabetologia 2012;55:421-431.
124. Zitomer NC, Mitchell T, Voss KA, et al. Ceramide Synthase Inhibition by Fumonisin B1 Causes Accumulation of 1-Deoxysphinganine. Journal of Biological Chemistry 2009;284:4786-4795.
125. Huang S, Cheng T-Y, Young DC, et al. Discovery of deoxyceramides and diacylglycerols as CD1b scaffold lipids among diverse groove-blocking lipids of the human CD1 system. Proceedings of the National Academy of Sciences 2011;108:19335-19340.
126. Martinez T, Chen X, Bandyopadhyay S, Merrill A, Tansey M. Ceramide sphingolipid signaling mediates Tumor Necrosis Factor (TNF)-dependent toxicity via caspase signaling in dopaminergic neurons. Molecular Neurodegeneration 2012;7:45.

Chapter 1:

Hereditary sensory and autonomic neuropathy type I (HSAN I) caused by a novel mutation in SPTLC2

S M Murphy*, D Ernst MSc *, Y Wei, M Laurà, Y-T Liu, J Polke, J Blake, J Winer, H Houlden, T Hornemann [#] ,M M Reilly [#]

* joint 1st authors. These authors contributed equally to the manuscript.

[#] joint senior authors

Accepted for publication in Neurology

Author contributions

Sinéad Murphy drafted manuscript, acquired, analysed and interpreted data
Daniela Ernst drafted manuscript, acquired, analysed and interpreted data
Yu Wei acquired, analysed and interpreted data, revised manuscript
Matilde Laura acquired, analysed and interpreted data, revised manuscript
Yo-Tsen Liu acquired, analysed and interpreted data, revised manuscript
James Polke acquired, analysed and interpreted data, revised manuscript
Julian Blake acquired, analysed and interpreted data, revised manuscript
John Winer acquired, analysed and interpreted data, revised manuscript
Henry Houlden acquired, analysed and interpreted data, revised manuscript
Thorsten Hornemann study concept, interpreted data, revised manuscript, supervised study
Mary Reilly study concept, interpreted data, revised manuscript, supervised study

Abstract

Objective:

To describe the clinical and neurophysiological phenotype of a family with hereditary sensory and autonomic neuropathy type I (HSAN I) due to a novel mutation in *SPTLC2* and to characterize the biochemical properties of this mutation.

Methods:

We screened 107 patients with HSAN who were negative for other genetic causes for mutations in *SPTLC2*. The biochemical properties of a new mutation were characterized in cell-free and cell based activity assays.

Results:

A novel mutation (A182P) was found in two subjects of a single family. The phenotype of the two subjects was an ulceromutilating sensory-predominant neuropathy as described previously for patients with HSAN I, but with prominent motor involvement and earlier disease-onset in the first decade of life. Affected patients had elevated levels of plasma dSLs. Biochemically the A182P mutation was associated with a reduced canonical activity but an increased alternative activity with alanine, which results in largely increased dSL levels, supporting their pathogenicity.

Conclusion:

This study confirms that mutations in *SPTLC2* are causing HSAN I and are associated with increased dSL formation.

Introduction

Hereditary sensory and autonomic neuropathy type 1 (HSAN I) is an autosomal dominant (AD) sensory neuropathy complicated by ulcerations and amputations, with variable autonomic and motor involvement[1]. To date, mutations in five genes have been reported to cause AD HSAN I[2-7].

Mutations in the enzyme serine palmitoyltransferase (SPT) cause HSAN I[8, 9]. SPT is a heteromeric enzyme composed of three subunits (SPTLC1-3) located at the outer membrane of the endoplasmic reticulum [10, 11]. It catalyzes the first and rate-limiting step in *de novo* sphingolipid synthesis: the condensation of L-serine and palmitoyl-CoA. Mutations in *SPTLC1* account for 12% of patients with HSAN[12]. More recently, mutations in *SPTLC2* were found to cause HSAN I with a similar phenotype[13]. HSAN I mutations cause a shift in the substrate specificity of SPT leading to the alternative use of L-alanine and L-glycine over its canonical substrate L-serine [14,15]. This forms an atypical category of 1-deoxy-sphingolipids (dSLs) lacking the C1 hydroxyl group which impedes their conversion into complex sphingolipids but also their canonical degradation. Elevated dSLs were found in the plasma and lymphoblasts of HSAN I patients[14] as well as in plasma and tissues of transgenic HSAN I mice[16]. DSLs were shown to be neurotoxic blocking neurite formation in cultured neurons[14].

Here we report a novel HSAN I mutation in *SPTLC2* that is associated with elevated plasma dSLs. Analysing SPT activity in isolated proteins as well as in living cells show that this mutant has reduced canonical activity but forms high levels of dSLs.

Methods

Standard Protocol Approvals, Registrations, and Patient Consents

Ethical approval for this study was obtained from the Joint Medical and Ethics Committee at the National Hospital for Neurology and Neurosurgery (NHNN). Written informed consent was obtained from all patients.

Patients

107 patients with HSAN were selected from our inherited neuropathy database including patients seen in the NHNN peripheral neuropathy clinics as well as patients whose DNA were referred from other hospitals for diagnostic and research testing. Most patients presented with distal progressive sensory loss, with or without ulceromutilating complications or autonomic dysfunction. Because of the overlap between Charcot-Marie-Tooth Type 2B (CMT2B) and HSAN I, we included patients with motor involvement; however, sensory features were predominant. Diagnosis was based on clinical phenotype in addition to neurophysiology. All patients were negative for mutations in *SPTLC1* and most were also negative for mutations in *RAB7*, *NGFB*, *FAM134B* and *NTRK1*. Three hundred and fifty-eight British control chromosomes were screened for control.

Patient assessment

Patients found to have mutations underwent detailed clinical and neurophysiological assessments including the Charcot-Marie-Tooth Neuropathy Score 2 (CMTNS2)[17]. Nerve conduction studies were performed using standard technique.

Genetic sequencing

All 12 exons and flanking introns of *SPTLC2* were amplified using Roche polymerase chain reaction (PCR) reagents. Sequence reactions were performed using Big Dye Terminator v3.1 Cycle Sequencing Kit (Applied Biosystems) and resolved on an ABI 3730xl Sequencer. See Supplemental Figure 1 for primers and primer conditions. Sequence variants were confirmed by repeat sequencing. PolyPhen2 (http://genetics.bwh.harvard.edu/pph/), SIFT (http://blocks.fhcrc.org/sift/SIFT.html) and aGVGD (http://agvgd.iarc.fr/), were used to predict the effect of the mutation on protein function.

Cloning

The A182P was introduced into the SPTLC2 cDNA by site-directed mutagenesis as described earlier[18] using the following primers: SPTLC2_A182P_fw: CAA CTA TCT TGG ATT TCC CCG GAA TAC TGG ATC ATG and SPTLC2_A182P_rv: CAT GAT CCA GTA TTC CGG GGA AAT CCA AGA TAG TTG. All constructs were verified by sequencing.

Stable expression of SPTLC2wt and the A182P mutation in HEK293 cells

HEK293 (ATCC) were stably transfected with the empty vector (control), SPTLC2wt or the A182P mutant as described previously[18]. Expression of the constructs was confirmed by RT-PCR and immune blotting (Supplemental Figure 2).

Immunostaining of stable expressed SPTLC2 variants in HEK293 cells

HEK293 cells transfected with wtSPTLC2 and SPTLC2-A182P were cultured in chamber culture slides (BD Falcon) to 50% confluence and fixed in 4% paraformaldehyde for 15 min at 37°C. Permeabilization was performed for 5min using ice-cold acetone. Cells were washed in double-distilled water and dried for some seconds. Unspecific binding sites were blocked with 1% horse serum in PBS for 30min. After washing in PBS, mouse anti-V5-tag antibody diluted 1:2000 (Serotec) in blocking solution together with rabbit anti-calnexin antibody 1:4000 (Sigma) were incubated for 2 hours. After 2 times washing in PBS, Alexa Fluor 594 conjugated secondary goat anti-mouse antibody (Invitrogen) diluted 1:1000 in blocking solution was incubated together with 30nM DAPI for 1 hour in the dark. Immunofluorescence of the V5 tagged SPTLC2 mutant and wildtype protein, calnexin and nucleinacid were detected with Zeiss Axiovert 200M using AxioVision 4 software.

Metabolic labeling assay

Transfected HEK293 cells were cultured in DMEM for three days before medium was changed to DMEM without L-serine (Genaxxon BioScience). After two hours pre-incubation, isotope labeled (2,3,3-d3, 15N) L-serine (1mM) and (2,3,3,3)-d4 labeled L-alanine (5mM, Cambridge Isotope Laboratories, Inc.) was added to the cells. In some cases, cells were treated with Fumonisin B1 (35uM) as described. Cells were

harvested after 24h, counted (Z2 Coulter Counter, Beckman Coulter) and pelleted (800xg, 5min at 4°C). Pellets were stored at -20°C.

SPT activity assay in isolated proteins and lipid base extraction

Total protein was extracted from frozen HEK293 cell pellets using SPT assay buffer (50mM HEPES pH8, 1mM EDTA, 0.2% Triton-X). 500ug total protein was added to a mix of 160uM palmitoyl-CoA (Sigma), 30uM pyridoxal-5'-phosphate (Sigma) and either 64mM L-serine or 320mM L-alanine (Sigma). The mix was incubated for 45min at 37°C under constant shaking at 800 rpm (Thermomixer comfort, Eppendorf). The *in vitro* SPT reaction was stopped by adding 500ul lipid extraction buffer containing 4 vol MetOH-KOH and 1 vol $CHCl_3$ spiked with 200 pmol isotopic labeled d7-sphinganine and d7-sphingosine (Avanti Polar Lipids) as internal extraction standards. Lipids were base-extracted and analysed as described[18].

Acid-base extraction and analysis of sphingoid bases

500ul MetOH including 200pmol internal standard (d7-sphinganine and d7-sphingosine, Avanti Polar Lipids) were added to 100ul of plasma or frozen cell pellets re-suspended in 100ul PBS. Lipid extraction was performed for 1hour at 37°C with constant agitation at 1000 rpm (Thermomixer comfort, Eppendorf). Precipitated protein was removed by centrifugation (5min at 16000xg). After transferring the supernatant into a new tube, lipids were extracted, acid-base hydrolysed and analyzed by LC-MS as described earlier[14].

Statistics

One-way ANOVA was used for statistical analysis. Significance was verified by Bonferroni multiple-correction. P-values less than 0.001 were considered significant unless otherwise stated (****$p < 0.0001$, ***$p < 0.001$, **$p < 0.01$, *$p < 0.05$). Statistical analysis was performed using GraphPad Prism5.

Results

Genetics

Sequencing of *SPTLC2* in 107 index patients with HSAN I revealed a novel mutation in one family. c.544G>C, A182P, was found in the index case (Figure 1A; III-2); this mutation was not present in 358 control chromosomes. One other affected member of this family who was tested carried the mutation (Figure 1A; IV-2).

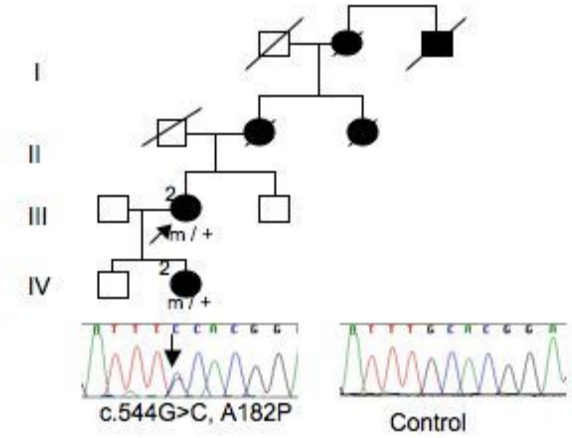

FIGURE 1A**: Pedigree of HSAN I family with A182P-SPTLC2 mutation**
Square = male; circle = female; diagonal line = deceased; filled symbol = affected; m / + = heterozygous for mutation; arrow = proband; electropherogram of affected patient and control

The A182P mutation affects a highly evolutionary conserved amino acid (Figure 1B); PolyPhen2 and SIFT both predict that this change would be damaging, while aGVGD classes the variant as class C25 where C65 is most likely to interfere with function and C0 less likely to interfere with function.

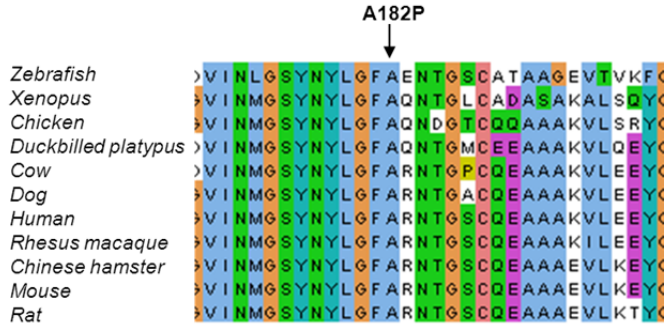

FIGURE 1B: Conservation of A182P in different species

Clinical details

The family had autosomal dominant (AD) inheritance (Figure 1A). Clinical features are documented in Table 1. Both patients had onset in the first decade, presenting with reduced sensation in the feet, with later development of motor weakness. Sensory loss occurred in a glove and stocking distribution; pinprick perception was affected to a greater extent than vibration perception, similar to patients with *SPTLC1* mutations[19]. III-2 had painful tingling in the hands while IV-2 had no history of pain. Sensory complications including ulcers and accidental burns occurred in both patients. In both patients severe wasting and weakness was present (Figure 1C). There were no symptoms of hearing loss or autonomic dysfunction.

FIGURE 1C: **SPTLC2 A182P patients**
Photograph of IV-2 (A, B) and III-2 (C, D) demonstrating marked wasting and weakness in upper and lower limbs

Neurophysiology

Table 2 describes the neurophysiology of the HSAN I patients. Although this was predominantly an axonal neuropathy, motor conduction velocities in the upper limbs were slow (<38 m/s) even in the patient III-2 who had reasonable upper limb motor amplitudes, a finding which we have previously documented in our HSAN I families with *SPTLC1* mutations[19].

Table 1: Clinical details

Patient	**Age last exam**	**Sex**	**AAO**	**Symptoms at onset**	**Positive sensory symptoms**	**Motor UL / LL**	**Sensory**	**Ulcers**	**Amputations**	**Reflexes**	**CMTNS2**
III-2	63	F	10	Numb feet	Painful tingling in hands	Severe distal UL and LL	Vib to knees, pin above wrists and above knees	Burns	No	Brisk UL, absent at ankles	25/36
IV-2	29	F	5	Numb feet	No	Mild proximal and severe distal UL / severe distal LL	Vib to ankle, pin above elbow and above knee	Burns	No	Brisk UL, reduced at ankle	27/36

Table 1: Clinical details

AAO = age at onset; UL = upper limbs; LL = lower limbs; CMTNS2 = Charcot-Marie-Tooth Neuropathy Score version 2 [17] F = female; Vib = vibration;

Table 2: Nerve conduction studies

Patient	**Median**				**Ulnar**				**Radial**	**Common peroneal**			**Sural**
	DML ms	**CV m/s**	**CMAP mV**	**SAP uV**	**DML ms**	**CV m/s**	**CMAP mV**	**SAP uV**	**SAP uV**	**DML ms**	**CV m/s**	**CMAP mV**	**SAP uV**
III-2	3.5	32	4.5	NR	3.9	33	3.1	NR	NR	NR		NR	NR
IV-2	4.1	25	0.2	NR	4.1	29	0.3	NR	NR	5.4	30	0.2	

Table 2: Nerve conduction studies

DML = distal motor latency; CV = conduction velocity; CMAP = compound motor action potential; SAP = sensory action potential; ms = milliseconds; m/s = metres per second; mV = millivolts; uV = microvolts

Plasma sphingoid- and deoxy-sphingoid base levels

Total sphinganine (SA) or sphingosine (SO) base levels showed no difference between SPTLC2-A182P patients and healthy controls, whereas dSL levels were elevated in plasma of the two A182P carriers. Higher dSL plasma levels were found in the more severely affected patient, IV-2 (Figure 3).

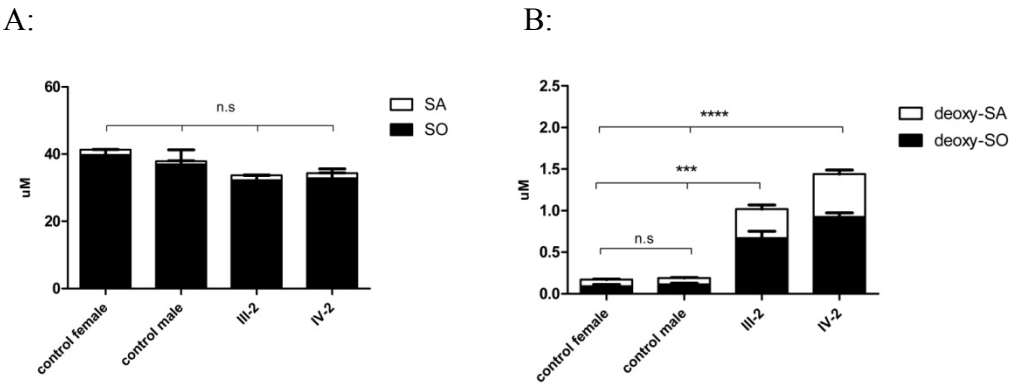

FIGURE 3: **Sphingoid base and deoxy-sphingoid base levels**
Total sphingoid base (**A**) and deoxy-sphingoid base (**B**) levels in plasma of patients and healthy controls. There are significant differences only for deoxy-sphingoid base levels in patients carrying the SPTLC2 A182P mutation ($p < 0.001$ for III-2 and $p < 0.0001$ for IV-2). Data are shown as mean, with error bars representing standard deviations. Error bars and standard deviation were calculated using 1-way ANOVA with Bonferroni's Multiple Comparison Test. SA, sphinganine; SO, sphingosine; 1-deoxySA, 1-deoxy-sphinganine; 1-deoxySO, 1-deoxysphingosine

Effect of the SPTLC2-A182P mutation on SPT activity

Most of the HSAN I mutations in *SPTLC1* and *SPTLC2* are associated with reduced canonical activity in a cell-free environment and increased dSL formation in living cells[8, 9, 13, 20]. The A182P mutant showed a 65% reduced activity with L-serine and a 3.5-fold increased activity with L-alanine when analysed in isolated proteins (Figure 4A-B). These results were confirmed by a metabolic labeling assay in living cells using isotope labeled (d3, N15) L-serine (1mM) and (d4) L-alanine (5mM) which leads to the formation of isotope labeled (M+3)SA and (M+3)deoxySA since one deuterium is lost during the reaction the condensation reaction[21]. This assay was performed in the presence or absence of Fumonisin B1 (FB1), an inhibitor of ceramide synthase (CerS). The inhibition of CerS leads to a significant accumulation of SA over time which is a measure for cellular SPT activity. Upon FB1 treatment, SPTLC2wt cells showed a 2-3 fold higher accumulation of (M+3) SA and (M+3)

deoxySA compared to controls (Figure 4C-D). The formation of (M+3) SA was decreased by 50% in the A182P mutant cells (Figure 4C). Compared to SPTLC2wt cells, (M+3) deoxySA formation was 15-fold higher in A182P cells (Figure 4D). In the absence of FB1 sphingoid bases are mostly metabolized into ceramides and complex sphingolipids which results in a predominant release of (M+3)SO after acid hydrolysis (Figure 4C). In contrast, deoxySLs were predominantly present as (M+3) deoxySA (Figure 4D). In SPTLC2wt cells the total sum of isotope labeled sphingoid bases was 50% higher in FB1 treated than in non-treated cells. In the absence of FB1 the canonical activity was the same in A182P and SPTLC2wt cells (Figure 4C). In the absence of FB1 no isotope labeled dSLs were found in SPTLC2wt cells. In contrast, labeled dSLs were detected in A182P cells although the total levels were about 8-fold lower than under FB1 treatment (Figure 4D). Since FB1 had no effect on SPT activity in isolated proteins (data not shown) we assume that the stimulatory effect of FB1 on SPT activity is indirect and probably associated with a recently described metabolic feedback regulation[22-24].

A: B:

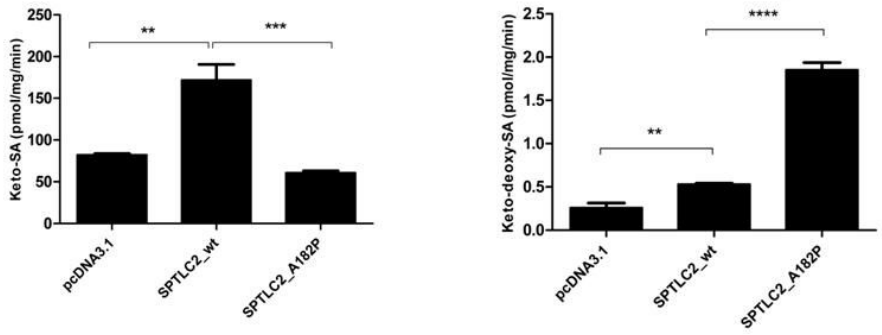

C: D:

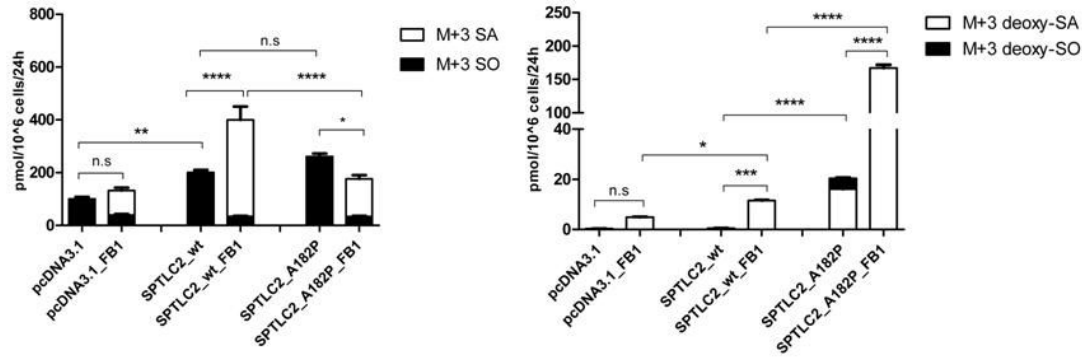

FIGURE 4: **SPT activity in cell-free conditions (A, B) and in intact HEK293 cells (C, D)**

SPT activity in isolated proteins with L-serine (**A**) and L-alanine (**B**) measured in 1mg total protein lysate extracted from HEK293 cells expressing wt or mutant SPTLC2

(**A**) The A182P mutation leads to a significant decrease ($p < 0.001$) in keto-SA compared to the SPTLC2 wt expressing control.

(**B**) The A182P mutation leads to a significant increase ($p < 0.0001$) in keto-deoxySA compared to the SPTLC2 wt expressing control.

(C) Canonical SPT activity measured in HEK293 cells

SPT activity in the SPTLC2 wildtype is increased in the presence of FB1 ($p < 0.0001$), while this FB1-dependant increase is lost in the mutant A182P. Without the usage of FB1, SPT activity is not different in the mutant compared to the wt SPTLC2.

(D) Generation of dSLs in HEK293 cells

The A182P mutation leads to a significant increase ($p < 0.0001$) in dSL species in the presence and absence of FB1compared to the SPTLC2 control. FB1 *per se* leads to generation of dSLs in SPTLC2 wt ($p < 0.001$) and to a large increase in dSLs in the mutant SPTLC2 ($p < 0.0001$).

Data are shown as mean, with error bars representing standard deviations. Error bars and standard deviation were calculated using 1-way ANOVA with Bonferroni's Multiple Comparison Test. Wt wildtype, SA sphinganine, SO sphingosine, deoxy-SA deoxy-sphinganine, deoxy-SO deoxy-sphingosine, dSLs deoxy-sphingolipids, FB1 Fumonisin B1, mg milligram

No differences in the spatial distribution were seen between STPLC2wt and the A182P mutant. Immune-histochemistry showed in both cases a co-localisation with the ER marker calnexin (Figure 5).

SPTLC2 wt:

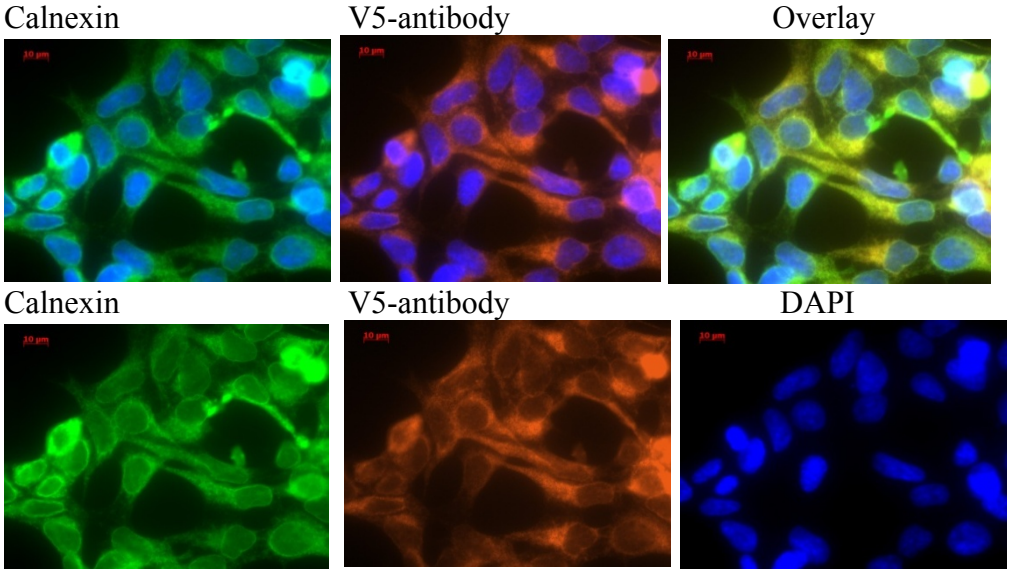

SPTLC2_A182P:

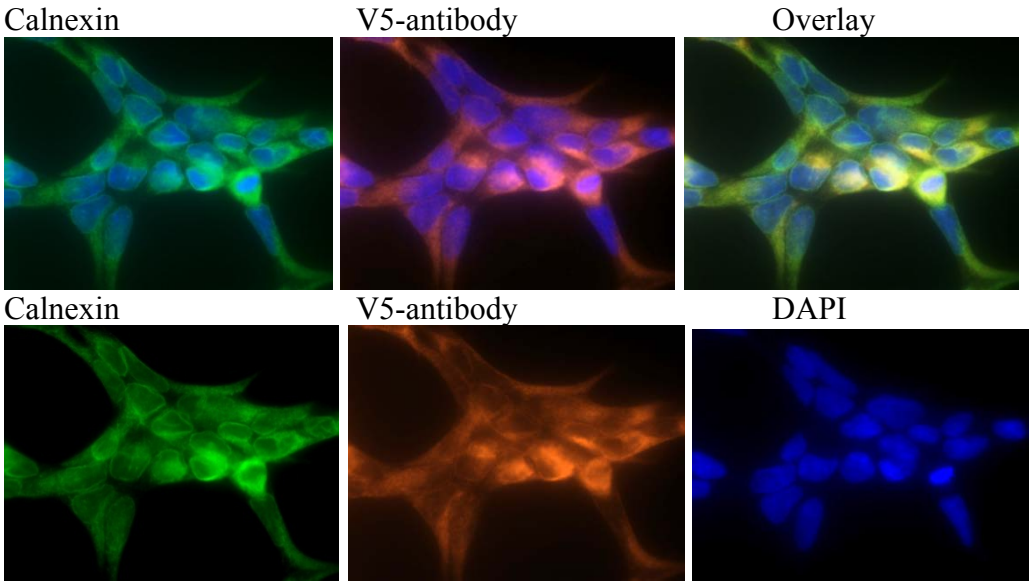

FIGURE 5: **Co-localization of HEK293-SPTLC2 wt and -A182P with ER marker Calnexin**

Localization of transfected wt (SPTLC2) and mutant-SPTLC2 (A182P) in HEK293 cells revealed co-localization of both variants with the ER marker calnexin (blue DAPI; green calnexin; red SPTLC2 variants.

Discussion

Mutations in *SPTLC1* are a well-established cause of HSAN I[8, 9, 19]. An initial study of 12 families with HSAN I did not find any patients with mutations in *SPTLC2*[25]. However, because of the known association of SPT with HSAN I, *SPTLC2* remained a functional candidate and a later study established that mutations in *SPTLC2* were also associated with HSAN I[13]. Our study provides genetic and functional data demonstrating that a novel A182P mutation found in one family is pathogenic, and gives detailed clinical and neurophysiological descriptions of the phenotype. The age of onset in this family was in the first decade, younger than is typically seen in HSAN I patients. To date, three HSAN I mutations in SPTLC2 have been described (V359M, G382V and I504F). Of these, one was associated with early onset in the first decade and other atypical features like motor conduction velocities in the demyelinating range, suggesting a wide phenotypic spectrum of HSAN I. Elevated blood dSL levels were confirmed in both A182P carriers with higher levels being found in the more severely affected daughter than the mother. The A182P mutant showed a significantly reduced activity with L-serine and increased activity with L-alanine when analysed in isolated proteins. This was confirmed by two metabolic labelling assays in living cells. The combined genetic, clinical and functional data confirm the association of this novel *SPTLC2* mutation with HSAN I. It further supports the concept that a pathological dSL formation underlies the pathogenesis of HSAN I indicating that HSAN I, in contrast to most other inherited neuropathies, is a metabolic disorder. The dSLs are therefore relevant HSAN I biomarkers to validate the functional consequences of genetic *SPTLC1* and *SPTLC2* variants.

Footnotes

This work was supported by the Gebert Rüf Stiftung.

Supplemental information

SPTLC2 exon	Forward primer	Reverse primer	Primer conditions
1	CCTACAGAGCCTGCCTTG	CGGTGTGGACTGGCGGAG	58 touchdown
2	GGTATAATTCAGCAAATCTC	TTTAACTGCATCTGGAATAG	60-50 touchdown
3	TAATGAAATTGCCCTTATAC	AATCATATTGTATCCTCAGC	60-50 touchdown
4	ATAGACTTTGTTCTCTCTGC	CTAAATGACATGACAAAGTG	60-50 touchdown
5	TCTGAAAAGGACACAACAC	TTTAGCTCACTCTGACTGC	51.3
6	AGCTATTAGTGTTTGTGGC	TCATTTATACTTTCAAGTGC	60-50 touchdown
7	TATCTGAGGCATGGTTTC	TAGACTAATGTTCCCTTCAG	65-55 touchdown
8	ATAATAATGAAGTGCCAAAC	GTATTATGAGCCTAAACCAG	60-50 touchdown
9	TCTAGAACTTAGAAGGAAAGG	TGCCTATTAGTAAACCTGAC	60-50 touchdown
10	GATAGAATGGAGATAGAGGAG	TAAGGACAAGACCATTTTC	60-50 touchdown
11	TTGAAATCTTTGAGGACAG	GCTCACAAGAACATCAAG	60-50 touchdown
12	GCACTAGACATAAGTCCTGC	ACAGAAGTGTGGTTCCTG	60-50 touchdown

SUPPLEMENTAL FIGURE 1: **Primer for sequencing**
PCR comprised the following steps for all exons except exons 1 and 5: 1) 95°C for 15 minutes, 2) 25 cycles of 95°C for 30 seconds, 60°C (reduced by 0.4°C per cycle) for 30 seconds, and 72°C for 45 seconds, 3) 13 cycles of 95°C for 30 seconds, 50°C for 30 seconds, and 72°C for 45 seconds, 4) 72°C for 10 minutes.
For exon 1: 1) 95°C for 15 minutes, 2) 38 cycles of 95°C for 30 seconds, 58°C (reduced by 0.4°C per cycle) for 30 seconds, and 72°C for 45 seconds, 3) 72°C for 10 minutes. 10% DMSO
For exon 5: 1) 95°C for 15 minutes, 2) 37 cycles of 95°C for 30 seconds, 51.3°C (reduced by 0.4°C per cycle) for 30 seconds, and 72°C for 45 seconds, 3) 72°C for 10 minutes.

A: B:

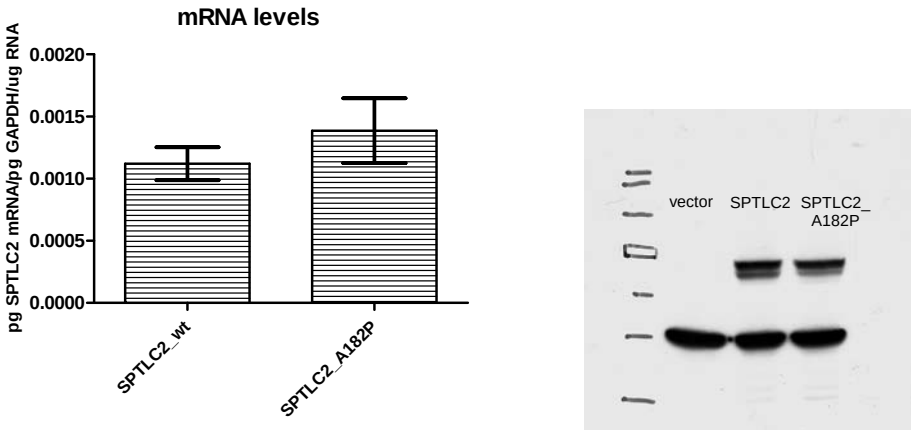

SUPPLEMENTAL FIGURE 2: **mRNA and protein expression in wt and mutant SPTLC2 transfected HEK293 cells**
mRNA **(A)** and protein **(B)** expression levels are not different in the expressed SPTLC2 wildtype and mutant in HEK293 cells
SPTLC2 protein 62.9kDa, and beta-actin 41.7kDa (loading control) detected with V5/His-antibody 1:200

References

1. Houlden H, Blake J, Reilly MM. Hereditary sensory neuropathies. Current Opinion in Neurology 2004;17:569-577.
2. Bejaoui K, Wu C, Scheffler MD, et al. SPTLC1 is mutated in hereditary sensory neuropathy, type 1. Nat Genet 2001;27:261-262.
3. Dawkins JL, Hulme DJ, Brahmbhatt SB, Auer-Grumbach M, Nicholson GA. Mutations in SPTLC1, encoding serine palmitoyltransferase, long chain base subunit-1, cause hereditary sensory neuropathy type I. Nat Genet 2001;27:309-312.
4. Rotthier A, Auer-Grumbach M, Janssens K, et al. Mutations in the SPTLC2 Subunit of Serine Palmitoyltransferase Cause Hereditary Sensory and Autonomic Neuropathy Type I. The American Journal of Human Genetics 2010;87:513-522.
5. Verhoeven K, De Jonghe P, Coen K, et al. Mutations in the Small GTP-ase Late Endosomal Protein RAB7 Cause Charcot-Marie-Tooth Type 2B Neuropathy. The American Journal of Human Genetics 2003;72:722-727.
6. Guelly C, Zhu P-P, Leonardis L, et al. Targeted High-Throughput Sequencing Identifies Mutations in atlastin-1 as a Cause of Hereditary Sensory Neuropathy Type I. The American Journal of Human Genetics 2011;88:99-105.
7. Klein CJ, Botuyan M-V, Wu Y, et al. Mutations in DNMT1 cause hereditary sensory neuropathy with dementia and hearing loss. Nat Genet 2011;43:595-600.
8. Dawkins JL, Hulme DJ, Brahmbhatt SB, Auer-Grumbach M, Nicholson GA. Mutations in SPTLC1, encoding serine palmitoyltransferase, long chain base subunit-1, cause hereditary sensory neuropathy type I. Nat Genet 2001;27:309-312.
9. Bejaoui K, Wu C, Scheffler MD, et al. SPTLC1 is mutated in hereditary sensory neuropathy, type 1. Nat Genet 2001;27:261-262.
10. Hanada K. Serine palmitoyltransferase, a key enzyme of sphingolipid metabolism. Biochimica et Biophysica Acta 2003;1632:16-30.
11. Hornemann T, Richard S, Rutti MF, Wei Y, von Eckardstein A. Cloning and initial characterisation of a new subunit for mammalian serine-palmitoyltransferase. J Biol Chem 2006;281:37275-37281.
12. Davidson GL, Murphy SM, Polke JM, et al. **Frequency of mutations in the genes associated with hereditary sensory and autonomic neuropathy in a UK cohort** J Neurol 2012;259:1673-1685.
13. Rotthier A, Auer-Grumbach M, Janssens K, et al. Mutations in the SPTLC2 subunit of serine palmitoyltransferase cause hereditary sensory and autonomic neuropathy type I. Am J Hum Genet 2010;87:513-522.
14. Penno A, Reilly MM, Houlden H, et al. Hereditary sensory neuropathy type 1 is caused by the accumulation of two neurotoxic sphingolipids. J Biol Chem 2010;285:11178-11187.
15. Zitomer NC, Mitchell T, Voss KA, et al. Ceramide synthase inhibition by fumosin B1 causes accumulation of 1-deoxysphinanine: a novel category of bioactive 1-deoxydeo bases and 1-deoxydihydroceramides biosynthesizes by mammalian cell lines and animals. J Biol Chem 2009;284:4786-4795.
16. Eichler FS, Hornemann T, McCampbell A, et al. Overexpression of the wild-type SPT1 subunit lowers deoxysphingolipid levels and rescues the phenotype of HSAN1. The Journal of Neuroscience 2009;29:14646-14651.
17. Murphy SM, Hermann DN, McDermott MP, et al. Reliability of the CMT neuropathy score (second version) in Charcot-Marie-Tooth disease. J Peripher Nerv Syst 2011;16:191-198.
18. Penno A, Reilly MM, Houlden H, et al. Hereditary Sensory Neuropathy Type 1 Is Caused by the Accumulation of Two Neurotoxic Sphingolipids. Journal of Biological Chemistry 2010;285:11178-11187.
19. Houlden H, King R, Blake J, et al. Clinical, pathological and genetic characterization of hereditary sensory and autonomic neuropathy type 1 (HSAN I). Brain 2006;129:411-425.
20. Verhoeven K, Coen K, De Vriendt E, et al. SPTLC1 mutation in twin sisters with hereditary sensory neuropathy type I. Neurology 2004;62:1001-1002.
21. Ikushiro H, Fujii S, Shiraiwa Y, Hayashi H. Acceleration of the substrate Calpha deproteination by an analogue of the second substrate palmitoyl-CoA in serine palmitoyltransferase. J Biol Chem 2008;283:7542-7553.
22. Breslow DK, Collins SR, Bodenmiller B, et al. Orm family proteins mediate sphingolipid homeostasis. Nature 2010;463:1048-1053.
23. Han S, Lone MA, Schneiter R, Chang A. Orm1 and Orm2 are conserved endoplasmic reticulum membrane proteins regulating lipid homeostasis and protein quality control. Proceedings of the National Academy of Sciences 2010;107:5851-5856.
24. Siow DL, Wattenberg BW. Mammalian ORMDL Proteins Mediate the Feedback Response in Ceramide Biosynthesis. Journal of Biological Chemistry 2012.

25. Dawkins JL, Brahmbhatt SB, Auer-Grumbach M, et al. Exclusion of serine palmitoyltransferase long chain base subunit 2 (SPTLC2) as a common cause for hereditary sensory neuropathy. Neuromuscul Disord 2002;12:656-658.

Chapter 2:

Novel HSAN I mutation in Serine Palmitoyltransferase resides at a putative SPTLC2 phosphorylation site that is involved in regulating amino acid substrate specificity

Daniela Ernst* and Sinéad M Murphy*, Karthik Sathiyanadan, Yu Wei, Alaa Othman, Ramona Papa, Matilde Laura, Yo-Tsen Liu, Julian Blake, Michael Donaghy, John Winer, Henry Houlden, Arnold von Eckardstein, Mary M Reilly[#] and Thorsten Hornemann[#]

* joint 1st authors. These authors contributed equally to the manuscript.
[#] joint senior authors

In submission process

Contributions

Daniela Ernst performed the experiments and wrote the manuscript
Sinéad M Murphy examined the S384F patients, provided their plasma, did the neurological and clinical tests and wrote the manuscript
Karthik Sathiyanadan and Yu Wei cloned the phospho-mutants
Alaa Othman developed the LC-MS ceramide method and assisted with the SPT modeling
Ramona Papa performed the 2D-gel experiments of HEK cells expressing the phospho-mutants
Matilde Laura, Yo-Tsen Liu, Julian Blake, Michael Donaghy, John Winer and Henry Houlden help with the patients examination
Arnold von Eckardstein supervised the work and reviewed the manuscript
Mary M Reilly and Thorsten Hornemann initiated the collaboration, supervised the work and revised the manuscript

Capsule

Background: The inherited neuropathy HSAN I is associated with increased formation of 1-deoxy-sphingolipids. No mechanistic details are known that lead to their generation.

Results: We report a novel HSAN I-causing mutation (SPTLC2-S384F) at the same position as a putative phosphorylation site.

Conclusion: S384 is a regulatory site in SPTLC2 that influences amino acid substrate-specificity of SPT

Significance: The regulation of 1-deoxy-sphingolipid formation is essential for understanding their physiological meaning**.**

Summary

1-Deoxy-sphingolipids (dSLs) are atypical sphingolipids which are formed by the enzyme serine palmitoyltransferase (SPT) due to a promiscuous use of L-alanine over its canonical substrate L-serine. Several missense mutations in SPT cause the rare, inherited sensory neuropathy HSAN I and are associated with pathologically increased dSL levels. Metabolic diseases like the metabolic syndrome and diabetes are also associated with an increased 1-dSL formation. The mechanism underlying the switch in substrate specificity for the wt SPT is not understood. In a comprehensive screen for new HSAN I mutations we identified a novel SPTLC2-S384F variant in two unrelated HSAN I families. Plasma samples from the index patients showed increased dSL levels and ectopic expression of the S384F mutant in HEK293 cells resulted in increased dSL generation. Two phosphorylation sites in the SPTLC2 subunit (S384 and Y387) were reported previously from an unbiased phospho-proteome screen. Both sites are located in close vicinity to the active site of the enzyme and might thereby be involved in regulating SPT activity and substrate specificity. A phosphorylation of SPTLC2 was confirmed by isoelectric focusing. We therefore tested the role of these two sites by creating a set of mutants which mimicked either a constitutively phosphorylated (S384D, S384E) or unphosphorylated (S384A, Y387F, Y387F+S384A) SPTLC2 subunit. Only the S384D but not the homologue S384E nor the negative mutants were associated with increased dSL formation. Our data suggest that phosphorylation at S384 could act as a molecular switch shifting SPT activity from metabolizing L-serine to L-alanine.

Chapter 2

Introduction

Serine palmitoyltransferase (SPT) catalyzes the condensation of L-serine and palmitoyl-CoA which is the first and rate limiting step of ceramide *de novo* synthesis [1, 2]. Under certain conditions the enzyme shows a switch in substrate specificity and uses also L-alanine as an alternative substrate. This reaction leads to the formation of an atypical class of 1-deoxy-sphingolipids (dSLs) which lack the C1 hydroxyl group of regular sphingoid bases[3, 4]. These atypical 1-deoxy-sphingoid bases are metabolized to 1-deoxy-(dihydro)-ceramides[4] but cannot be converted to higher substituted sphingolipids due to the missing hydroxyl group. Accordingly, they are not degraded by the canonical sphingolipid catabolism which involves the phosphorylation at C1 to form sphingosine-1-phosphate as a catabolic intermediate (Supplemental Figure 1).

Several point mutations in *SPTLC1* and *SPTLC2* cause the rare inherited sensory neuropathy HSAN I (Hereditary Sensory and Autonomic Neuropathy type I)[5-12]. All confirmed HSAN I mutations in SPT revealed a reduced canonical activity with L-serine in isolated proteins and a significantly increased activity with L-alanine in intact cells[3, 12]. Elevated dSL levels are found in plasma and peripheral nerve tissue (PNS) from transgenic HSAN I mice[13] and in the plasma of patients[3, 12] and are therefore considered to be a biochemical hallmark for HSAN I. Moreover, patients with a deregulated carbohydrate metabolism like the metabolic syndrome and diabetes[14-16] exhibit elevated dSL plasma levels, even though there are no underlying mutations in SPT. This shows that not only the mutant, but also the wildtype SPT is capable to form dSL under certain conditions. Moreover, the presence of Fumonisin B1 (FB1) - an inhibitor of the downstream ceramide synthase (CerS) - significantly increases in dSL formation by SPT[4]. Whether dSLs have a physiological role in lipid metabolism is not clear yet. Deoxy-ceramides were found as scaffold lipids facilitating lipid antigen presentation and suggesting a role in the innate immunity[17]. In a recent report, dSLs were demonstrated to accumulate together with ceramides upon TNFa stimulation[18]. However, the wt SPT forms dSLs only under certain conditions which argues for a regulatory mechanism allowing SPT to shift between L-serine and L-alanine utilization.

A recent unbiased global proteomic approach revealed the presence of two phosphorylation sites (S384 and Y387) in the SPTLC2 subunit of SPT[19]. Both sites are in close proximity to the PLP binding motive (K379) and therefore good candidates to be involved in the regulation of SPT activity and substrate specificity. Here, we investigate whether a phosphorylation of S384 could act as a regulatory switch to shift substrate specificity of SPT between L-serine and its alternative substrate L-alanine.

Chapter 2

Experimental Procedures

Ethical approval for this study was obtained from the Joint Medical and Ethics Committee at the National Hospital for Neurology and Neurosurgery (NHNN). Written informed consent was obtained from all patients.

Patients

One hundred and seven patients with HSAN were selected from our inherited neuropathy database. The database includes patients seen in the peripheral neuropathy clinics in NHNN as well as patients whose DNA were referred from other hospitals for diagnostic and research testing. All patients selected had a clinical diagnosis of HSAN, presenting with progressive distal sensory loss, with or without ulceromutilating complications or autonomic dysfunction. Because of the overlap between Charcot-Marie-Tooth Type 2B (CMT2B) and HSAN I, patients with motor involvement were included however, sensory features were always predominant. Diagnosis was based on clinical phenotype in addition to neurophysiology. All patients were negative for mutations in *SPTLC1* and most were also negative for mutations in *RAB7*, *NGFB*, *FAM134B* and *NTRK1*. Four hundred and seventy-eight British control chromosomes were screened for the S384F mutation.

Patient assessment

All patients found to have mutations were seen and had detailed clinical and neurophysiological assessments performed, including assessment of neuropathy severity using the Charcot-Marie-Tooth Neuropathy Score 2 (CMTNS2)[20]. Nerve conduction studies were performed using standard techniques.

Genetic sequencing

All 12 exons and flanking introns of *SPTLC2* were amplified using Roche polymerase chain reaction (PCR) reagents. Sequence reactions were performed using Big Dye Terminator v3.1 Cycle Sequencing Kit (Applied Biosystems) and resolved on an ABI 3730xl Sequencer. See Supplementary Table 1 for primers and primer conditions. Sequence variants were confirmed by repeat sequencing. Three commonly used prediction programmes, PolyPhen2 (http://genetics.bwh.harvard.edu/pph/), SIFT (http://blocks.fhcrc.org/sift/SIFT.html) and aGVGD (http://agvgd.iarc.fr/), were used to predict the effect of the mutations on protein function.

Cloning

SPTLC2 cDNA was amplified by PCR from a cDNA library and cloned into a mammalian pcDNA 3.1D/V5-His-TOPO expression vector. The *SPTLC2* mutations S384D, S384E, S384A, S384F, S384A+Y387F, Y387F and G382V were introduced by site-directed mutagenesis (primer sequences Supplementary Figure 2A). All constructs were verified by sequencing.

Stable expression of mutant and wildtype SPTLC2 in HEK293 cells

HEK293 cells (ATCC) were cultured in DMEM (Sigma-Aldrich) with 10% fetal calf serum (FisherScientific FSA15-043) and penicillin/streptomycin (100 U/ml and 0.1 mg/ml, respectively, Sigma-Aldrich). Stable transfection was performed using TurboFect (Thermo Scientific) under selection of 400µg/ml Geneticin (Gibco, Invitrogen). Expression of the constructs was confirmed by RT-PCR and immune blotting.

2D-PAGE analysis

Total proteins of CHO cells (grown for three days in Ham-F12 supplemented with 10% FCS) were extracted either in the presence or absence of a phosphatase-inhibitor cocktail (Roche). The aliquot without phosphatase inhibitor was treated with alkaline phosphatase (FastAP, Thermo Scientific) for 30min at 37°C. 1mg of total protein each was mixed with DeStreak™ Rehydration Solution (Amersham Biosciences) to a final volume of 100ul and loaded on a Immobiline™ DryStrip (GE Healthcare), together with 0.5% IPG buffer (Amersham Biosciences) by passive rehydration over-night. Strip and buffer covered a pH ranged from pH 6-11. Iso-electric focusing was carried out on an Ettan IPGphor (Amersham Biosciences) according to following conditions: Step1: 300V, 200kVh; step 2: 1000V, 300kVh; step 3: 5000V, 4500kVh; step 4: 5000V, 2000kVh; step 5: 500V, hold. All steps were performed at 20°C, for 3hours with a maximal current of 50uA per strip. Focused proteins were subsequently equilibrated stepwise in 65mM DTT and 135mM iodacetamide (both in 1M Tris, 6M Urea, 30% v/v glycerol, 2% w/v SDS, 0.01% v/v bromphenolblue) with intermediate washing. Proteins were separated in the second dimension on a 12% SDS-PAGE, followed by western-blotting (PVDF membrane) and immunostaining using a polyclonal SPTLC2 antibody [2] in 1:3000 dilution in 4% milk powder.

Cell-based SPT activity assay

200 000 HEK293 cells stably transfected with the empty vector (control), SPTLC2wt and SPTLC2-mutants (S384D, S384E, S384F, S384A, S384A+Y387F, Y387F) were seeded and cultured as described above. After 3 days, the conditioned medium was exchanged with L-serine and L-alanine deficient DMEM (Genaxxon BioScience). After a pre-incubation of two hours in this medium, isotope labeled (2,3,3)-d3 L-serine (1mM) together with 5mM (2,3,3,3)-d4 labeled L-alanine (Cambridge Isotope Laboratories, Inc.) were added to the cells (in some experiments ($3C_{13}$)-labeled L-alanine was used instead as stated in the text). After 24h or 48h (as stated in the text), the cells were washed twice with PBS, harvested and counted (Z2 Coulter Counter, Beckman Coulter). Cells were centrifuged (800xg, 5min at 4°C) and pellets were stored at -20°C for lipid extraction and analysis. The isotope labeled sphingoid bases are referred to as m+2 (from d3 L-serine) m+3 (from d4 L-alanine) or m+1 (from $3C_{13}$ L-alanine).

SPT activity assay in isolated proteins and lipid base extraction

Total protein was extracted from frozen HEK293 cell pellets using SPT assay buffer (50mM HEPES pH8, 1mM EDTA, 0.2% Triton-X). 500ug total protein was added to a mix of 160uM palmitoyl-CoA (Sigma), 30uM pyridoxal-5'-phosphate (Sigma) and either 64mM L-serine or 320mM L-alanine (Sigma). The mix was incubated for 45min at 37°C under constant shaking at 800 rpm (Thermomixer comfort, Eppendorf). SPT reaction was stopped by adding 500ul lipid extraction buffer containing 4 vol MetOH-KOH and 1 vol CHCl3 spiked with 200 pmol isotopic labeled d7-sphinganine and d7-sphingosine (Avanti Polar Lipids) as internal extraction standards. Lipids were base-extracted and analyzed on a TSQ Quantum Ultra MS analyzer (Thermo Scientific) as described earlier[3].

Kinetics with L-alanine

400 000 HEK293 cells stable expressing SPTLC2wt or SPTLC2-S384D were cultured as described above. At day two, 0-35mM (2,3,3,3)-d4 labeled L-alanine (Sigma) diluted in PBS was added to the cells without changing the media. Cells were cultured for 48h, washed twice in PBS, harvested and counted (Z2 Coulter Counter, Beckman Coulter). Cells were centrifuged (800xg, 5min at 4°C) and pellets were stored at -20°C until lipid extraction and acid-base extraction.

Acid-base extraction and analysis of sphingoid bases

500 ul MetOH including 200pmol internal standard (d7-sphinganine and d7-sphingosine, Avanti Polar Lipids) were added to 100ul of plasma or frozen cell pellets prior re-suspending in 100ul PBS. Lipid extraction was performed for 1hour at 37°C with constant agitation at 1000 rpm (Thermomixer comfort, Eppendorf). Precipitated protein was removed by centrifugation for 5min at 16000xg and the supernatant was transferred to a new tube. Lipids were acid-hydrolysed (in 4.8% HCL final overnight at 65°C), neutralized by adding 1.5M KOH (final concentration) and were further extracted with chloroform (92.6% v/v) under basic conditions (0.15N NH_4OH). Sphingoid bases were analyzed on a TSQ Quantum Ultra MS analyzer (Thermo Scientific) as described earlier[3] with minor changes (see under analysis of ceramide species).

Extraction and analysis of deoxy-ceramide and normal ceramide species

For the ceramide and deoxy-dihydro-ceramide analysis, total sphingolipid extraction was done as before[3, 21] with some modifications. In brief, cell pellet was re-suspended in 100 µl PBS. To this suspension, 1ml of methanol /chloroform (2:1) was added and spiked with 200 pmol of the internal standard C12 ceramide (d18:1, 12:0). The mix was shaken in a thermo-mixer at 37°C for 1 hour. Then, 0.5 ml of chloroform was added followed by 200 µl of alkaline water (500µl NH_4OH (25%) in 250ml H_2O and 20µl Bromphenol blue (2.5%). The mixture was centrifuged at 16100 *g* for 5 minutes. The upper phase was removed and the lower phase was washed three times with 1 ml alkaline water and dried under N_2. Base hydrolysis using methanolic KOH was performed to remove the phospholipids. To the dried extracted lipids, 0.5 ml of methanolic -KOH: chloroform (4:1) was added and the mix was treated as mentioned in the first extraction step. The dried extracted lipids were stored at -20°C until the LC/MS analysis was performed.

The lipids were re-suspended in 100 µl methanol and then separated on a C_{18} column (Uptispere 120 Å, 5µm, 125 × 2 mm, Interchim, Montluçon, France) with ammonium acetate (5mM) in water and methanol (1:1) as mobile phase A and methanol as the mobile phase B. The isocratic gradient was run as follows (22% mobile phase A, 78% mobile phase B for 20 minutes then mobile phase B 100% for 25 minutes and then 22% mobile phase A, 78% mobile phase B for 5 minutes).

The lipids were detected with an MS detector (TSQ Quantum Ultra, Thermo, Reinach, BL, Switzerland) using atmospheric pressure chemical ionization (APCI) as the ionization source.

Precursor ion scan was performed to identify ceramides with the fragment (m/z 264.3) and deoxy-dihydro-ceramides with (m/z 286.3) at 20mV collision energy. The (M+H)+ parent ions for each ceramide (d18:1,16:0 and d18:1,24:1) and deoxy-dihydro-ceramide (m18:0,16:0 and m18:0,24:1) were quantified by normalizing the area under the peak to the internal standard and the protein concentration. Peak analysis and quantification was done in Xcalibur® (Thermo Scientific, Reinach, BL, Switzerland).

Statistics

One-way ANOVA was used for statistical analysis. Significance was further verified by Bonferroni multiple-correction. P-values less than 0.001 were considered significant unless otherwise stated according to the following definition: ****$p < 0.0001$, ***$p < 0.001$, **$p < 0.01$, *$p < 0.05$. Statistical analysis was performed using GraphPad Prism5.

Results

Report of a novel HSAN I-causing mutation in the SPTLC2 subunit resides at the phospho-site Ser384

In order to find novel SPT mutations associated with HSAN I, we sequenced the *SPTLC2* gene in 107 patients with HSAN I. In two unrelated index cases we identified a novel c.1151C>T (S384F) *SPTLC2* variant. This variant was not present in 478 control chromosomes. Further studies showed that all affected members of these families who were tested also carried the mutation (Figure 1A).

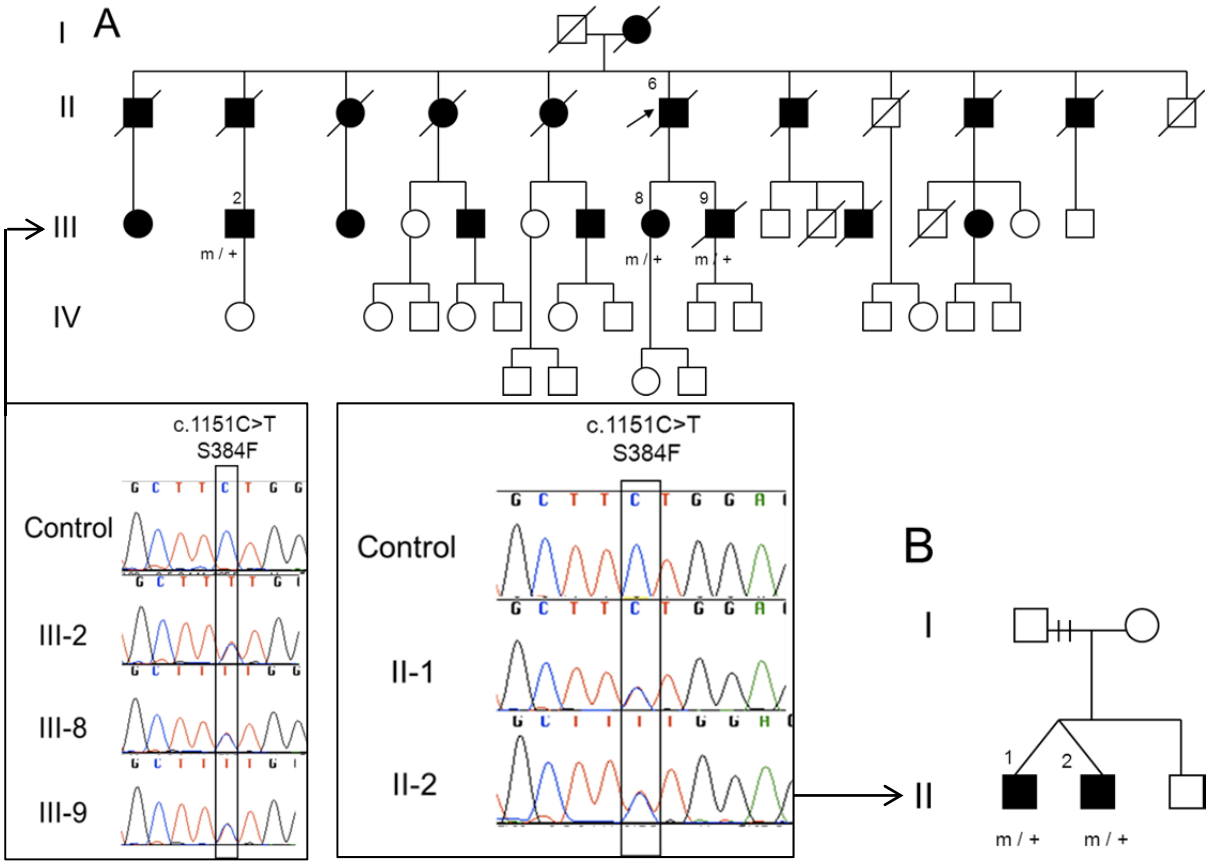

FIGURE 1A: **Pedigree of two HSAN I families with S384F SPTLC2 mutation**
Square = male; circle = female; diagonal line = deceased; filled symbol = affected; m / + = heterozygous for mutation; arrow = proband; electropherogram of affected patients and control. Shown are two families **A** (III-2, III-8 and III-9) and **B** (II-1 and II-2).

The S384 residue is conserved in mammals but replaced by alanine in lower vertebrates (Figure 1B). PolyPhen2 and SIFT both predict that this change would be damaging.

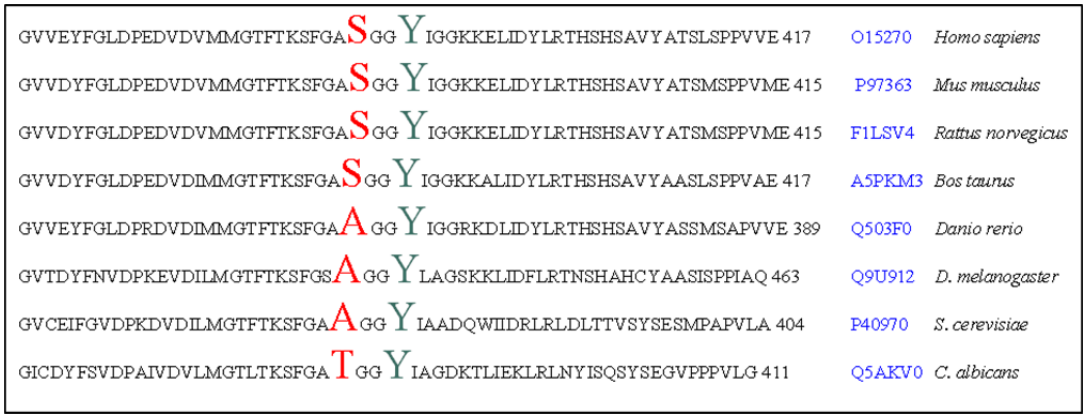

FIGURE 1B: **Conservation of S384 and Y387 among species**
Multiple protein alignment of the SPTLC2 orthologous from human (*Homo sapiens*), mouse (*mus musculus*), rat (*Rattus norwegicus*), taurus (*Bos Taurus*), zebrafish (*Danio rerio*), fly (*Drosophila melanogaster*), baker's yeast (*Saccharomyces cerevisiae*) and *Candida albicans*

Clinical details

The two S384F families could not be genealogically linked. Family A had clear autosomal dominant (AD) inheritance (Figure 1A). Clinical features are documented in Table 1. In comparison to other HSAN I families, patients from the two S384F families had a rather late onset of disease in the fourth or fifth decade. Most patients presented with reduced sensation in the feet with later development of motor weakness. Sensory loss occurred in a glove and stocking distribution; pinprick was affected to a greater extent than vibration perception, similarly to patients with *SPTLC1* mutations [22]. Sensory complications including ulcers and accidental burns occurred in all patients and some individuals had amputations. Motor involvement occurred in all families, though to a variable extent. The disease showed clinical heterogeneity even within families, e.g., III-8 having only mild distal lower limb weakness at 65 years, while her sibling III-9 had significant proximal and distal upper and lower limb weakness and required a wheelchair since 65 years. None of the patients had significant autonomic symptoms.

Family	Age last exam	Sex	AAO	Symptoms at onset	Positive sensory symptoms	Motor UL / LL	Sensory	Ulcers	Amputations	Reflexes	CMTNS2 (CMTES2)
Family A											
III-2	54	M	Mid 30s	Reduced sensation in feet	Shooting pains	N / N	Pin to mid shin	No	No	Preserved	(6/28)
III-8	65	F	Early 40s	Numbness in feet	Shooting pains	N / mild distal weakness	Vib to ankle, Pin to wrist and above knee	Yes	BKA, toes	Absent at ankle	13/36
III-9	71	M	40s	Numbness in feet	Shooting pains	Mild proximal and severe distal UL and LL weakness	Vib to costal margin, pin to face	Yes	No	Absent in LL	35/36
Family B											
II-1	47	M	30s	Pain in feet	Shooting pains	Mild distal UL weakness / N	Vib to ankles, pin to elbows and above knee	Yes	BKA, Toes	Absent at ankles	19/36
II-2	45	M	33	Numb feet	Shooting pains	N / N	Vib to ankles, pin to mid-palm and below knees	Yes	No	Preserved	ND

TABLE 1: **Clinical details of SPTLC2 S384F patients**
AAO = age at onset; UL = upper limbs; LL = lower limbs; CMTNS2 = Charcot-Marie-Tooth Neuropathy Score version 2 [20]; CMTES2 = CMT Examination Score, a subset of the CMTNS2; M = male; F = female; N = normal; ND = not done; Vib = vibration; BKA = below knee amputation

Neurophysiology

Details of the neurophysiology from the S384F patients are shown in Supplemental Table 2. Overall, nerve conduction studies demonstrated a sensorimotor axonal neuropathy. Sensory action potentials were absent in the lower limbs and reduced or absent in the upper limbs. Motor responses were absent or reduced in the lower limbs and normal or reduced amplitude in the upper limbs. Motor conduction velocity ranged from normal (>50 m/s) to within the demyelinating range (<38 m/s) similar to what is seen in our families with *SPTLC1* mutations[23].

Plasma sphingoid- and deoxy-sphingoid base levels

The composition of plasma sphingolipids was analyzed in four S384F patients and compared to plasma from three random HSAN I patients with a C133W mutation and two healthy controls (Figure 2A+B). Total sphingolipid plasma levels were not different for S384F and C133W carriers, compared to healthy controls (Figure 2A). In contrast, total dSL levels (deoxySO+deoxySA) were significantly higher in the plasma of patients with the S384F mutation (Figure 2B). The dSL plasma levels in S384F carriers were comparable to those with the C133W mutation and ranged from 1.5-5uM.

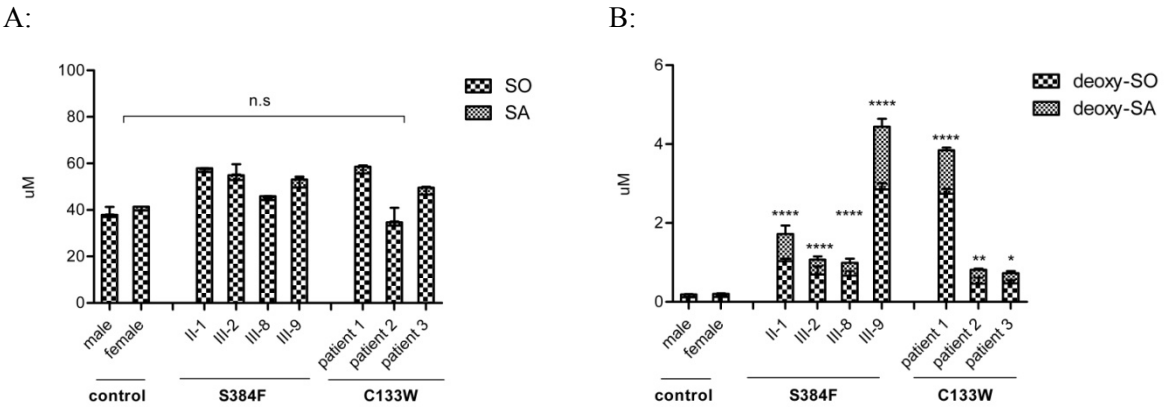

FIGURE 2: **Clinical characterization of the novel HSAN I mutation S384F**
Total lipids from plasma of four S384F and three C133W patients were extracted and total sphingoid- (**A**) and deoxy-sphingoid base (**B**) levels analyzed after acid-base hydrolysis. All carriers of the S384F as well as the C133W mutations had significant elevated deoxy-sphingoid base levels without differences in their normal sphingoid base contents compared to healthy controls. Data are shown as mean, with error bars representing standard deviations. Error bars and standard deviation were calculated using 1-way ANOVA followed by Bonferroni's Multiple Comparison Test with ****p < 0.0001, ***p < 0.001, **p < 0.01, *p < 0.05.

SPTLC2 is phosphorylated *in vivo*

In an unbiased global phospho-proteomic approach Olsen *et al.* found two phosphorylation sites (S384 and Y387) in the SPTLC2 subunit of SPT[19]. A posttranslational modification of SPTLC2 was confirmed by 2D-PAGE and western blot in a CHO cell extract. The isoelectric focusing revealed a typical punctuated migration pattern for SPTLC2 (Figure 3, left panel) which was reduced to a single spot upon treatment with alkaline phosphatase (Figure 3, right panel).

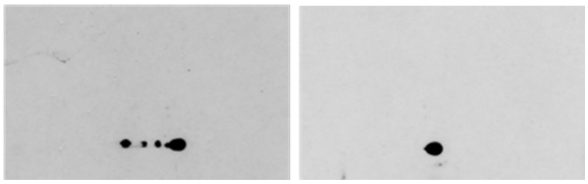

FIGURE 3: **SPTLC2 phosphorylation pattern is lost after phosphatase treatment**
Total proteins of CHO cells (grown for three days in Ham-F12 supplemented with 10% FCS) were extracted in the presence of phosphatase-inhibitors (left panel) or treated with alkaline phosphatase (right panel). The extract was subjected to iso-electrical focusing in the first dimension and separated on a 12% SDS-PAGE in the second dimension. SPTLC2 was detected with a polyclonal antiSPTLC2 antibody.

Effect of a constitutive phosphorylated and un-phosphorylated SPTLC2 on SPT activity

To investigate the influence of the two putative phosphorylation sites S384 and Y387 on SPT activity and substrate specificity we created a set of mutants which either mimicked a constitutively phosphorylated (S384D, S384E) or an un-phosphorylated state of the enzyme (S384A, Y387F, S384A+Y387F). The phosphorylation at Y387 could not be mimicked. The mutant SPTLC2 subunits were stably expressed in HEK293 cells and expression levels were similar for mRNA and protein (Supplemental Figure 2B+C).

HEK cells expressing the wtSPTLC2 subunit also revealed a typical phosphorylation pattern after isoelectric focusing (Supplemental Figure 4A) that is different in the mutants where the two phosphosites were knocked-out (S384A and Y387F, Supplemental Figure 4B+C).

We analyzed the effect of the mutations on SPT activity in transfected HEK293 cells. In isolated proteins the canonical activity of the phosphorylation mimicking mutants (S384D and S384E) was 50-60% reduced, but was not different in the negative mutants S384A, Y387F or S384A+Y387F compared to the wild type (Figure 4A). With L-alanine we observed a 2.5 fold increased activity in the S384D mutant but not for the homologous S384E variant or the negative mutants S384A, Y387F, S384A+Y387F (Figure 4B). These results were compared to a previously reported SPTLC2 HSAN I mutation (G382V)[12] which is located in close proximity to the identified two phospho-sites. In a cell-free environment, the G382V mutant

showed a 70% decreased activity with L-serine (Figure 4A) but no significant activity with L-alanine (Figure 4B) although increased dSL formation was previously found in G282V expressing HEK293 cells and in lymphoblasts of G382V carriers[12]. However, the levels of deoxySA that have been produced in cells during culture, were elevated in both, S384D and G382V expressing cells, but not in SPTLC2wt or S384A, Y387F and S384A+Y387F (Figure 4C). This indicates that SPT shows distinct activities when measured in isolated proteins or living cells.

A:

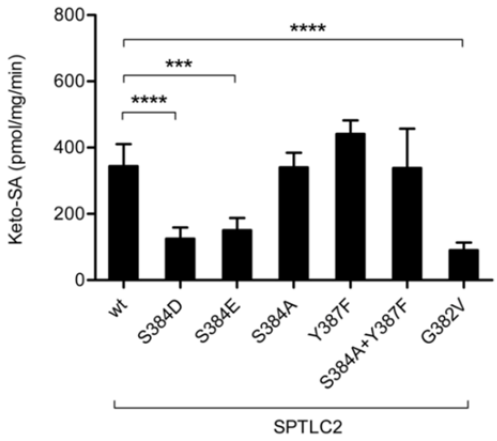

B:

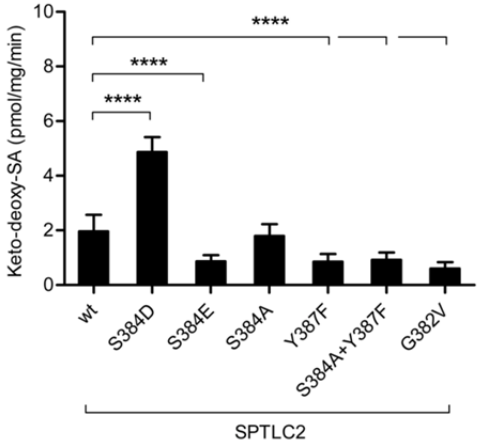

C:

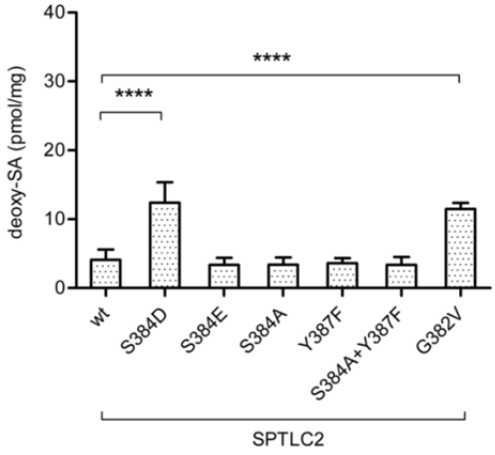

FIGURE 4**: Activity of SPTLC2 phosphomutants in isolated proteins**
SPT Activity was analyzed in isolated proteins extracted from HEK293 cells stably transfected with either wildtype SPTLC2 or the SPTLC2 mutants S384D, S384E, S384A, Y387F, S384A+Y384F and G382V. The activity in cell-free conditions was determined in the presence of **(A)** L-serine or **(B)** L-alanine. **(C)** DeoxySA levels (non-acylated) in cells expressing either SPTLC2wt or the mutants S384D, S384E, S384A, Y387F, S384A+Y384F and G382V. All data are shown as mean, with error bars representing standard deviations. Error bars and standard deviation were calculated using 1-way ANOVA followed by Bonferroni's Multiple Comparison Test with ****$p < 0.0001$, ***$p < 0.001$, **$p < 0.01$, *$p < 0.05$.

We therefore performed a metabolic labeling assay with SPTLC2wt or mutant expressing HEK293 cells to analyze the mutant's activity in intact cells. Cells were cultured in the presence of isotope labeled (d3) L-serine and (d4) L-alanine which resulted in the formation of (m+2) SA and (m+2) SO or (m+3) deoxySA, respectively since one of the deuteriums is lost during the SPT condensation reaction[24]. Like in cell-free conditions, we observed a 2-3 fold higher dSL formation in the S384D cells but not in cells expressing the homolog S384E or the negative mutants (S384A, Y387F and S384A+Y387F) (Figure 5A). Although we observed a reduced activity with L-serine for the S384D and S384E mutant in isolated proteins (Figure 4A) we did not see any reduced formation of (m+2) SO and (m+2) SA in living cells (Figure 5B). Analysis of the lipid species revealed that ceramides were mostly present as d18:1;16:0 and d18:1;24:1 (Figure 5C) whereas deoxy-ceramides were conjugated to the same fatty acids but primarily found in the dihydro-form, m18:0;16:0 and m18:0;24:1 (Figure 5D). S384D expressing cells had significantly higher total deoxy-dihydro-ceramide levels than cells expressing the S384E or the negative mutants (Figure 5D).

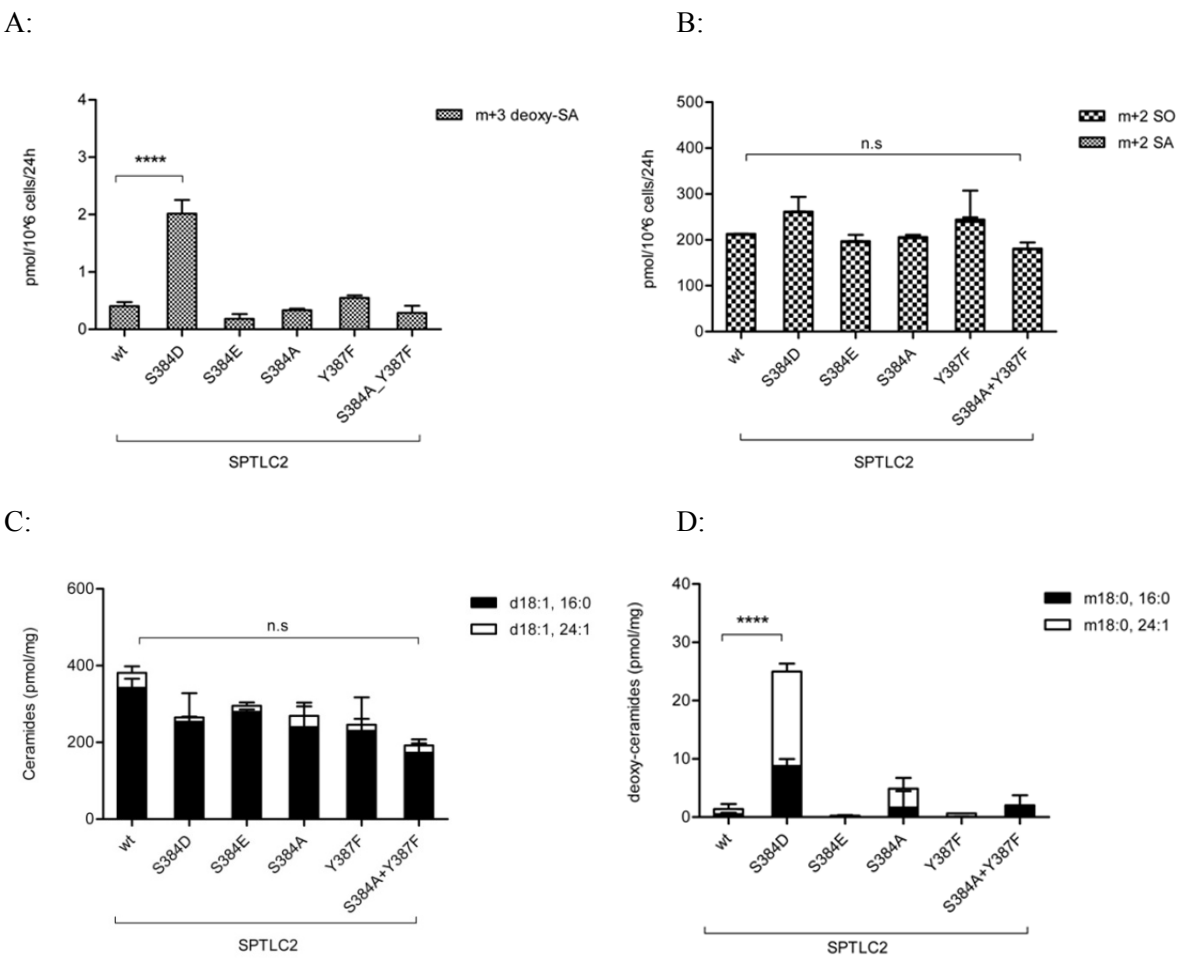

FIGURE 5**: Activity of SPTLC2 phosphomutants in HEK cells**

SPT Activity was analyzed in intact HEK293 cells which were stably transfected with either wildtype SPTLC2 or the SPTLC2 mutants S384D, S384E, S384A, Y387F, S384A+Y384F and G382V.
(A+B) Incorporation of isotope labeled (2,3,3)-d3 L-serine (1mM) and (2,3,3,3)-d4 labeled L-alanine (5mM) within 24h. The extracted lipids were subjected to an acid-base hydrolysis as described in experimental procedure and the free isotope labeled sphingoid bases analyzed LC-MS. The resulting sphingoid bases originating from d3 L-serine and d4 L-alanine are referred to as (m+2) and (m+3) respectively.
(C+D) Total lipids were extracted from SPTLC2wt and mutants expressing cells and ceramide (C) and deoxy-ceramide species (D) analyzed by LC-MS. All data are shown as mean, with error bars representing standard deviations. Error bars and standard deviation were calculated using 1-way ANOVA followed by Bonferroni's Multiple Comparison Test with ****p < 0.0001, ***p < 0.001, **p < 0.01, *p < 0.05.

Increasing concentrations of (d4)-L-alanine in the medium elevated dSL formation only in S384D expressing cells, but not in SPTLC2wt cells (Figure 6). This shows that formation of dSLs in the wt SPT is not directly associated with any increased supply of alanine.

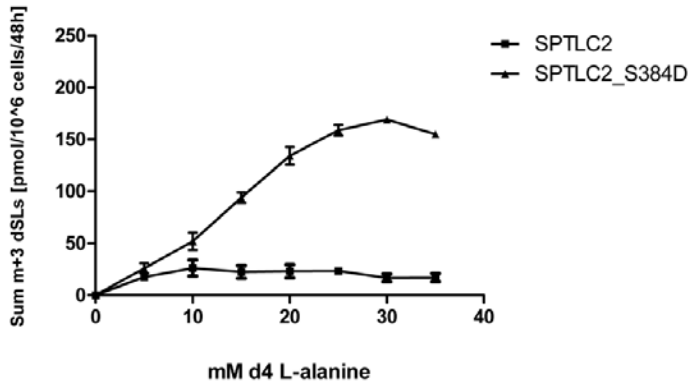

FIGURE 6**: L-alanine kinetics in wt SPTLC2 and phosphorylation mimicking mutant S384D**
Deoxy-sphingolipid formation in response to increasing amounts of d4 L-alanine in the medium of SPTLC2wt and S384D expressing cells. Cells were cultured in the presence of d4 L-alanine (0-35mM) for 48h. After harvesting the cells the total lipids were extracted and the sphingoid base profile analyzed by LC-MS after acid-base hydrolysis. The sphingoid bases were quantified relative to the internal extraction standards (d7 SO and d7 SA). The graph shows the sum of labeled (m+3) deoxySA and (m+3) deoxySO.

Effect of the HSAN I associated SPTLC2-S384F mutation on SPT activity

The HSAN I-causing S384F mutation led to a decreased activity with L-serine and an increased activity with L-alanine in a cell-free environment that was similar to the S384D mutant (Figure 7A). However, the metabolic labeling assay in intact cells did not reveal any reduced formation of (m+2) SO and (m+2) SA (Figure 7B) but a significantly increased dSL formation which was even 2-3 fold higher compared to the S384D mutation (Figure 7C). Like wt SPTLC2 protein, the mutant SPTLC2 variants (S384D, S383E, S384A, Y387F,

S384A+Y387F) co-localized with the ER marker calnexin, rendering it unlikely that mislocation is leading to the observed differences in SPT activity (Supplemental Figure 5).

A:

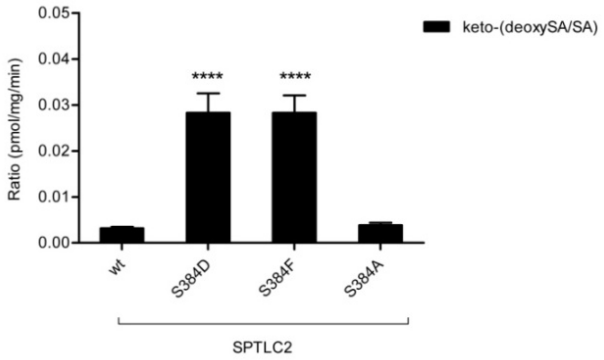

B:

C:

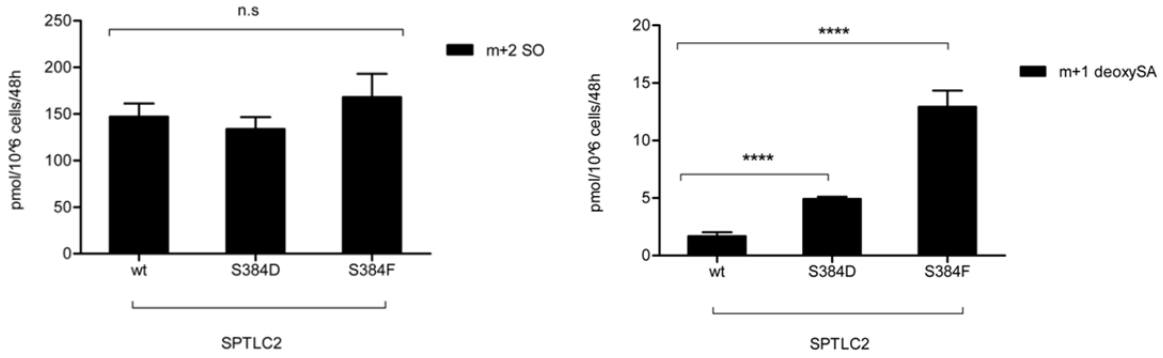

FIGURE 7**: Biochemical characterization of the novel HSAN I mutation**
SPT activity was analyzed in a cell-free environment (A) and in intact HEK293 cells (B+C) which were stably transfected with SPTLC2 (wt), the phosphorylation mimicking S384D or the SPTLC2-HSAN I associated mutation S384F. **(A)** Activity in isolated proteins was determined in the presence of L-serine or L-alanine. S384F and S384D both showed a decrease for L-serine activity and an increase for L-alanine activity. Free sphingoid bases were quantified relative to internal extraction standards (d7SO and d7SA). Shown is the ratio of keto-deoxySA/keto-SA per min.
B+C) Cells were grown in DMEM lacking L-serine, supplemented with isotope labeled (2,3,3)-d3 L-serine (1mM) together with 5mM ($3C_{13}$)- labeled L-alanine and incubated for 48h. Lipids were extracted, acid-base hydrolysed and analyzed using LC-MS. Sphingoid bases were quantified relative to internal extraction standards (d7 SO and d7 SA). The resulting sphingoid bases are referred to m+2 for d3 L-serine and m+1for $3C_{13}$ L-alanine **(B)**. m+2 sphingoid base levels were not different in the analyzed mutants compared to the wt **(C)**.
Data are shown as mean, with error bars representing standard deviations. Error bars and standard deviation were calculated using 1-way ANOVA followed by Bonferroni's Multiple Comparison Test with ****$p < 0.0001$, ***$p < 0.001$, **$p < 0.01$, *$p < 0.05$.

Discussion

Elevated dSL levels are a hallmark for the inherited neuropathy HSAN I[5-12] which is caused by several mutations in SPT. Low levels of dSLs are also present in the plasma of healthy individuals and have been shown to increase in metabolic disorders like the metabolic syndrome or diabetes[14-16]. Thus, not only the mutated but also the wt SPT is capable to form dSLs. However, an increased availability of L-alanine does not automatically lead to increased dSL formation which shows that these lipids are not simply formed as by-products of the canonical SPT reaction (Figure 6). This indicated that additional factors are required to induce a shift in substrate specificity in the wildtype enzyme.

In a screen for novel HSAN I mutations in SPT, we identified a new SPTLC2-S384F variant in two unrelated HSAN I families. In line with previously reported HSAN I mutations[5-12] this variant was associated with increased dSL plasma levels in the four patients. Their plasma levels were comparable to previously reported HSAN I mutations (e.g. SPTLC1-C133W). Clinically, the S384F mutation is associated with a "classical" HSAN I phenotype primarily affecting sensory- and to a lower extent also motor functions. However, as for other HSAN I mutations, there is considerable clinical heterogeneity between the patients even from the same family.

Interestingly, an unbiased systematic approach to characterize the phospho-proteome in EGF stimulated HeLa cells revealed that S384 together with Y387 in SPTLC2 are modified by phosphorylation. The consequence of this SPTLC2 phosphorylation was not investigated by the authors in detail but was shown to be independent to the EGF stimulus and did not follow a kinetic pattern[19]. Isoelectric focusing revealed a significant heterogeneity in the isoelectric point (pI) for the SPTLC2 subunit (Figure 3, Supplemental Figure 4A). This heterogeneity was lost after alkaline phosphatase treatment which further supports the concept of a phosphorylated SPTLC2. The two identified residues, S384 and Y387, are located in close proximity to the PLP binding motive and are thereby well positioned for being involved in regulating enzyme activity.

We therefore investigated the putative regulatory role of these sites on SPT activity by creating a set of mutants which mimicked either a constitutively phosphorylated (S384D, S384E) or non-phosphorylated (S384A, Y387F, S384A+Y387F) protein. In isolated proteins, the S384D and S384E mutant showed reduced activity with L-serine and only the S384D and not the homologue S384E mutant revealed increased activity with L-alanine. Likewise, a

reduced activity with L-serine and an increased activity with alanine were observed in the novel HSAN I-causing S384F mutation but not in those mutants that mimicked a non-phosphorylated state of the enzyme (S384A, Y387F, S384A+Y387F). This indicates that the switch between L-serine and L-alanine activity requires specific structural conditions at S384 and is not caused by a general or arbitrary amino acid exchange at this position. As a limitation, we could not investigate the effect of a phosphorylation at Y387. These results were confirmed in living cells by a metabolic labeling assay using isotope labeled L-serine and L-alanine. Again, dSL formation was increased in S384D and S384F expressing cells but not in the S384E or the negative mutants.

We noticed differences in SPT activity when analyzed in isolated proteins and in living cells. In detail, we observed a decreased canonical activity for the S384D, S384E, S384F and G382V mutant in isolated proteins but the analysis in living cells revealed no differences in the formation of serine based sphingoid bases (sphingosine and sphinganine). These, at first sight contradictory results might be explained by the influence of several factors which were reported to control SPT activity and *de novo* sphingolipid synthesis. Recent reports showed that sphingolipid *de novo* production is tightly controlled by a group of small proteins (ORMDL1, 2 and 3) to prevent a harmful overproduction of sphingolipids by SPT. The ORM proteins act as negative regulators and inhibit SPT activity in response to elevated cellular sphingolipid levels[25-27]. In yeast un-phosphorylated ORM proteins bind to SPT and inhibit sphingolipid *de novo* formation[27]. In case of a sphingolipid deficiency, the ORM proteins are phosphorylated, dissociate from the SPT complex and activate *de novo* synthesis by SPT. In addition, two other small proteins (ssSPTa and b) have been reported to regulate the overall SPT activity and specificity for certain acyl-CoAs [28].

It is important to note that *de novo* synthesis is not the only route for a cell to generate sphingolipids. The cell can metabolize sphingolipids also from external sources for example from lipoproteins in the culture medium and it is likely that *de novo* synthesis by SPT is down regulated if the availability of exogenous sphingolipids from the medium is sufficient. This prevents any toxic overproduction of ceramides which will lead to apoptosis. The concept that cellular *de novo* generation of sphingolipids is essentially suppressed in case of a sufficient sphingolipid supply, might explain why we did not see differences in the incorporation of isotope labeled L-serine between SPTLC2 wt and S384D/E/F expressing cells, although the activity in isolated proteins is significantly reduced in these mutants. Under the condition of down regulated sphingolipid *de novo* synthesis, the reduced total activity of the mutants might

not be a limiting factor anymore. Consequently, the alternative SPT activity with L-alanine is independent of this regulation, since the activity pattern of the mutants with alanine was the same in isolated proteins and intact cells.

However, the regulatory mechanism underlying the shift in substrate specificity and dSL formation for wt SPT is not known. Our data suggest that phosphorylation of SPTLC2 at S384 can shift the activity of the enzyme towards the use of L-alanine. This shift might be either caused by structural changes in the active site, or by binding of additional factors to the SPT enzyme. Notably, an increased activity with L-alanine was only seen in the S384D but not for the homolog S384E mutation although aspartate (D) and glutamate (E) are structural homologues and differ only by one methyl-group in length. This indicates that the switch in activity between serine and alanine requires specific structural changes and is not caused by any mutation at this position. Interestingly, a closely located HSAN I mutation (G382V) did not show any increased dSL formation in a cell-free environment, although an elevated dSL formation was shown in G382V expressing HEK293 cells and also in lymphoblasts of G382V carriers[12]. The difference in cell-free conditions compared to intact cells was also observed for other HSAN I mutants (discussed in the general conclusions section) and suggests that other cellular factors contribute to the substrate specificity of SPT.

Earlier data from our group suggested that the active mammalian SPT is an octamer with a mass of about 460kD and probably composed of four heterodimers each formed by one SPTLC1 and either an SPTLC2 or SPTLC3 subunit [29, 30]. Unfortunately, the x-ray structure for the mammalian SPT is not re-solved yet. However, the molecular structure of the prokaryotic SPT is re-solved from two sphingolipid generating bacteria, *Sphingomonas paucimobilis* and *Sphingobacterium multivorum*[22, 31]. In contrast to the mammalian enzyme, the prokaryotic SPT is a homodimer and either soluble (*S. paucimobilis*) or loosely attached to the inner cell membrane (*S. multivorum)*[32]. The PLP binding motif (FT**K**SXXXX$\mathbf{X_{Ser384}}$G) in the x-ray structure from *S. multivorum* (PDB ID: 3A2B) is organized as a coil surrounded by two beta-sheets (Supplemental Figure 3A). Modeling the mammalian sites S384 and Y387 into this structure indicates that Ser384 is positioned directly in the core of the PLP binding motif, pointing outside towards the PLP-binding pocket whereas Y387 is localized on the beta-sheet and pointing away from the binding pocket (Supplemental Figure 3B). This indicates that residue S384 rather than Y387 could be accessible for a kinase from outside.

Like the S384D, also the HSAN I associated S384F variant shows increased dSL formation in isolated proteins. Although phenylalanine is a non-charged amino acid, the bulky aromatic

side group might mimic similar structural changes as a phosphorylated S384. Although the activity with L-alanine in isolated proteins was similar for the S384D and S384F, the latter showed a 2-3-fold higher dSL formation in the metabolic labeling assay in living cells. This again indicates that additional factors influence the cellular activity of SPT with L-alanine.

In addition to their suggested neurotoxicity in HSAN I, dSLs are not yet known to exert any physiological function. The finding that a specific phosphorylation in SPT could act as a molecular switch to shift the substrate specificity of the enzyme from L-serine to L-alanine further supports the idea for a specific physiological function of dSLs in cellular lipid metabolism. However, the exact function, underlying regulatory mechanisms and associated signaling pathways remain subjects for future studies.

Footnotes

This work was supported by the Gebert Rüf Stiftung.

Supplemental Information

I. FIGURES

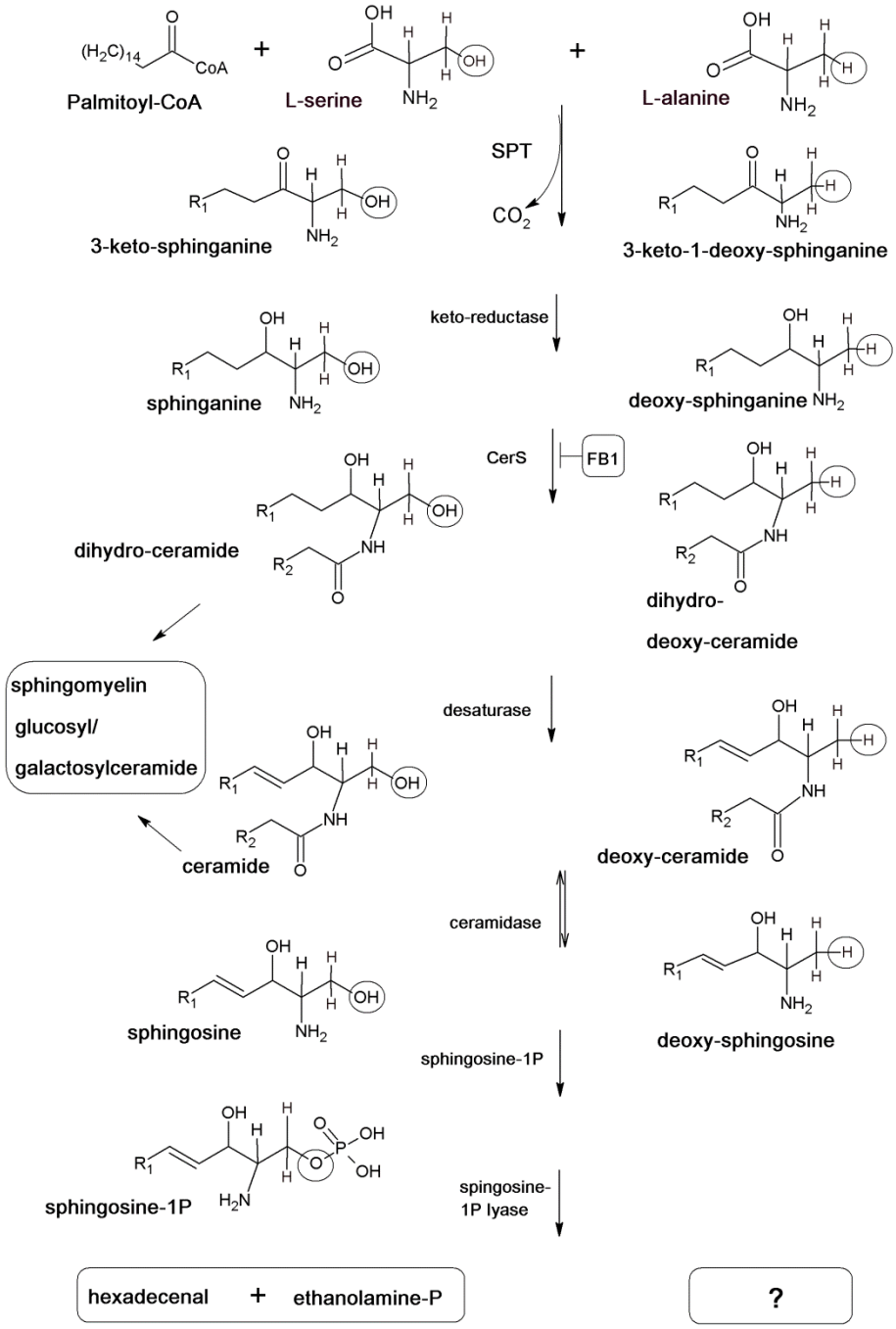

SUPPLEMENTAL FIGURE 1: **Pathway illustration of sphingolipid *de novo* synthesis with L-serine and L-alanine aminoacid substrate**

S384D_fw:5'-TCA CAA AGA GTT TTG GTG CTG ATG GAG GAT ATA TTG GAG GC-3'
S384D_rv:5'-GCC TCC AAT ATA TCC TCC ATC AGC ACC AAA ACT CTT TGT GA-3'

S384E_fw:5'-TTC ACA AAG AGT TTT GGT GCT GAG GGA GGA TAT ATT GGA GGC AAG-3'
S384E_rv:5'-CTT GCC TCC AAT ATA TCC TCC CTC AGC ACC AAA ACT CTT TGT GAA-3'

S384F_fw:5'-CAA AGA GTT TTG GTG CTT TCG GAG GAT ATA TTG GAG GC-3'
S384F_rv:5'-GCC TCC AAT ATA TCC TCC GAA AGC ACC AAA ACT CTT TG-3'

S384A_fw:5'-CAC AAA GAG TTT TGG TGC TGC AGG AGG ATA TAT TGG AGG CA-3'
S384A_rv:5'-TGC CTC CAA TAT ATC CTC CTG CAG CAC CAA AAC TCT TTG TG-3'

S384A+Y387F_fw:5'-CAA AGA GTT TTG GTG CTG CTG GTG GAT TTA TTG GAG GCA AGA AGG-3'
S384A+Y387F_rv:5'-CCT TCT TGC CTC CAA TAA ATC CAC CAG CAG CAC CAA AAC TCT TTG-3'

Y387F_fw: 5'-GAG TTT TGG TGC TTC TGG TGG ATT TAT TGG AGG CAA GAA GG-3'
Y387F_rv:5'-CCT TCT TGC CTC CAA TAA ATC CAC CAG AAG CAC CAA AAC TC-3'

G382V_fw:5'-GAA CGT TCA CAA AGA GTT TTG TTG CTT CTG GAG GAT ATA TTG G-3'
G382V_rv:5'-CCA ATA TAT CCT CCA GAA GCA ACA AAA CTC TTT GTG AAC GTT C-3'

SUPPLEMENTAL FIGURE 2A: **Primer pairs for site-directed mutagenesis in SPTLC2**

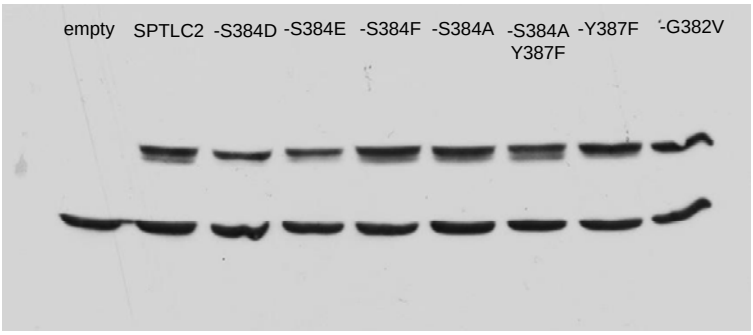

SUPPLEMENTAL FIGURE 2B: **Protein expression control of the stable transfected HEK293 mutants**
Expression levels of wild type SPTLC2 and the SPTLC2 mutants in stably transfected HEK293 cells. The proteins were separated on a 12% SDS Page and detected by a V5-tag antibody (higher bands). Beta-actin was used as the loading control (lower bands).

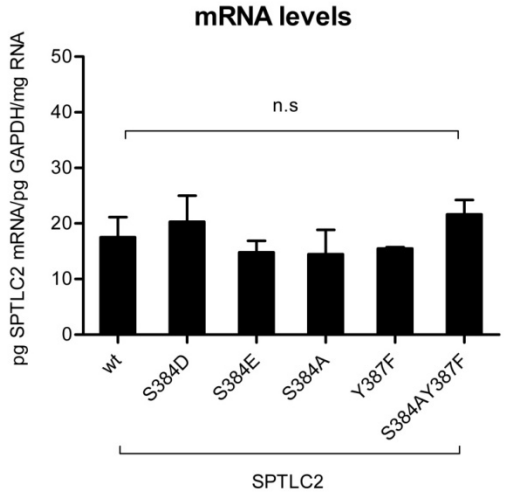

SUPPLEMENTAL FIGURE 2C: **SPTLC2 mRNA levels in the HEK293 mutants**
mRNA expression of wild type SPTLC2 and the SPTLC2 mutants in stably transfected HEK293 cells. Expression levels of GAPDH were used for normalization.

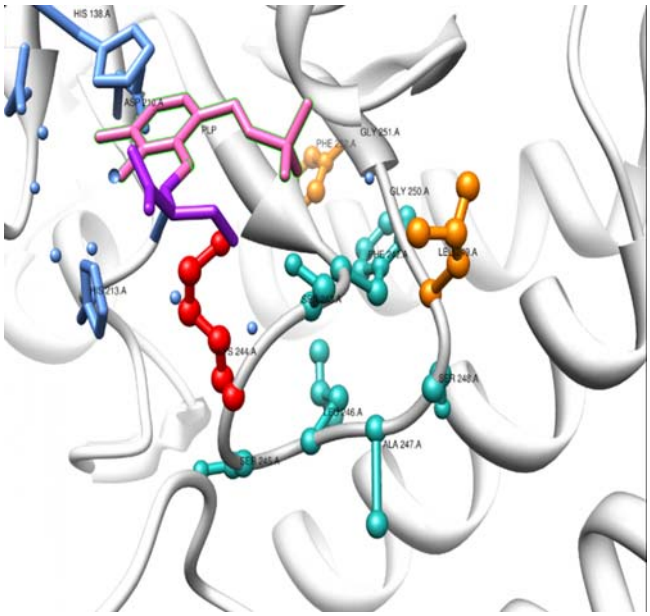

SUPPLEMENTAL FIGURE 3A:
Structure of SPT in *sphingobacterium multivorum* (PDB:3A2B)
SPT structure of *S. multivorum* was illustrated using UCSF Chimera 1.6.2.
Lys244 (Lys379) in red and Leu249 (Ser384) in orange are located in the coil structure surrounded by 2 beta-sheets whereas the second phosphosite Phe252 (Tyr387) in orange is found on the beta-sheet outside the PLP-binding motif sequence. Other aminoacids located on the coil structure are illustrated in turquois (Ser248, Ala247, Leu246, Ser245, Ser243, Phe242). The substrate (serine-PLP) is bound to Lys244 (purple-pink). His138 and His213 (blue) are important for coordinating the right position of the substrate.

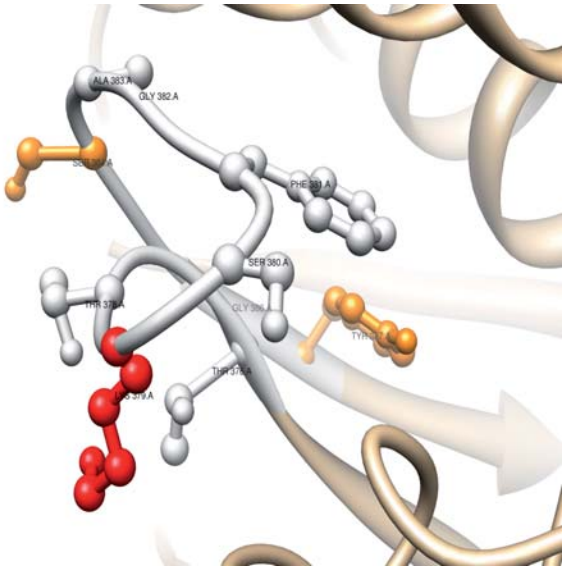

SUPPLEMENTAL FIGURE 3B:
Structural modeling of SPTLC2 phosphosites in *sphingobacterium multivorum*
The sequence of the mammalian SPTLC2 subunit was modeled into the protein structure of *S. multivorum* (PDB:3A2B) using SWISS-MODEL (http://swissmodel.expasy.org). The results are illustrated using USCF Chimera 1.6.2. Both phosphosites (Ser384 and Tyr387) are shown in orange and the Schiff-base forming Lys379 in red. Lys379 and Ser384 are both located on the coil structure of the inner core of the PLP-binding motif (FT**K**SXXX**X**$_{\mathbf{Ser}}$G) whereas the second phosphosites Tyr387 is located on the beta-sheet.

A: SPTLC2wt
Endogenous and transfected protein

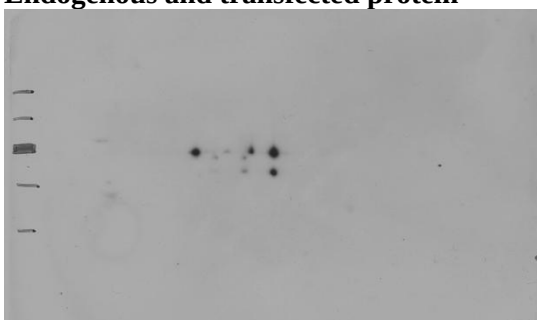

B: SPTLC2-S384A
Endogenous and transfected mutant protein

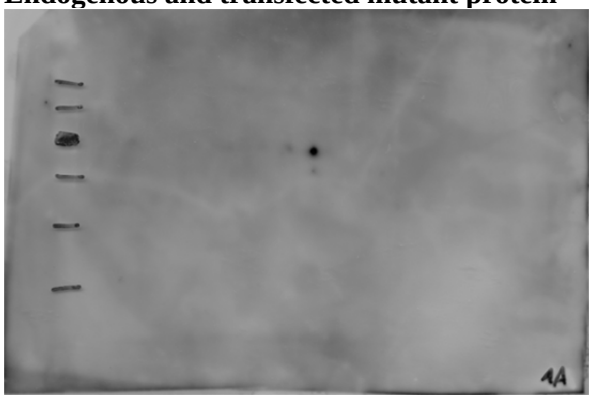

C: SPTLC2-Y387F
Endogenous and transfected mutant protein

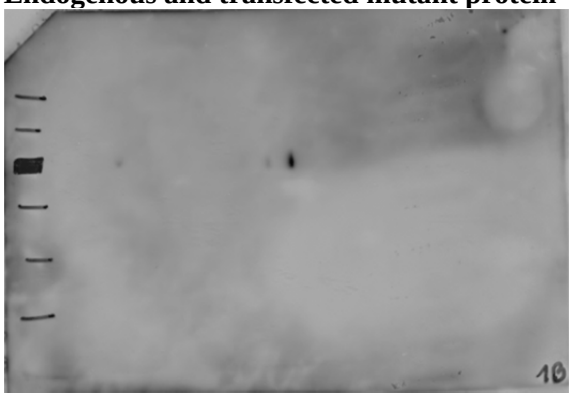

D: SPTLC2-S384A
Only transfected mutant protein

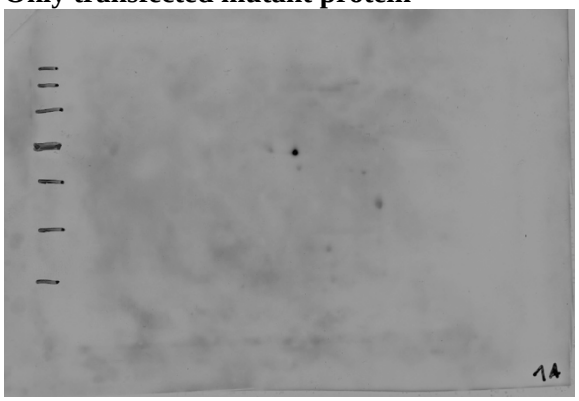

E: SPTLC2-Y387F
Only transfected mutant protein

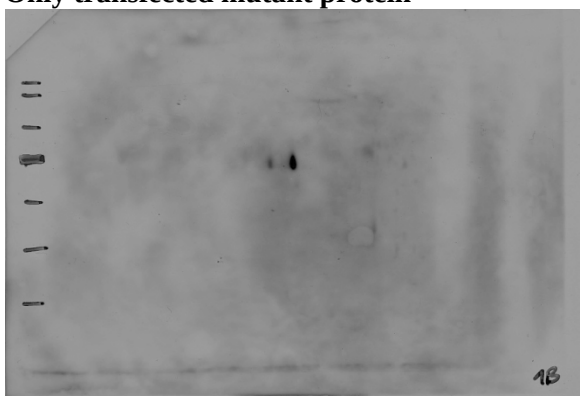

SUPPLEMENTAL FIGURE 4: **2D-gel analysis of the HEK293 phospho-mutants**
HEK293 cells expressing wt (SPTLC2) and mutant-SPTLC2 (S384A, Y387F) were analyzed on a 2D-gel. Endogenous and transfected SPTLC2 were detected using a polyclonal antibody[2] (1:3000) whereas the use of an anti-V5-antibody 1:2000 (Serotec) allows exclusively detection of the transfected SPTLC2 variants. The wt (SPTLC2) transfected HEK cells revealed a phosphorylation pattern **(A)**, that is changed in the HEK cells expressing the mutated SPTLC2 **(B-E)** suggesting that the phosphorylation sites are lost in the mutants.

HEK-empty

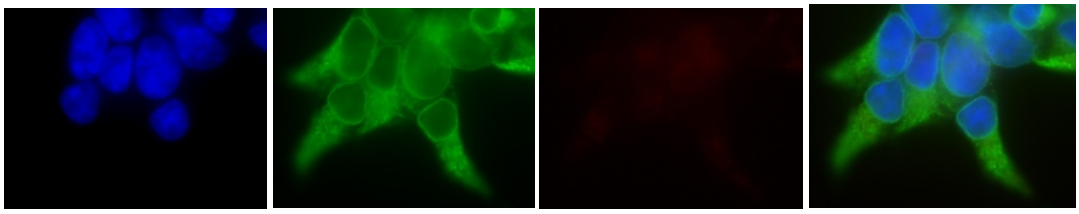

HEK-SPTLC2

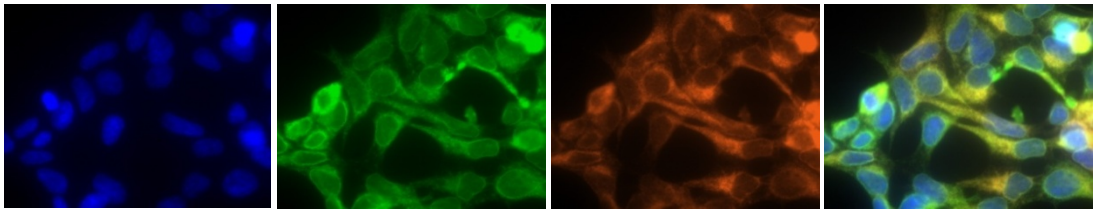

HEK-SPTLC2_S384D

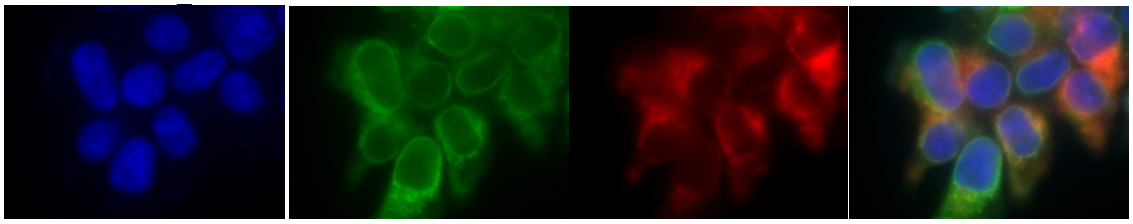

HEK-SPTLC2_S384E

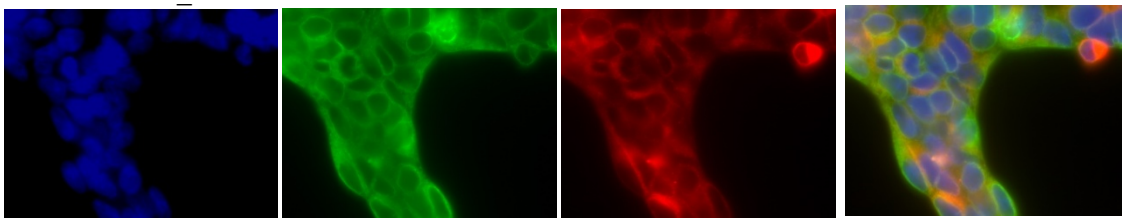

HEK-SPTLC2_S384A

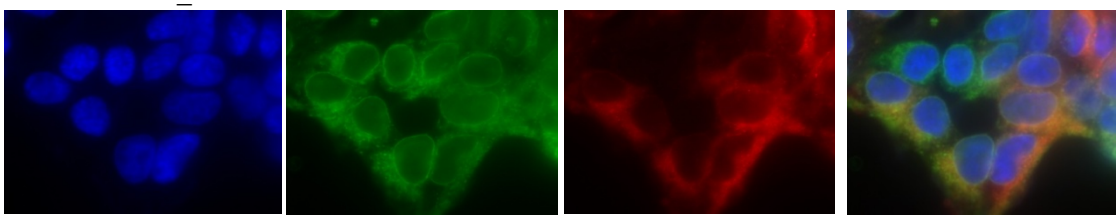

HEK-SPTLC2_S384F

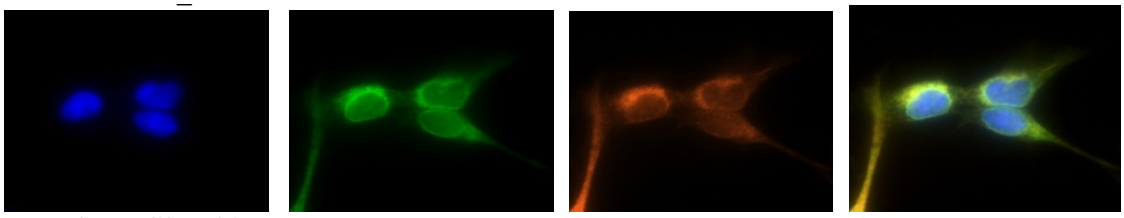

HEK-SPTLC2_Y387F

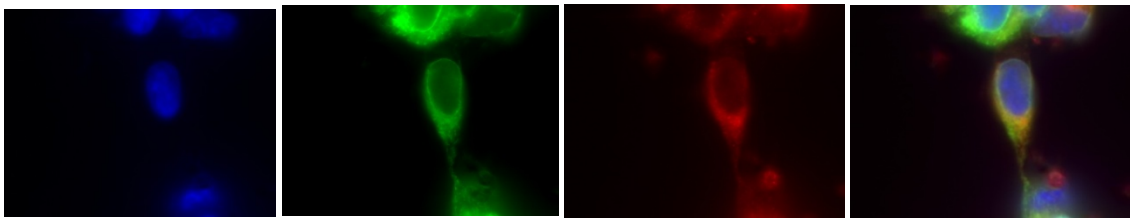

HEK-SPTLC2_S384A_Y387F

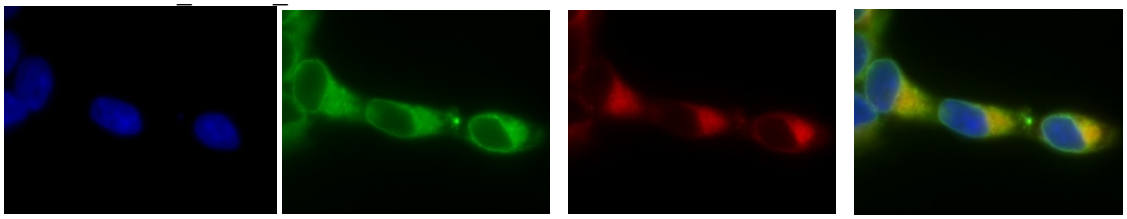

SUPPLEMENTAL FIGURE 5: **Co-localization of transfected wt and mutant SPTLC2 variants with ER marker calnexin in HEK293**

Localisation of transfected vector (empty), wt (SPTLC2) and mutant-SPTLC2 (S384D, S384E, S384A, Y387F, S384A+Y387F) was analyzed in HEK293 cells revealed co-localisation of all variants with the ER marker calnexin (blue DAPI; green calnexin; red SPTLC2 variants. HEK293 cells were cultured in chamber culture slides (BD Falcon) to 50% confluence and fixed in 4% paraformaldehyde for 15min at 37°C. Permeabilization was performed for 5min using ice-cold acetone. Cells were washed in double-distilled water and dried for some seconds. Unspecific binding sites were blocked with 1% horse serum in PBS for 30min. After washing in PBS, mouse anti-V5-tag antibody diluted 1:2000 (Serotec) in blocking solution together with rabbit anti-calnexin antibody 1:4000 (Sigma) were incubated for 2 hours. After 2 times washing in PBS, Alexa Fluor 594 conjugated secondary goat anti-mouse antibody (Invitrogen) diluted 1:1000 in blocking solution was incubated together with 30nM DAPI for 1 hour in the dark. Immunofluorescence of the V5 tagged SPTLC2 mutant and wildtype protein, calnexin and nuclein acid were detected with Zeiss Axiovert 200M using AxioVision 4 software

II. TABLES

SPTLC2 exon	Forward primer	Reverse primer	Primer conditions
1	CCTACAGAGCCTGCCTTG	CGGTGTGGACTGGCGGAG	58 touchdown
2	GGTATAATTCAGCAAATCTC	TTTAACTGCATCTGGAATAG	60-50 touchdown
3	TAATGAAATTGCCCTTATAC	AATCATATTGTATCCTCAGC	60-50 touchdown
4	ATAGACTTTGTTCTCTCTGC	CTAAATGACATGACAAAGTG	60-50 touchdown
5	TCTGAAAAGGACACAACAC	TTTAGCTCACTCTGACTGC	51.3
6	AGCTATTAGTGTTTGTGGC	TCATTTATACTTTCAAGTGC	60-50 touchdown
7	TATCTGAGGCATGGTTTC	TAGACTAATGTTCCCTTCAG	65-55 touchdown
8	ATAATAATGAAGTGCCAAAC	GTATTATGAGCCTAAACCAG	60-50 touchdown
9	TCTAGAACTTAGAAGGAAAGG	TGCCTATTAGTAAACCTGAC	60-50 touchdown
10	GATAGAATGGAGATAGAGGAG	TAAGGACAAGACCATTTTC	60-50 touchdown
11	TTGAAATCTTTGAGGACAG	GCTCACAAGAACATCAAG	60-50 touchdown
12	GCACTAGACATAAGTCCTGC	ACAGAAGTGTGGTTCCTG	60-50 touchdown

SUPPLEMENTAL TABLE 1**: Primer pairs for sequencing SPTLC2**

PCR comprised the following steps for all exons except exons 1 and 5: 1) 95°C for 15 minutes, 2) 25 cycles of 95°C for 30 seconds, 60°C (reduced by 0.4°C per cycle) for 30 seconds, and 72°C for 45 seconds, 3) 13 cycles of 95°C for 30 seconds, 50°C for 30 seconds, and 72°C for 45 seconds, 4) 72°C for 10 minutes.
For exon 1: 1) 95°C for 15 minutes, 2) 38 cycles of 95°C for 30 seconds, 58°C (reduced by 0.4°C per cycle) for 30 seconds, and 72°C for 45 seconds, 3) 72°C for 10 minutes. 10% DMSO
For exon 5: 1) 95°C for 15 minutes, 2) 37 cycles of 95°C for 30 seconds, 51.3°C (reduced by 0.4°C per cycle) for 30 seconds, and 72°C for 45 seconds, 3) 72°C for 10 minutes.

Patient	Median				Ulnar				Radial	Common peroneal			Posterior tibial			Superficial peroneal	Sural
	DML ms	CV m/s	CMAP mV	SAP uV	DML ms	CV m/s	CMAP mV	SAP uV	SAP uV	DML ms	CV m/s	CMAP mV	DML ms	CV m/s	CMAP mV	SAP uV	SAP uV
A II-6	5.3	42		NR	6	28		NR									
A III-8	3.0	58	7.0	NR	2.9		8.7	NR	13	NR						NR	NR
A III-9	NR			NR	NR			NR	NR	NR							
B II-1	3.9	49	6.1	NR	2.5	46	2.5	NR	2	3.5	42	3.3					
B II-2	3.7	50	8.6	7	3.2	56	9.4	2	21	NR			NR			NR	NR

SUPPLEMENTAL TABLE 2**: Nerve conduction studies in SPTLC2 S384F patients**

DML = distal motor latency; CV = conduction velocity; CMAP = compound motor action potential; SAP = sensory action potential; ms = milliseconds; m/s = metres per second; mV = millivolts; uV = microvolts. Shown are members of the two families A (III-2, III-8, III-9) and B (II-1, II-2)

References

1. Hanada K. Serine palmitoyltransferase, a key enzyme of sphingolipid metabolism. Biochimica et Biophysica Acta (BBA) - Molecular and Cell Biology of Lipids 2003;1632:16-30.
2. Hornemann T, Richard S, Rütti MF, Wei Y, von Eckardstein A. Cloning and Initial Characterization of a New Subunit for Mammalian Serine-palmitoyltransferase. Journal of Biological Chemistry 2006;281:37275-37281.
3. Penno A, Reilly MM, Houlden H, et al. Hereditary Sensory Neuropathy Type 1 Is Caused by the Accumulation of Two Neurotoxic Sphingolipids. Journal of Biological Chemistry 2010;285:11178-11187.
4. Zitomer NC, Mitchell T, Voss KA, et al. Ceramide Synthase Inhibition by Fumonisin B1 Causes Accumulation of 1-Deoxysphinganine. Journal of Biological Chemistry 2009;284:4786-4795.
5. Bejaoui K, Wu C, Scheffler MD, et al. SPTLC1 is mutated in hereditary sensory neuropathy, type 1. Nat Genet 2001;27:261-262.
6. Dawkins JL, Hulme DJ, Brahmbhatt SB, Auer-Grumbach M, Nicholson GA. Mutations in SPTLC1, encoding serine palmitoyltransferase, long chain base subunit-1, cause hereditary sensory neuropathy type I. Nat Genet 2001;27:309-312.
7. Bi H, Gao Y, Yao S, Dong M, Headley AP, Yuan Y. Hereditary sensory and autonomic neuropathy type I in a Chinese family: British C133W mutation exists in the Chinese. Neuropathology 2007;27:429-433.
8. Houlden H, King R, Blake J, et al. Clinical, pathological and genetic characterization of hereditary sensory and autonomic neuropathy type 1 (HSAN I). Brain 2006;129:411-425.
9. Klein CJ, Wu Y, Kruckeberg KE, et al. SPTLC1 and RAB7 mutation analysis in dominantly inherited and idiopathic sensory neuropathies. Journal of Neurology, Neurosurgery & Psychiatry 2005;76:1022-1024.
10. Geraldes R, de Carvalho M, Santos-Bento M, Nicholson G. Hereditary sensory neuropathy type 1 in a Portuguese family—electrodiagnostic and autonomic nervous system studies. Journal of the Neurological Sciences 2004;227:35-38.
11. Rotthier A, Baets J, Vriendt ED, et al. Genes for hereditary sensory and autonomic neuropathies: a genotype–phenotype correlation. Brain 2009;132:2699-2711.
12. Rotthier A, Auer-Grumbach M, Janssens K, et al. Mutations in the SPTLC2 Subunit of Serine Palmitoyltransferase Cause Hereditary Sensory and Autonomic Neuropathy Type I. The American Journal of Human Genetics 2010;87:513-522.
13. Garofalo K, Penno A, Schmidt BP, et al. Oral l-serine supplementation reduces production of neurotoxic deoxysphingolipids in mice and humans with hereditary sensory autonomic neuropathy type 1. The Journal of Clinical Investigation 2011;121:4735-4745.
14. Bertea M, Rutti M, Othman A, et al. Deoxysphingoid bases as plasma markers in Diabetes mellitus. Lipids in Health and Disease 2010;9:84.
15. Othman A, Rütti M, Ernst D, et al. Plasma deoxysphingolipids: a novel class of biomarkers for the metabolic syndrome? Diabetologia 2012;55:421-431.
16. Wang-Sattler R, Yu Z, Herder C, et al. Novel biomarkers for pre-diabetes identified by metabolomics. Mol Syst Biol 2012;8.

17. Huang S, Cheng T-Y, Young DC, et al. Discovery of deoxyceramides and diacylglycerols as CD1b scaffold lipids among diverse groove-blocking lipids of the human CD1 system. Proceedings of the National Academy of Sciences 2011;108:19335-19340.

18. Martinez T, Chen X, Bandyopadhyay S, Merrill A, Tansey M. Ceramide sphingolipid signaling mediates Tumor Necrosis Factor (TNF)-dependent toxicity via caspase signaling in dopaminergic neurons. Molecular Neurodegeneration 2012;7:45.

19. Olsen JV, Blagoev B, Gnad F, et al. Global, In Vivo, and Site-Specific Phosphorylation Dynamics in Signaling Networks. Cell 2006;127:635-648.

20. Murphy SM, Herrmann DN, McDermott MP, et al. Reliability of the CMT neuropathy score (second version) in Charcot-Marie-Tooth disease. Journal of the Peripheral Nervous System 2011;16:191-198.

21. R. T. Riley WPNEWAHM. Alteration in sphingolipid metabolism: bioassays for fumonisin- and ISP-I-like activity in tissues, cells and other matrices. Natural Toxins 1999;7:407-414.

22. Yard BA, Carter LG, Johnson KA, et al. The Structure of Serine Palmitoyltransferase; Gateway to Sphingolipid Biosynthesis. Journal of Molecular Biology 2007;370:870-886.

23. Houlden H, King R, Blake J, et al. Clinical, pathological and genetic characterization of hereditary sensory and autonomic neuropathy type 1 (HSAN I). Brain 2006;129:411-425.

24. Ikushiro H, Fujii S, Shiraiwa Y, Hayashi H. Acceleration of the Substrate Cα Deprotonation by an Analogue of the Second Substrate Palmitoyl-CoA in Serine Palmitoyltransferase. Journal of Biological Chemistry 2008;283:7542-7553.

25. Siow DL, Wattenberg BW. Mammalian ORMDL Proteins Mediate the Feedback Response in Ceramide Biosynthesis. Journal of Biological Chemistry 2012.

26. Han S, Lone MA, Schneiter R, Chang A. Orm1 and Orm2 are conserved endoplasmic reticulum membrane proteins regulating lipid homeostasis and protein quality control. Proceedings of the National Academy of Sciences 2010;107:5851-5856.

27. Breslow DK, Collins SR, Bodenmiller B, et al. Orm family proteins mediate sphingolipid homeostasis. Nature 2010;463:1048-1053.

28. Han G, Gupta SD, Gable K, et al. Identification of small subunits of mammalian serine palmitoyltransferase that confer distinct acyl-CoA substrate specificities. Proceedings of the National Academy of Sciences 2009;106:8186-8191.

29. Han G, Gable K, Yan L, et al. The Topology of the Lcb1p Subunit of Yeast Serine Palmitoyltransferase. Journal of Biological Chemistry 2004;279:53707-53716.

30. Hornemann T, Wei Y, von eckardstein A. Is the mammalian serine palmitoyltransferase a high-molecular-mass complex? Biochem J 2007;405:157-164.

31. Ikushiro H, Islam MM, Okamoto A, et al. Structural Insights into the Enzymatic Mechanism of Serine Palmitoyltransferase from Sphingobacterium multivorum. Journal of Biochemistry 2009;146:549-562.

32. Ikushiro H, Islam MM, Tojo H, Hayashi H. Molecular Characterization of Membrane-Associated Soluble Serine Palmitoyltransferases from Sphingobacterium multivorum and Bdellovibrio stolpii. Journal of Bacteriology 2007;189:5749-5761.

Chapter 3:

Deoxy-sphingolipids are generated in monocytes during PMA stimulated differentiation into macrophages

Daniela Ernst, Markus Rütti, Yu Wei, Marco van Eijck, Arnold von Eckardstein, Thorsten Hornemann

Not submitted

Contributions:

Daniela Ernst performed the experiments and wrote the manuscript

Markus Rütti measured the amino acids

Marco van Eijck provided the primary monocytes

Thorsten Hornemann and Arnold von Eckardstein supervised the work and revised the manuscript

Summary

Background: 1-Deoxy-sphingolipids (dSLs) are an atypical class of sphingolipids that were found to accumulate in the plasma of patients with the rare inherited neuropathy HSAN I (Hereditary neuropathy type I) which is caused by several missense mutations in serine palmitoyltransferase. Plasma from healthy individuals also contains low but detectable dSL levels which are increased in patients with certain metabolic disorders (metabolic syndrome, diabetes type 2). Very little is known about the factors that are involved in the generation and downstream processing of these atypical lipids.

Results: Sphingoid base profiling of several commonly used cell lines revealed high dSL levels in the macrophage cell line RAW264.7 as well as in HEK293 cells. Monocytic cell lines like THP1 or HL60 did not show dSL formation to the same extent. We therefore investigated the change in the sphingoid base profile in THP1 cells during PMA stimulated monocyte to macrophage differentiation with the aim to identify metabolic factors that regulate dSL formation. Upon differentiation, THP1 cells increasingly generated dSLs at the expense of forming sphinganine- the canonical SPT product. The increase in dSL generation was accompanied by an increase in intracellular alanine concentration whereas the serine concentration did not alter over the period of differentiation. The SPT protein expression profiles changed in a manner that correlated temporally with the dSL formation and intracellular alanine concentration. We observed a conversion of deoxySA to deoxy-ceramide (by the appearance of deoxySO backbones) even in the presence of the CerS inhibitor Fumonisin B1. Furthermore, the formation of deoxySO (and deoxySO containing sphingolipids) -but not of deoxySA (and deoxySA containing sphingolipids) - was dependent on the presence of PMA. The PMA dependant deoxySO generation was further stimulated in the presence of FB1. This activity pattern was shown to be specific in THP1 monocytes since the addition of PMA to HEK293 cells resulted in the opposite effect and rather inhibited dSL generation. Increased dSL formation during differentiation was confirmed in human primary monocytes.

Conclusion: We showed that dSL formation is a coordinated process during monocyte to macrophage differentiation. The metabolism of dSLs is influenced by PMA and FB1, both known activators of PKC and correlates with intracellular changes in the amino acid metabolism. Our results indicate that the formation of dSLs is of physiological relevance during monocyte to macrophage differentiation.

Introduction

The first step of sphingolipid *de novo* biosynthesis is the condensation of L-serine and palmitoyl-CoA. This reaction is catalyzed by serine palmitoyltransferase (SPT) in a pyridoxal 5'phosphate dependent manner[1]. SPT consists of three subunits, SPTLC1/2/3 together with small SPT subunits, ssSPTa/b that were reported to modulate SPT activity and the acyl-CoA substrate specificity[1-3]. The overall SPT complex composition is not known yet but was suggested to consist of a functional heterodimer of SPTLC1 together with SPTLC2/3 in combination with the small SPT subunits (ssSPTa/b) and to be organized in a higher mass complex[2-4]. Besides the canonical L-serine substrate, SPT can also use L-alanine and L-glycine to a certain extent which results in the formation of 1-deoxy-sphingolipids (dSLs)[5, 6].

Assuming that dSLs are metabolized in the same way as the serine-derived sphingolipids, their further processing requires N-acylation, a reaction that is catalysed by a ceramide synthase isoform (CerS) and results in deoxy-dihydro-ceramides. A desaturase (DES) introduces a C4 double-bond into the deoxy-sphinganine backbone leading to the unsaturated deoxy-ceramide. During degradation the N-acyl chain is removed by the action of a ceramidase, resulting in the free deoxy-sphingosine (deoxySO); (see Figure 1A). So far, it was shown that dSLs are acylated to deoxy-dihydro-ceramides [6], but their further downstream metabolism remains unknown. As dSLs lack the C1-hydroxyl group, they can neither be metabolized to complex sphingolipids nor degraded by the canonical catabolic pathway.

Deoxy-sphingolipids were reported to be generated in cells during longer culture periods and in response to Fumonisin B1, a mycotoxin and inhibitor of CerS [5-8]. Besides, dSL levels were described to increase together with ceramides in response to TNF treatment in dopaminergic neurons. Here, they reduced the cell viability in a dose-dependent manner and inhibited neurite outgrowth and branching in cultured DRG neurons [9]. In addition, dSLs were found to be elevated in the plasma of patients affected with metabolic syndrome or diabetes type 2 (T2D)[10-12]. Recently, deoxy-ceramide was reported to act as a scaffold lipid facilitating the presentation of the lipid antigen for recognition by T-cells. Deoxy-ceramides, due to their hydrophobicity, help the lipid antigen to navigate for its presentation by the CD1b receptor[13]. This discovery established a physiological context where dSLs could play a role in innate immunity.

The objective of this study was to reveal factors that contribute to the generation of dSLs in wildtype SPT and to gain information about the downstream processing of deoxy-sphingolipids.

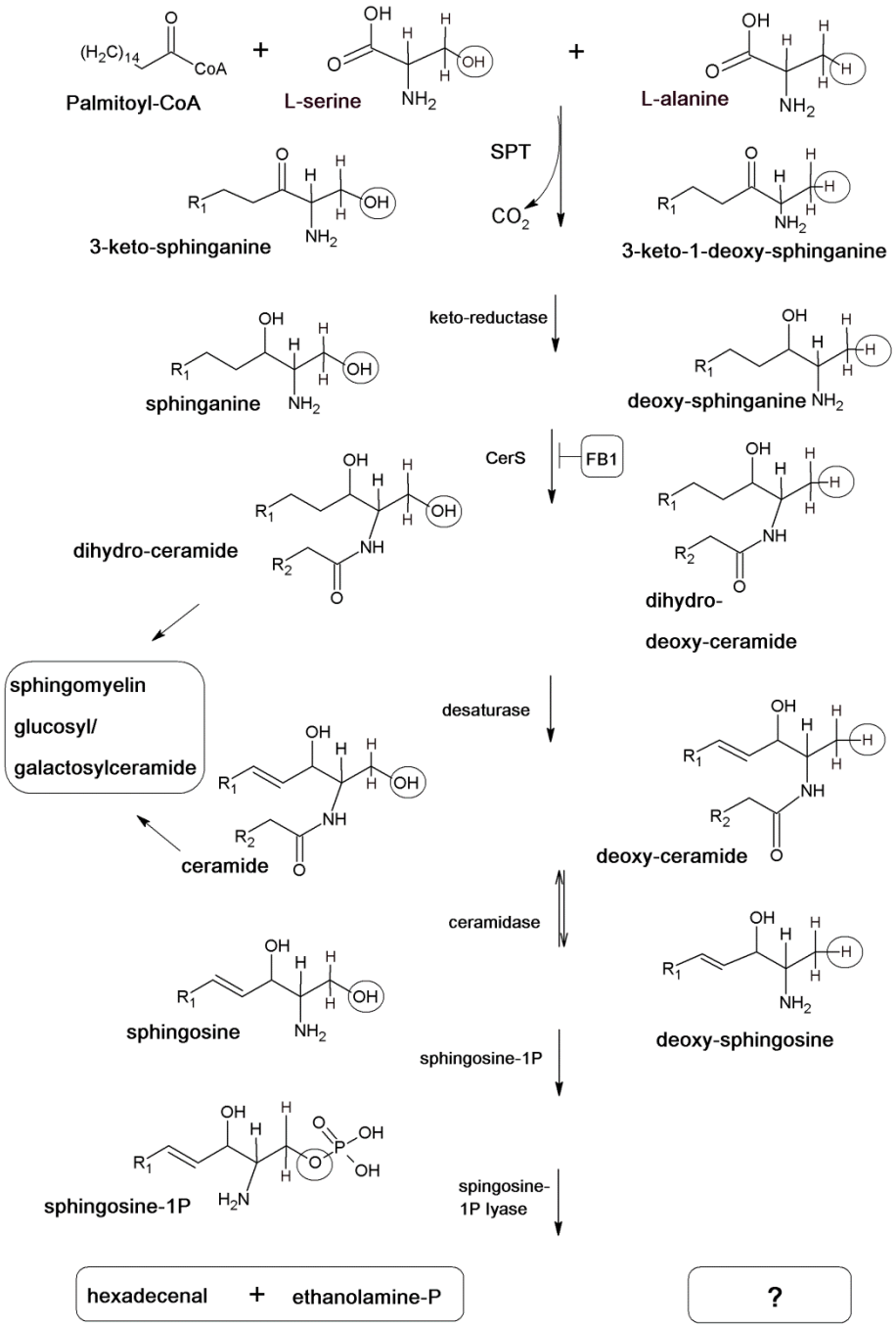

FIGURE 1A: **Sphingolipid *de novo* synthesis pathway with L-serine and L-alanine**

Chapter 3

Experimental Procedures

Cell culture

HEK293, COS-1, HeLa, HepG2 and NIH/3T3 RAW cells were cultured in DMEM, CHO and LYB in Ham F12, JURKAT in RPMI 1640, PC12 in RPMI1640 with 5% horse serum, T84 in 50% DMEM and 50% Ham-F12, JEG in MEM and JAR in RPMI 1640; all cell lines were supplemented with 10% FCS. HL60 cells were cultured in IMDM with 4mM L-Glutamine and 20% FCS and THP1 cells in RPMI containing 2mM L-glutamine, 4.5g/L glucose, 1mM sodium-pyruvate and 10% FCS. EBV transformed lymphocytes were cultured in RPMI 1640 supplemented with 15% FCS, 2mM L-glutamine, 1mM sodium-pyruvate, 0.075% sodium-bicarbonate and 1mM HEPES. One hundred U/ml and 0.1 mg/ml penicillin/streptomycin (FisherScientific FSA15-043), respectively were present in all culture media. The cell lines were obtained from ATCC and the media from Sigma-Aldrich. THP1 cells were differentiated into macrophages using 200nM PMA (in ethanol).

Protein extraction and determination of concentration

Protein was extracted by re-suspension of the cell pellet in cold lysis buffer (50mM HEPES, 5mM EDTA and 0.2% Triton-X). After 30min incubation on ice, the extract was centrifuged for 5min at 16.000x g at 4°C (Eppendorf). Protein concentration was determined using the Bradford Protein Assay (Biorad) according to manufacturer's instructions.

Analysis of total sphingoid base content and SPT protein expression in primary human monocytes

Monocytes were isolated from human buffy coats and cultured in the presence of RPMI containing 10% horse serum for 6 days and were subsequently stimulated with PMA, solvent control (DMSO) or were left untreated for 24h or 72h. The culture media was collected for amino acid measurement (analysis done at the Functional Genomic Center Zürich, Switzerland). The cells were harvested, the protein was extracted and 100ug total protein was used for acid-base lipid extraction. Two hundred pmol deuterated internal extraction standards (d7-C18SA, d7-C18SO, d5-m17:0) were added to the protein extract prior to extraction. Twenty ug total protein was separated using a 12% SDS-PAGE gel, immuno-blotted and stained using anit-SPTLC1[3] (1:2000), anti-SPTLC2[3] (1:3000) and GAPDH (1:5000, Abnova) antibodies. THP1 differentiation status was monitored via the upregulation of CD14 (1:1000, Serotec).

Fumonisin B1 dependent SPT activity assay

Fumonisin B1 (Sigma) was added to the medium of exponentially growing cells in a final concentration of 13.85uM. As a negative control, myriocin (25uM, Sigma) was added together with Fumonisin B1. Twenty-four hours after Fumonisin B1 addition, cells were washed twice with cold PBS, harvested and counted (Z2 Coulter Counter, Beckman Coulter). Cells were centrifuged (800xg, 5min at 4°C) and pellets were stored at -20°C until lipid extraction.

Lipid extraction and hydrolysis

Total lipids were extracted from cells according to the method of Riley *et al.*[14]. The extracts were either base -or acid and base hydrolyzed as stated in the text. Lipid extraction, hydrolysis and LC-MS analysis was performed as previously described[5]. The quantified lipids were normalized to cell number (per million cells) relative to the internal extraction standard (as stated in the text).

Measurement of amino acids

For analysis of the intracellular amino acids, the internal amino acid standard (beta-amino-butyrate, Sigma) was added to the cell pellets and included in the lipid extraction procedure (acid-base or base-only). Five -hundred ul of the watery upper phase (see under section lipid extraction and hydrolysis of Penno *et al.*[5]) or 500ul of conditioned media was collected and after adding perchloric acid to 0.25M final concentration, the sample was centrifuged at 16000 x g for 10min at 4°C. The amino acids present in the supernatant were derivatized online with ortho-phthaldialdehyde[14] containing 0.001% v/v 3-mercaptopropionic acid (OPA-MPA) in a ratio of 37.5% (supernatant) to 62.5% (OPA-MPA). One minute post derivatization, the OPA-amino acids were directly injected and analyzed on a Shimadzu HPLC system using an Agilent Zorbax Eclipse AAA column (4.6, 150, 5um) and fluorescence detection. Chromatographic conditions were chosen according to the standard "Eclipse" analysis protocol (Agilent).

Results and discussion

I. Analysis of the sphingolipid profile and SPT protein expression in different cell lines

To get an overview of the generation or metabolism of dSLs, we compared the sphingoid base profiles of various commonly used cell lines from human, mouse, rat and hamster. The cells were cultured for three days, the lipids were extracted and the sphingoid base profile was analysed by LC-MS after an acid hydrolysation step (Figure 1B). Hereby the analysed sphingoid backbones represent the total amount of sphingolipids or deoxy-sphingolipids present in these cells[5].

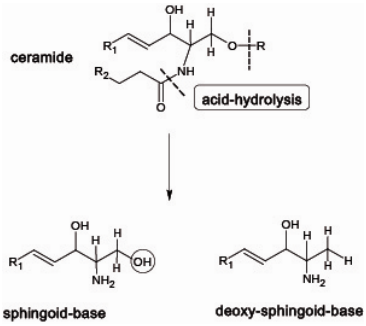

FIGURE 1B**: Illustration of sphingoid bases after acid-base hydrolysis**

Profile of sphingolipid species in various cell lines

Sphingosine was the major sphingoid base in all cell lines, at highest concentration in T84, JEG, JAR and Hela cells. Lower amounts of sphingosine backbones were detected in HEK, CHO and COS cells (Figure 1C).

C16-derived sphingoid bases were detected in the highest amounts in T84, PC12, JEG and JAR cells (Figure 1D). C16-derived sphingoid bases result from the condensation of myristoyl-CoA (instead of palmitoyl-CoA) with L-serine, a reaction that is catalysed by the SPTLC3 subunit possibly in combination with ssSPTb[2,3]. The general amount of C16-based sphingoid bases did not correlate with the amount of C18 sphingoid bases, indicating that the sphingolipid species are formed by distinct pathways.

Deoxy-sphingolipids accumulated to a different extent in the analysed cell lines. The highest amount of dSLs (50pmol/1mio cells) was found in RAW cells, a mouse leukemic macrophage cell line. Human embryonic kidney cells (HEK293) also had significant levels (20pmol/1 mio cells) in comparison to other cell lines (Figure 1E). Deoxy-sphingolipid levels in these cells did not correlate with the total levels of C18 sphingoid bases which are shown as the sum of sphingosine and sphinganine (SO+SA) (Figure 1C). This indicates that in RAW and HEK293

cells, dSLs are generated due to a specific switch in the activity towards L-alanine, rather than as a by-product of the general SPT activity. Differences between the cell lines were also seen with respect to the formed dSL species. Deoxy-sphinganine (deoxySA) was the major dSL found in most cell lines (Figure 1E). However, in human colonic adenocarcinoma T84 cells and human placenta cells (JEG), deoxySO was the predominant dSL (Figure E). The majority of serine-based sphingolipids in the cells were found in the sphingosine form whereas the alanine-derived metabolites were mostly found in the dihydro-sphingosine form (deoxySA). This difference could either stem from the CerS step or the desaturase step in the synthesis pathway. Since the analysed sphingolipids were chemically hydrolysed we are not able to distinguish between those steps. For that purpose the analysis of the (deoxy-) ceramide species is necessary.

C:

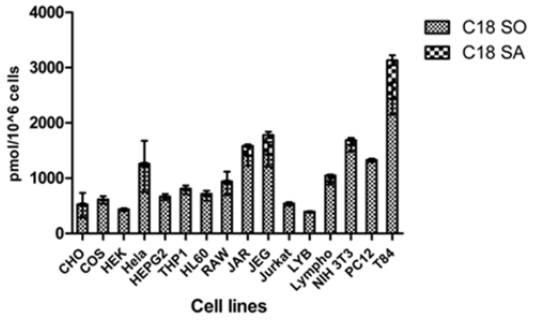

D:

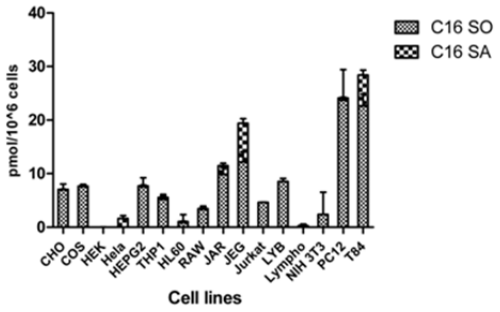

E:

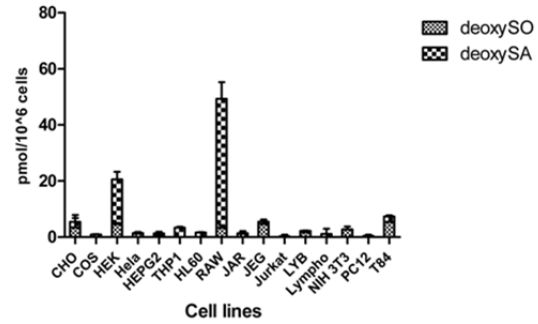

FIGURE 1C-E**: Total C18- and C16-based sphingoid and deoxy-sphingoid bases in different cell lines**

Cells were cultured for 3 days in their respective media (experimental procedures), harvested and counted and the lipids were methanol-chloroform extracted. Lipids were acid-base hydrolyzed and the resulting sphingoid bases analyzed using LC-MS. Sphingoid bases were quantified relative to an internal extraction standard (C17SO) and to 1 mio cells.

SPT protein expression pattern

Second, we compared the expression profile of SPTLC1 and SPTLC2 in the various cell lines (Figure 1F). They differed in the expression of both SPT subunits, with high expression of SPTLC1 (55kDa) and SPTLC2 (62kDa) in RAW, HEK293, JEG, JAR, COS (among others) and low expression in monocyte cell lines like THP1 and HL60 cells. Furthermore, signals corresponding to smaller SPT proteins were detected. Using an anti-SPTLC2 antibody[3], a protein of 32kDa size was detected in almost every cell line analysed (except THP1, JEG, CHO and LYB cells). Using an anti-SPTLC1 antibody[3], a protein correlating to 25kDa in size was detected in COS, HEK293, HL60wt, with the highest expression in T84 cells.

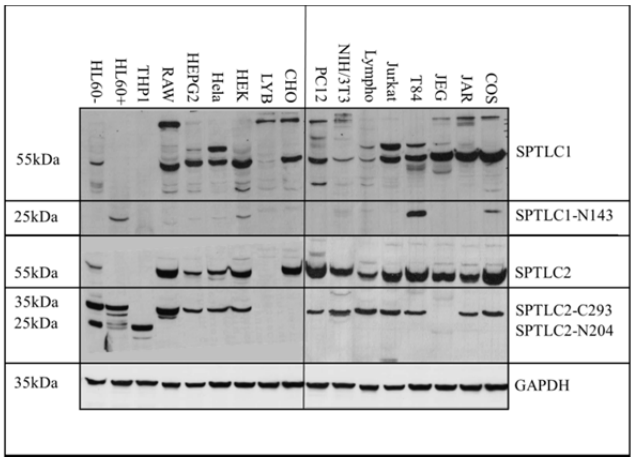

FIGURE 1F**: Protein expression profile of analysed cell lines**
Protein extracts of different cell lines were separated on a 12% SDS-PAGE gel, immune-blotted and -stained. Detection was performed using antibodies against SPTLC1, SPTLC2[3] and GAPDH (Abnova). Indicated sizes according to molecular size standard (PageRuler^{TM}, Thermo Scientific). Sizes of respective proteins: SPTLC1 55kDa, SPTLC2 62kDa; SPT splice variants, SPTLC1-N162 25kDa, SPTLC2-C293 32.6kDa and SPTLC2-N204 24.5kDa; GAPDH 37 kDa. HL 60+/- indicates expression of a functional (+) or non-functional (-) CB_2-receptor.

Identification of several SPT splice variants

A systematic EST (Expressed Sequence Tag) database screen was performed to search for potential splice variants of SPT. This revealed several possible splice variants for both SPT subunits.

hSPTLC1-N143, a splice variant of SPTLC1, is composed of the first 143 amino acids of the N-terminus. For SPTLC2, three splice variants were found. hSPTLC2-N162 contains 162 amino acids of the N-terminus and hSTPLC2-N204, is composed of the N-terminal 204 amino acids. A third splice variant of SPTLC2, namely hSPTLC2-C293, possesses 293 amino acids of the C-terminal end, thereby including the PLP binding motif -the catalytic center of the condensation reaction. Previous research in our group discovered that mRNA of these

splice variants is expressed in a tissue specific manner and is also detectable on the protein level (data not shown). Three of these potential splice variants correlate in size with the smaller proteins that were detected in the cell lines (hSPTLC2-C293 32kDa, hSPTLC2-N204 25kDa and hSPTLC1-N143 25kDa, Figure 1F). However, cloning and individual over-expression of theses splice variants in HEK293 cells affects neither SPT activity nor cell growth (not shown).

II. Monitoring dSL generation during monocyte to macrophage differentiation

Deoxy-sphingolipids were found at considerable concentrations in macrophages but were hardly present in monocyte cell lines like THP1 or HL60 cells (Figure 1E). We therefore set out to monitor dSL levels during PMA (phorbol-12-myristate-13-acetate) stimulated differentiation of THP1 monocytes into macrophages. After the addition of PMA to cultured THP1 cells, they start to differentiate in a time-dependant manner into macrophages. The differentiation status can be monitored by the up-regulation of macrophage specific surface markers like CD14 or CD16[15]. To analyze exclusively the *de novo* generated products of SPT during the differentiation period, we used Fumonisin B1, a potent inhibitor of CerS to block the downstream pathway (Figure 1A)[16]. This blockage leads to a time dependant accumulation of SPT products that directly correlate with SPT activity. After the addition of PMA to cultured THP1 cells (time point 0), FB1 was additionally added after 0, 5, 10, 21, 46, 71 and 96 hours of PMA supplementation. After 24h of FB1 incubation and hence pathway blockage, the cells were harvested, and the lipids were extracted and base hydrolysed, enabling only the non-acylated (lyso-) sphingolipids to be included in the analysis. The SPT *de novo* products sphinganine (SA) and deoxy-sphinganine (deoxySA) were analysed by LC-MS and quantified relative to the synthetic internal standard C17SO.

Deoxy-sphingolipid generation increased during PMA stimulated differentiation of monocytes into macrophages

During the PMA stimulated differentiation of monocytes into macrophages, no SA was generated by SPT upon FB1 inhibition (Figure 2A, Supplementary Figure 1A). In contrast, 21 hours after PMA addition, SPT started to generate the alanine-derived dSLs (deoxySA and deoxySO) in the presence of FB1 (80pmol/1mio cells). The generation of these dSLs increased in an almost linear manner during the differentiation process and reached a total of 600pmol/1mio cells after 96 hours (Figure 2A, Supplementary Figure 1B). Thus, the more the monocytes differentiated into the macrophage-like phenotype, the more dSLs were generated.

To compare the effect of PMA in another cell line, we chose HEK293 cells as they were also able to generate dSLs (Figure 1E).

A: B:

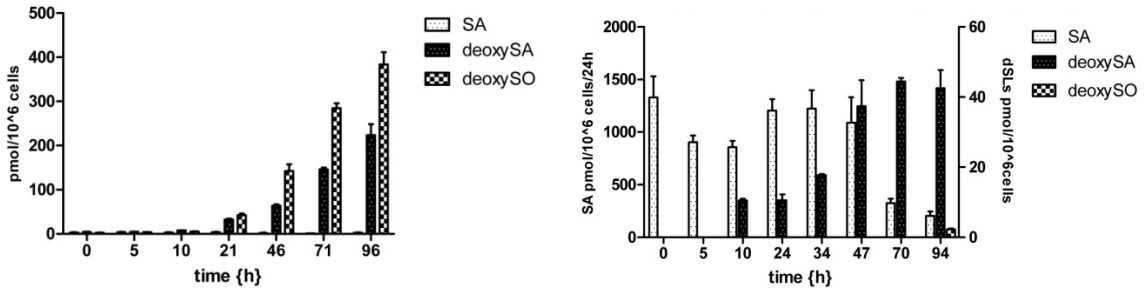

FIGURE 2A+B**: SPT activity in PMA stimulated THP1 cells and HEK293 cells**
THP1 (A) and HEK293 cells (B) were cultured in the presence of 200nM PMA (given at timepoint 0). At each indicated time point (0, 5, 10, 21, 46, 71, 96h), FB1 (13.85uM) was added to the cells and incubated for 24h, leading to an accumulation of the direct SPT products SA and deoxySA (Figure 1A). Cells were harvested, and lipids were base extracted allowing the free (non-acylated) sphingoid bases to be measured with LC-MS. Sphingoid bases were quantified relative to the internal extraction standard (C17SO) and to 1 mio cells.

HEK cells accumulated SA steadily up to 1200 pmol in the first 47 hours of the culture period, but after 70 and 94hours only 200-300pmol of SA was accumulated (Figure 2B, Supplementary Figure 1C). HEK293 cells also generated increasing amounts of dSLs during this period but to a lesser degree than THP1 cells during differentiation. In THP1 cells, dSL levels reached 600pmol in sum (deoxySO+deoxySA), whereas HEK cells accumulated 40pmol in the late culture phase (Figure 2A+B, Supplementary Figure 1C). Upon FB1 stimulation, HEK cells produced deoxySA, but deoxySO was not detected in higher amounts (Figure 2B). In the presence of FB1, CerS is potently inhibited, thus preventing N-acylation, further metabolism by DES, and hence the formation of its downstream products SO or deoxySO (Figure 1A). In this context, it is surprising that the alanine-derived downstream product deoxySO is being generated during THP1 differentiation in an even higher amount than its precursor deoxySA, despite the presence of FB1 (Figure 2A, Supplementary Figure 1A).

FB1 is a known activator of PKC[17, 18]. On the other hand, sphingoid bases like SO and SA, that accumulate upon FB1 treatment, were reported to inhibit PKC[19]. In the presence of PMA, THP1 cells, in contrast to HEK cells, failed to accumulate SA upon FB1 stimulation. Therefore activation of PKC by FB1 is not influenced by delayed accumulation of SA. Prior to the addition of PMA (see timepoint -24h in Supplemental Figure 1A) THP1 cells do

accumulate SA upon FB1 stimulation, suggesting that PMA interferes with the FB1-related CerS inhibition.

C: D:

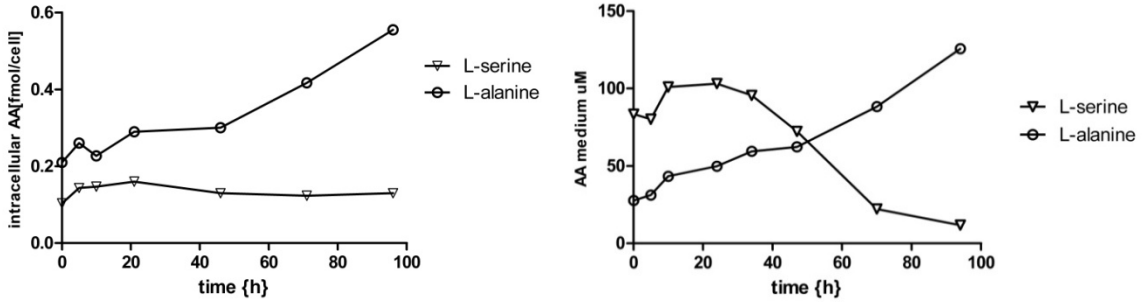

FIGURE 2C+D: **Intracellular amino acid levels in THP1 cells during differentiation (C) and in the culture media of HEK293 cells during culture (D)**
Intracellular aminoacid levels were measured in the watery phase that was collected during the process of lipid extraction (see experimental procedures). Aminoacids (intracellular or in the culture medium) were derivatized using OPA-MPA and analysed by HPLC relative to the internal standard (beta-aminobutyrate).

We included the measurement of the intracellular amino acids substrates, L-serine and L-alanine, in THP1 cells in this set-up (Figure 2C) and compared it to the amino acid levels in the media during HEK cell culture (Figure 2D) as intracellular levels in HEK293 cells could not be measured due to technical problems.

In THP1 cells we observed an increase in the intracellular L-alanine concentration (0.25 fmol-0.6 fmol per cell) during the differentiation that correlated with the increased dSL generation (Figure 2A+C). At the same time, the intracellular L-serine concentration did not increase during the differentiation process and stagnated at 0.1-0.13 fmol per cell (Figure 2C). In HEK cells, L-alanine increased in the culture medium, whereas L-serine decreased (Figure 2D). Thus, the amino acid levels in the culture media correlated with the generated SA and deoxySA in HEK cells. These data suggest that dSLs increase correlates to a general increase in alanine.

FB1 increased the generation of deoxySO during PMA stimulated THP1 differentiation

Analysing the influence of FB1 on deoxySO levels revealed, that in the late culture phase, free deoxySO levels in the presence of FB1 were higher, compared to their total cellular amount without FB1 treatment (Figure 2E). The levels of the precursor metabolite deoxySA were not different when analyzed in these two conditions (Figure 2F). This indicates that FB1 stimulated deoxySO generation without changes in deoxySA levels. As there is neither accumulation of SA throughout the differentiation process (Figure 2A) the apparent

contradiction of deoxySO generation in the presence of FB1 might be explained by an interference of PMA with FB1 innhibition. This is supported by the observation that prior the addition of PMA to THP1 cells (at timepoint -24h), the cells accumulated SA upon FB1 stimulation (Supplemental Figure 1A). It has been reported that FB1 stimulates dSL generation, although the mechanism was not described[6]. Here, we confirm the increase of dSL generation by FB1 in THP1-derived macrophages, with the notion that the increased dSL species is deoxySO and not deoxySA, as expected in the presence of FB1.

E:

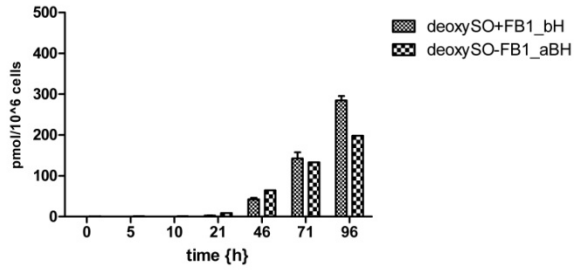

F:

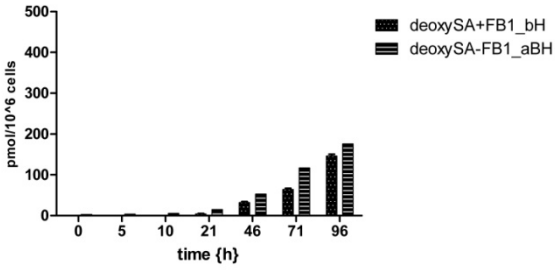

FIGURE 2E+F: **Deoxy-sphingoid base levels in THP1 cells in the presence and absence of FB1**

THP1 cells were grown in the presence of 200nM PMA added at time point 0. At each indicated time point (0, 5, 10, 21, 46, 71, 96h) the cells were harvested and the lipids were acid-base hydrolysed (aBH) or in the case of FB1 treatment, base-hydrolysed (bH), allowing only the free (non-acylated) deoxy-sphingoid bases to be included in the measurement with LC-MS. FB1 (13.85uM) was added to the cells 24h prior to harvesting. For example at 46h harvest: FB1 was added 22h after PMA addition and further cultured for 24h. Sphingoid bases were quantified relative to the internal extraction standard (C17SO) and to 1 mio cells.

SPT protein expression profile changed in a controlled manner during differentiation that correlated temporally with the increase in dSLs

Ninety-six hours after PMA stimulation, THP1 monocytes differentiated into macrophages, a process that was monitored by the up-regulation of the macrophage surface marker CD14 (Figure 2G). Analyzing the SPT expression profile of THP1 cells during differentiation revealed the up-regulation of both SPT subunits (SPTLC1 -55kDa and SPTLC2 -62kD), which was more pronounced for the SPTLC2 subunit (Figure 2G).

Besides the SPTLC2 subunit, two other SPTLC2 immunoreactive bands with approximate molecular weight of 32kDa and 25kDa could be detected. The 25kDa protein expression decreased during differentiation whereas the 32kDa protein was stably expressed. The 32kDa protein was detected in other cell lines as well, whereas the 25kDa protein was exclusively expressed in monocyte cell lines like THP1 or HL60 cells (Figure 1F). However, analyzing the peptides corresponding to the two small SPTLC2 proteins, after separation on an SDS-

PAGE and an in-gel digestion, did not reveal SPTLC2 specific peptides using shotgun mass spectrometry analysis (data not shown). Therefore we could not confirm that these small proteins are splice variants of the SPTLC2 full length protein.

The analysis of SPT protein expression profile during PMA stimulated differentiation revealed a change in the expression of SPT subunits. The timecourse of SPTLC2 expression correlated universely with the timecourse of 25kDa SPTLC2 expression. At the same time, L-alanine started to accumulate in the cells (Figure 2C) and dSL levels increased (Figure 2A).

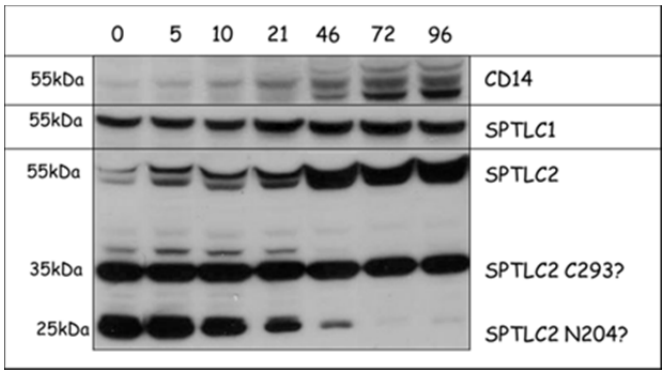

FIGURE 2G: **SPT protein expression in THP1 during differentiation**
Total protein was extracted and separated on a 12% SDS-PAGE. Differentiation status was monitored via CD14 (1:1000) up-regulation. SPTLC1 (1:1500) and SPTLC2 (1:1250) antibodies[3] were used to monitor the expression profile of the SPT subunits and their potential splice variants. Indicated sizes according to molecular size standard (PageRuler^{TM}, Thermo Scientific).

<u>The generation of deoxySO and the increase in intracellular L-alanine but not the increase in deoxySA are dependent on the presence of PMA in THP1 cells</u>

It has been reported that dSLs increase with the duration of culture[6]. To investigate whether the increased generation of dSLs during THP1 differentiation is due to the differentiation status and not caused by any culturing effect, we compared the total amount of dSLs in THP1 cells in the presence or absence of PMA. The early dSL metabolite deoxySA was not affected by the presence of PMA (Figure 3A). In contrast, its downstream metabolite deoxySO was generated only in presence of PMA (Figure 3B). Intracellular L-alanine levels also increased only upon PMA stimulation whereas intracellular L-serine levels were not affected by the PMA treatment (Figure 3E). The presence of PMA lead to increased concentrations of serine-derived sphingoid bases (SO and SA) compared to non-PMA treated (Figure 3C+D).

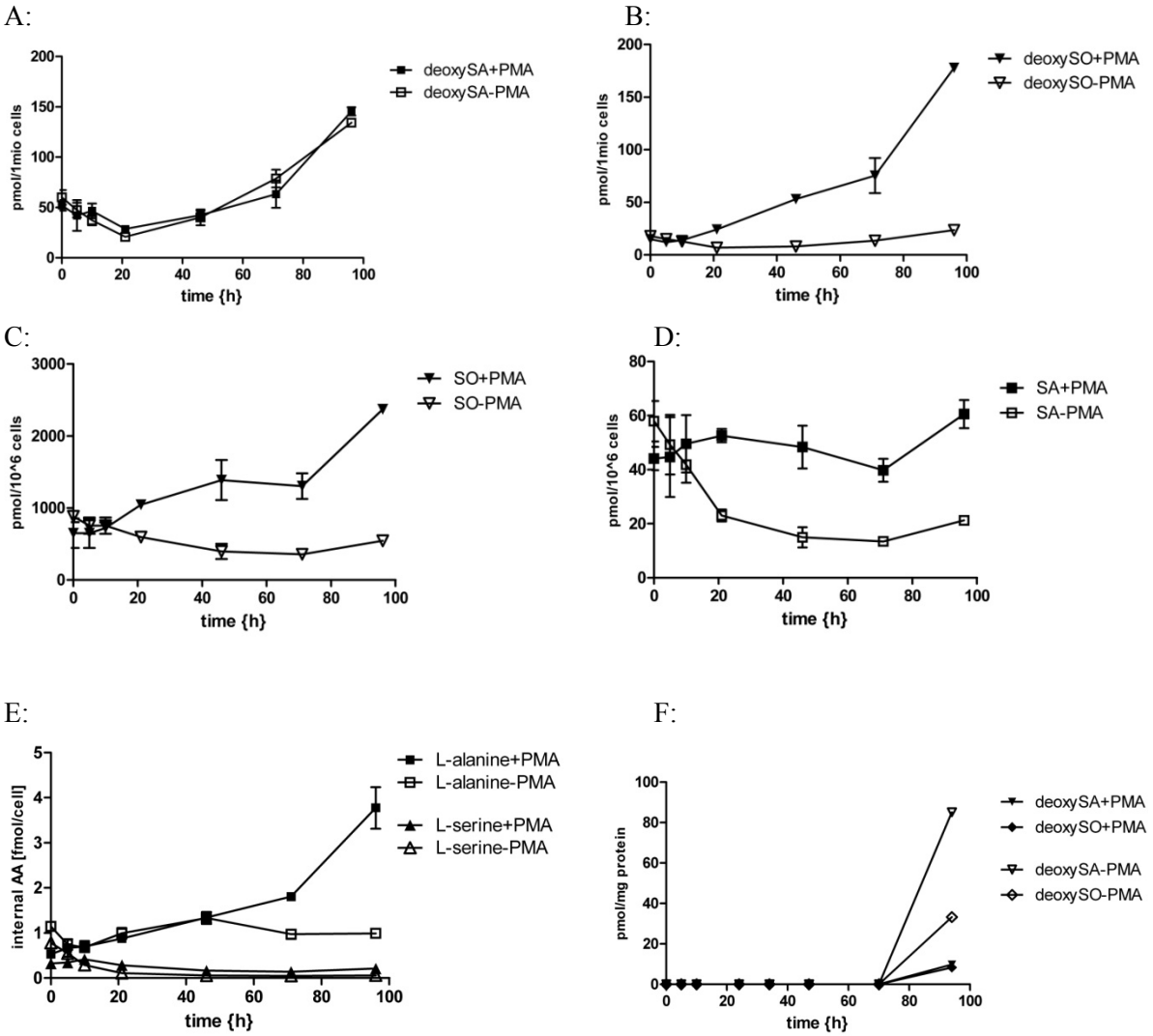

FIGURE 3: **Effect of PMA on the sphingolipid and intracellular amino acid profile**
THP1 (**A-D**) and HEK293 (**F**) cells were cultured either in the presence or absence of 200nM PMA (added at time point 0). After 5, 10, 21, 46, 71 and 96 hours, the cells were harvested, and the lipids were extracted, acid-base hydrolysed and analysed with LC-MS. Resulting sphingoid bases were quantified relative to the respective internal standard (THP1 cells C17SO, HEK293 d7 SO) and per 1 mio cells. (**E**) Intracellular aminoacid levels in THP1 cells were measured in the watery phase that was collected during the process of lipid extraction (see experimental procedures). Intracellular aminoacids were analysed by HPLC relative to the internal standard beta-aminobutyrate.

In HEK293 cells PMA had an opposing effect, as it inhibited deoxySA and deoxySO generation during culture (Figure 3F). As the serine-derived sphingoid bases were not affected by PMA during HEK cell culture (not shown), the inhibition effect of PMA was specific for the alanine-derived sphingoid bases. PMA belongs to the family of phorbolesters and is a potent direct activator of cPKCs and nPKCs [20-22]. In contrast to diacylglycerol, which only transiently activates PKC, PMA stimulates PKC irreversibly. It is well known that PKC isozymes can have unique and sometimes opposing roles in signalling or disease states[23, 24]. It has even been reported that the same isozyme can lead to ambiguous responses in the same

cell line, depending on the context of the stimuli[25]. This could explain the different responses of the THP1 and HEK293 cells to the PMA treatment. In THP1 cells we observed a PMA dependent increase of deoxySO, while deoxySA levels were unchanged. This could be explained by the activation of SPT and its downstream enzymes (CerS and DES) by PMA via PKC, that would result in a rapid metabolism of deoxySA to deoxySO. On the other hand, PMA could inhibit the degradation of deoxySO.

The increased generation of dSLs during monocyte to macrophage differentiation was confirmed in primary human macrophages

In line with the results reported above on dSL formation, dSL levels also increased in primary human monocytes during differentiation into macrophages (Figure 4A). Likewise, the major dSL metabolite was deoxySO (90pmol/mg protein) compared to deoxySA (58pmol/mg protein). The total SL content was also increased in primary human macrophages during differentiation (Figure 4A).

A:

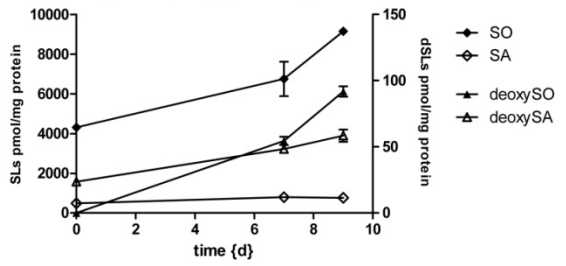

B:

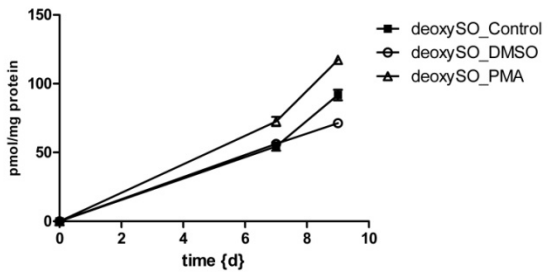

C:

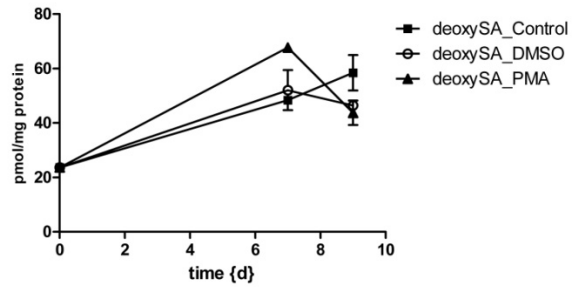

D:

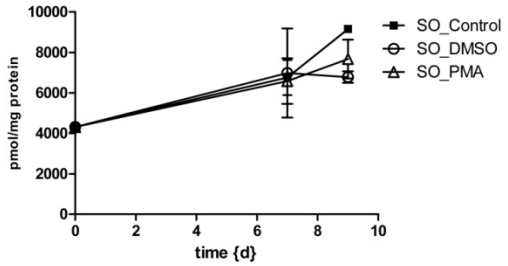

E:

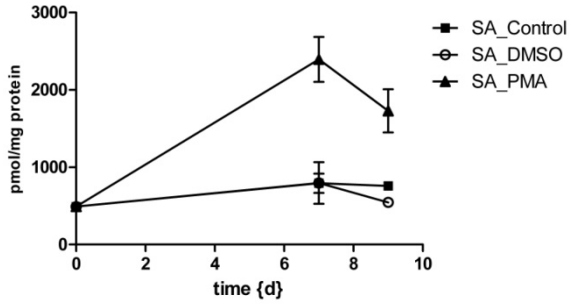

FIGURE 4: **Sphingolipid profile in human macrophages**
Monocytes were isolated from human buffy coats and cultured for 9 days for differentiation into macrophages. At day 6, no treatment (A), PMA or solvent (B-E) was added to the cells. Cells were harvested at day 0, 7 and 9, lipids were extracted and acid-base hydrolysed, and the total SL and dSL content was measured using LC-MS relative to the internal standard (d5 deoxymethyl-sphinganine) and 1 mg total protein.

To control for a possible PMA-related effect, at day 6 PMA and DMSO (solvent) were added to the cells. Due to limited material no aliquot was harvested at day 6 at the time of treatment. Therefore the SL and dSL levels at day 6 are not known, hampering the determination of the exact increase at day 7 and 9 (Figure 4B-E). Nevertheless, at day 7 and 9, the deoxySO content in PMA treated cells was slightly higher than in untreated cells (Figure 4B) whereas total SO content was faintly decreased (Figure 4D). Besides, aminoacids in the culture medium were analysed. We observed an increase in L-alanine during the differentiation that was accompanied by a decrease in L-serine (Figure 4F).

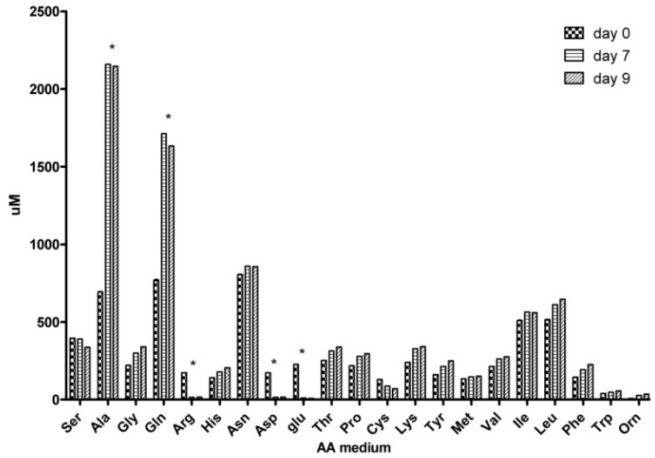

FIGURE 4F: **Aminoacid profile in the media measured during culture of human macrophages**
Aminoacid measurement was carried out at the Functional Genomic Center Zürich
http://www.fgcz.ch/supportmodes/proteinservice/aminoacidanalysis

We did not measure the intracellular amino acid levels, and hence do not know if the alanine concentration in the cells followed the same pattern and increased during the differentiation. In this context we also detected changes of other amino acids in the culture media during differentiation (Figure 4F). Analysing the protein expression during differentiation confirmed the up-regulation of SPTLC1 as well as SPTLC2 in primary monocyte-derived macrophages (Figure 4G). Next to the full length SPTLC proteins, smaller anti-SPTLC1 and anti-SPTLC2 35kDa bands were detected. The expression of the smaller SPTLC1 but not of the smaller SPTLC2 protein was up-regulated during the differentiation (Figure 4G).

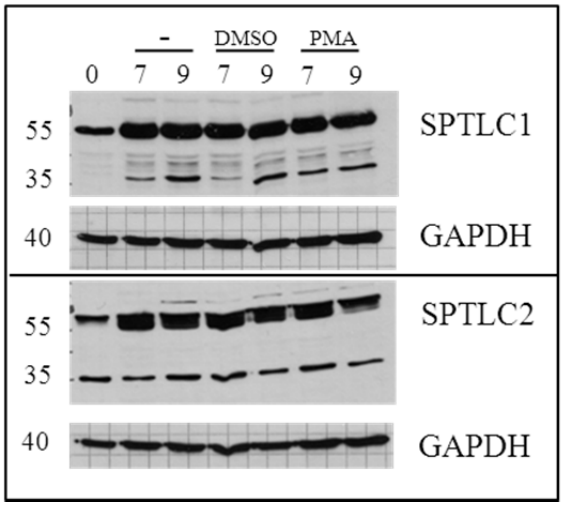

FIGURE 4G: **Expression profile of SPT proteins in human macrophages**
Total protein was extracted and separated on a 12% SDS-PAGE. SPTLC1 (1:1500) and SPTLC2 (1:1250) antibodies[3] were used to monitor the expression profile of the SPT subunits; GAPDH (1:5000, Abnova) was used as the loading control. Indicated sizes according to molecular size standard (PageRuler™, Thermo Scientific)

Conclusions and outlook

We showed that dSLs generation is increased during PMA driven THP1 differentiation, an event that is accompanied by the intracellular accumulation of L-alanine. The generation of deoxySO was dependent on the presence of PMA, and was paradoxically increased by the upstream CerS inhibitor FB1. The PMA/FB1 dependant deoxySO generation was specific to THP1 macrophages. In HEK cells we rather observe the opposite effect, namely inhibited dSL generation. Phorbolesters like PMA as well as Fumonisin B1 are strong activators of PKC that both interact with the diacyglycerol binding site of PKC[17, 18]. By contrast, sphingoid bases like SO and SA, were reported to inhibit PKC[19]. Increased activation of PKC isoforms is involved in many diseases [26-34] including diabetic complications, like diabetic neuropathy[35, 36]. In this context it is interesting to note that dSLs were shown to be elevated in the metabolic syndrome with the later risk of T2D[11, 12]. Whether PKC activation is involved in the signalling events that contribute to the generation of dSLs in general, or specifically in the monocyte-macrophage context, needs to be addressed in detail by using specific inhibitors/activators of the various PKC isoforms.

We confirmed increased dSL generation in human primary monocyte-derived macrophages. Interestingly this was independent of PMA stimulation. This further establishes a physiological relevance for dSLs. The question why dSL are generated during macrophage maturation is not clear yet.

Monocyte recruitment into inflamed vessels is believed to promote atherosclerosis. A functional link between sphingolipids and cholesterol efflux of macrophages was described by Tamehiro *et al.* He and his colleagues identified the SPTLC1 subunit as a binding partner of ABCA1 in THP1 monocyte-macrophages as well as in mouse liver. Binding of ABCA1 to SPTLC1 was found to inhibit cholesterol efflux activity, thereby maximizing the cellular cholesterol in cells with a demand in membrane synthesis[37]. Moreover Par3, a scaffolding factor that recruits signaling molecules into multiprotein complexes, was identified as another binding partner of SPTLC1 in THP1-derived macrophages. The knock-down of Par3 or SPTLC1 both decreased SPT activity and chemotaxis-induced migration of THP1 monocytes[38]. If dSLs are involved in these events needs to be addressed in future experiments.

Footnotes

This work was supported by the Forsschungskommision Zürich.

We thank Dr. Peter Hunziker from the Functional Genomic Center Zürich for the analysis of the amino acids in the media of primary monocytes during differentiation into macrophages.

Supplementary information

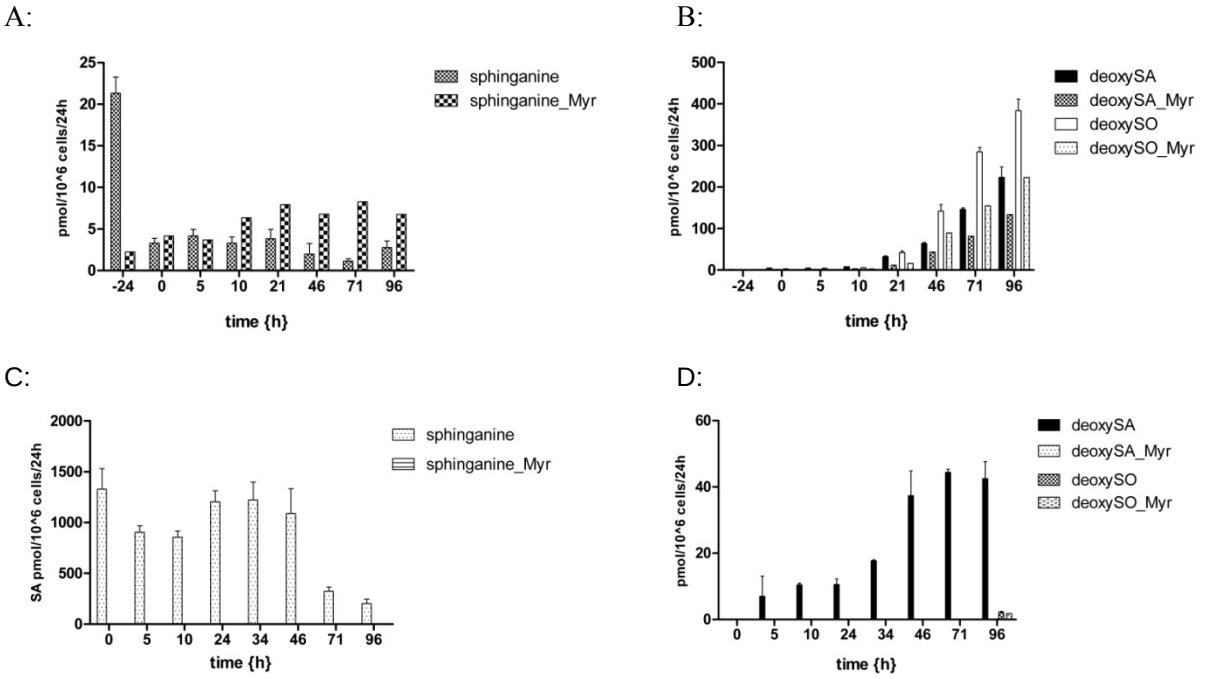

SUPPLEMENTARY FIGURE 1: **Myriocin controls for FB1 treated cells**
THP1 cells (A+B) and HEK293 cells (C+D) were grown in presence of 200nM PMA and supplemented with 13.85mM FB1 that blocks CerS and leads to an accumulation of SPT products. PMA was added at time point 0, FB1 was given at indicated time points and incubated for another 24h. Note: at time point -24h in THP1 cells no PMA was present. To control for an FB1 related sphingoid base accumulation, myriocin that blocks SPT, was added together with FB1 in a separate set-up.

References

1. Hanada K. Serine palmitoyltransferase, a key enzyme of sphingolipid metabolism. Biochimica et Biophysica Acta (BBA) - Molecular and Cell Biology of Lipids 2003;1632:16-30.
2. Han G, Gupta SD, Gable K, et al. Identification of small subunits of mammalian serine palmitoyltransferase that confer distinct acyl-CoA substrate specificities. Proceedings of the National Academy of Sciences 2009;106:8186-8191.
3. Hornemann T, Richard S, Rütti MF, Wei Y, von Eckardstein A. Cloning and Initial Characterization of a New Subunit for Mammalian Serine-palmitoyltransferase. Journal of Biological Chemistry 2006;281:37275-37281.
4. Hornemann T, Wei Y, von eckardstein A. Is the mammalian serine palmitoyltransferase a high-molecular-mass complex? Biochem J 2007;405:157-164.
5. Penno A, Reilly MM, Houlden H, et al. Hereditary Sensory Neuropathy Type 1 Is Caused by the Accumulation of Two Neurotoxic Sphingolipids. Journal of Biological Chemistry 2010;285:11178-11187.
6. Zitomer NC, Mitchell T, Voss KA, et al. Ceramide Synthase Inhibition by Fumonisin B1 Causes Accumulation of 1-Deoxysphinganine. Journal of Biological Chemistry 2009;284:4786-4795.
7. Rotthier A, Auer-Grumbach M, Janssens K, et al. Mutations in the SPTLC2 Subunit of Serine Palmitoyltransferase Cause Hereditary Sensory and Autonomic Neuropathy Type I. The American Journal of Human Genetics 2010;87:513-522.
8. Rotthier A, Penno A, Rautenstrauss B, et al. Characterization of two mutations in the SPTLC1 subunit of serine palmitoyltransferase associated with hereditary sensory and autonomic neuropathy type I. Human Mutation 2011;32:E2211-E2225.
9. Martinez T, Chen X, Bandyopadhyay S, Merrill A, Tansey M. Ceramide sphingolipid signaling mediates Tumor Necrosis Factor (TNF)-dependent toxicity via caspase signaling in dopaminergic neurons. Molecular Neurodegeneration 2012;7:45.
10. Bertea M, Rutti M, Othman A, et al. Deoxysphingoid bases as plasma markers in Diabetes mellitus. Lipids in Health and Disease 2010;9:84.
11. Othman A, Rütti M, Ernst D, et al. Plasma deoxysphingolipids: a novel class of biomarkers for the metabolic syndrome? Diabetologia 2012;55:421-431.
12. Brozinick JT, Hawkins E, Hoang Bui H, et al. Plasma sphingolipids are biomarkers of metabolic syndrome in non-human primates maintained on a Western-style diet. Int J Obes 2012.
13. Huang S, Cheng T-Y, Young DC, et al. Discovery of deoxyceramides and diacylglycerols as CD1b scaffold lipids among diverse groove-blocking lipids of the human CD1 system. Proceedings of the National Academy of Sciences 2011;108:19335-19340.
14. Riley RT, Norred WP, Wang E, Merrill AH. Alteration in sphingolipid metabolism: bioassays for fumonisin- and ISP-I-like activity in tissues, cells and other matrices. Natural Toxins 1999;7:407-414.
15. Daigneault M, Preston JA, Marriott HM, Whyte MKB, Dockrell DH. The Identification of Markers of Macrophage Differentiation in PMA-Stimulated THP-1 Cells and Monocyte-Derived Macrophages. PLoS ONE 2010;5:e8668.
16. Wang E, Norred WP, Bacon CW, Riley RT, Merrill AH. Inhibition of sphingolipid biosynthesis by fumonisins. Implications for diseases associated with Fusarium moniliforme. Journal of Biological Chemistry 1991;266:14486-14490.
17. Gopee NV, Sharma RP. Selective and transient activation of protein kinase C α by fumonisin B1, a ceramide synthase inhibitor mycotoxin, in cultured porcine renal cells. Life Sciences 2004;74:1541-1559.
18. Yeung JM, Wang H-Y, Prelusky DB. Fumonisin B1Induces Protein Kinase C Translocation via Direct Interaction with Diacylglycerol Binding Site. Toxicology and Applied Pharmacology 1996;141:178-184.
19. Smith ER, Jones PL, Boss JM, Merrill AH. Changing J774A.1 Cells to New Medium Perturbs Multiple Signaling Pathways, Including the Modulation of Protein Kinase C by Endogenous Sphingoid Bases. Journal of Biological Chemistry 1997;272:5640-5646.
20. Rovera G, O'Brien T, Diamond L. Induction of differentiation in human promyelocytic leukemia cells by tumor promoters. Science 1979;204:868-870.
21. Niedel JE, Kuhn LJ, Vandenbark GR. Phorbol diester receptor copurifies with protein kinase C. Proceedings of the National Academy of Sciences 1983;80:36-40.
22. Castagna M, Takai Y, Kaibuchi K, Sano K, Kikkawa U, Nishizuka Y. Direct activation of calcium-activated, phospholipid-dependent protein kinase by tumor-promoting phorbol esters. Journal of Biological Chemistry 1982;257:7847-7851.
23. Chen L, Hahn H, Wu G, et al. Opposing cardioprotective actions and parallel hypertrophic effects of δPKC and εPKC. Proceedings of the National Academy of Sciences 2001;98:11114-11119.

24. Murriel CL, Mochly-Rosen D. Opposing roles of δ and εPKC in cardiac ischemia and reperfusion: targeting the apoptotic machinery. Archives of Biochemistry and Biophysics 2003;420:246-254.
25. Basu A, Pal D. Two Faces of Protein Kinase Cδ: The Contrasting Roles of PKCδ in Cell Survival and Cell Death. TheScientificWorldJOURNAL 2010;10:2272-2284.
26. Bowling N, Walsh RA, Song G, et al. Increased Protein Kinase C Activity and Expression of Ca2+-Sensitive Isoforms in the Failing Human Heart. Circulation 1999;99:384-391.
27. Dempsey EC, Cool CD, Littler CM. Lung disease and PKCs. Pharmacological Research 2007;55:545-559.
28. Ishii H, Jirousek MR, Koya D, et al. Amelioration of Vascular Dysfunctions in Diabetic Rats by an Oral PKC β Inhibitor. Science 1996;272:728-731.
29. Koyanagi T, Noguchi K, Ootani A, Inagaki K, Robbins RC, Mochly-Rosen D. Pharmacological inhibition of epsilon PKC suppresses chronic inflammation in murine cardiac transplantation model. Journal of Molecular and Cellular Cardiology 2007;43:517-522.
30. Li JUN, Gobe G. Protein kinase C activation and its role in kidney disease (Review Article). Nephrology 2006;11:428-434.
31. Michie AM, Nakagawa R. The link between PKCα regulation and cellular transformation. Immunology Letters 2005;96:155-162.
32. Simonis G, Braun MU, Kirrstetter M, Schön SP, Strasser RH. Mechanisms of Myocardial Remodeling: Ramiprilat Blocks the Expressional Upregulation of Protein Kinase C-[epsilon] in the Surviving Myocardium Early After Infarction. Journal of Cardiovascular Pharmacology 2003;41:780-787.
33. Tuttle KR. Protein kinase C-β inhibition for diabetic kidney disease. Diabetes Research and Clinical Practice 2008;82, Supplement 1:S70-S74.
34. Palaniyandi SS, Sun L, Ferreira JCB, Mochly-Rosen D. Protein kinase C in heart failure: a therapeutic target? Cardiovascular Research 2009;82:229-239.
35. Geraldes P, King GL. Activation of Protein Kinase C Isoforms and Its Impact on Diabetic Complications. Circulation Research 2010;106:1319-1331.
36. Nishikawa T, Edelstein D, Brownlee M. The missing link: A single unifying mechanism for diabetic complications. Kidney Int 2000;58:S26-S30.
37. Tamehiro N, Zhou S, Okuhira K, et al. SPTLC1 Binds ABCA1 To Negatively Regulate Trafficking and Cholesterol Efflux Activity of the Transporter†. Biochemistry 2008;47:6138-6147.
38. Tamehiro N, Mujawar Z, Zhou S, et al. Cell Polarity Factor Par3 Binds SPTLC1 and Modulates Monocyte Serine Palmitoyltransferase Activity and Chemotaxis. Journal of Biological Chemistry 2009;284:24881-24890.

General Conclusions

Canonical SPT activity: The enzymatic reaction and the influence of the metabolic context

In chapter 1 we described a novel HSAN I-causing mutation (A182P) in the SPTLC2 subunit. SPT activity of this mutant was analyzed in transfected HEK293 cells in a cell-free assay and in living cells using metabolic labeling. The A182P mutation showed a decreased activity with L-serine in cell-free conditions although the cell-based metabolic labeling assay revealed no differences in the *de novo* formation of sphingolipids in mutant-expressing cells compared to wt cells (chapter 1, Figure 4A+C). We therefore assumed that SPT activity within the cells is generally reduced due to metabolic feedback inhibition when enough sphingolipids can be provided from external sources (serum or lipoproteins from medium). In these conditions the activity of the mutant SPT might be nevertheless sufficient to provide enough *de novo* generated sphingolipids although the Vmax of the mutant seems to be reduced as shown in the cell-free assay (chapter 1, Figure 4A). A recent report supports this concept by demonstrating that SPT activity in cultured cells is largely inhibited under normal medium conditions. This inhibitory effect is probably mediated by ORMDL proteins and yet unknown additional factors which seem to be present in the serum of the culture media[1].

Deoxy-sphingolipid generation: Different mechanisms can lead to the same result

In this report we showed for the first time that dSL formation in a cell-free environment is increased in SPT with specific mutations compared to the wt enzyme. This indicates that dSLs are generated due to a structural impact of these mutations on the enzyme resulting in a decreased activity with serine and an increased activity with alanine. The new A182P mutation showed, like most HSAN I mutations, a reduced canonical activity and resulted additionally in increased dSL generation in isolated proteins and also in living cells (Figure 1A-C). This was not observed for some other HSAN I mutations. Comparing different SPT HSAN I mutants revealed that not all of them exhibit activity with alanine in a cell-free environment (Figure 1B). Analyzing activity in isolated proteins, only the here described SPTLC2-A182P, -S384F, and to a minor extent -I504F resulted in a direct formation of dSLs, whereas SPTLC2-G382V, -T409M and V359M along with two analyzed SPTLC1-mutants, -

General conclusions

C133W and -S331F, did not show formation of dSLs in isolated proteins (Figure 1B+chapter 2, Figure 7A).

A:

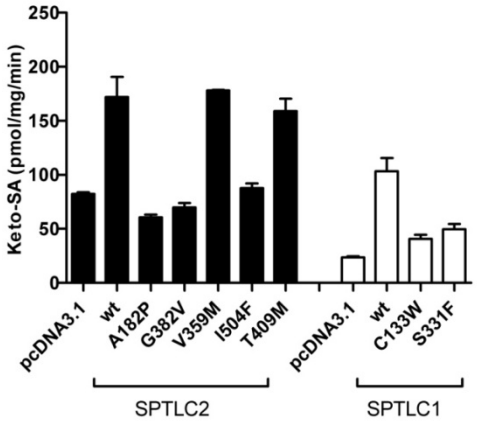

B:

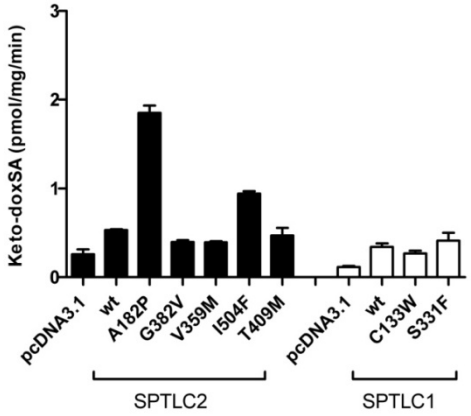

C:

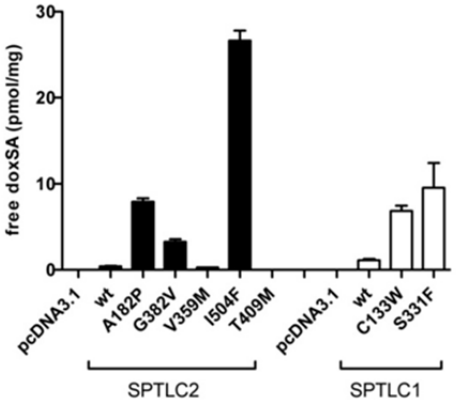

FIGURE 1: **Comparison of SPT activity in HSAN I mutants in cell-free conditions**
SPT activity was analyzed in isolated protein of HEK293 cells which were stably transfected with vector control (pcDNA3.1), wildtype (SPTLC2), SPTLC2 (A182P, G382V, V359M, I504F, T409M) and SPTLC1 (C133W, S331F) mutations that are causing HSAN I.
The activity was determined in the presence of **(A)** L-serine or **(B)** L-alanine. **(C)** Free (non-acylated) deoxySA that was generated in the cells during culture. Sphingoid bases (after base extraction) were quantified relative to internal extraction standards (d7SO and d7SA) and 1mg of total protein.

However, all HSAN I mutations which were also genetically confirmed were associated with an increased dSL formation in transfected cells (Figure 1C)[2-6]. Elevated dSL levels were also confirmed in available plasma samples of HSAN I patients[2-6]. This indicates that dSL generation can be based on different mechanisms. Those mutants that show a significant activity with alanine in cell-free conditions probably directly affect the SPT structure, whereas those which fail to have this effect, but increase dSL formation in living cells might require additional cellular factors to metabolize alanine. Furthermore, a phosphorylation site (S384)

in SPTLC2 that has been identified in a global screen[7], was shown to be involved in regulating the activity of SPT with L-serine and L-alanine, respectively. We showed that mimicking a permanently phosphorylated serine384 (S384D) resulted in a robust increase in dSL generation in isolated proteins and in living cells (chapter 2, Figure 4B+5A). Remarkably, a very similar S384E mutation did not show this effect, indicating that dSL formation by the S384D mutation is specific and not simply caused by an arbitrary aminoacid exchange at residue 384. In that context we also reported a second novel HSAN I mutation (S384F) that resides at the very same position and results in the same activity shift as was observed for the S384D mutant. We therefore speculated that either phosphorylation or the exchange of the S384 with a bulky amino acid like phenylalanine induces a structural change in SPT which leads to the observed shift in activity. However, this hypothesis needs to be further proven by identifying the kinase which is responsible for the phosphorylation of SPTLC2. As a consequence of our findings an activation of this kinase should also result in increased dSL formation.

Those HSAN I mutations (SPTLC2-G382V; T409M; V359M; SPTLC1 -C133W;-S331F) that do form dSLs in cellular but not in cell-free conditions probably have a different mechanism to generate dSLs. These HSAN I mutations possibly affect the binding or activity of a factor which might co-regulate dSL formation. In addition, factors which regulate the cellular amino acid levels could also be directly or indirectly involved in regulating the dSLs. It can be speculated that SPT itself might also influence amino acid synthesis or transportation. This assumes that sphingolipid and amino acid synthesis (e.g. serine and alanine) are functionally connected. The previously reported Serinc proteins might provide this missing link. Serinc was reported to connect SPT with PGDH, the first enzyme in the serine synthesis pathway[8]. A more indirect link between these two pathways was reported in yeast, where sphingolipid synthesis increased upon amino acid starvation, which is first sensed by the Npr2/Npr3 complex[9] and results in the phosphorylation of ORM1 via the TORC1 downstream effector kinase Npr1[10]. The increase in complex sphingolipids was suggested to stimulate the nutrient scavenging general amino acid Gap1 permease activity at the plasma membrane as a response to starvation[11]. To investigate this in more detail, future experiments need to analyze the composition of the mammalian SPT complex, especially comparing wt and HSAN I mutants. Another difference we observed between HSAN I mutants and phosphorylation mimicking mutants was the type of generated deoxy-ceramides. We showed in previous work that dSLs in HSAN I cells are predominantly present as non-acylated sphingoid bases[12], whereas dSLs formed by the wt enzyme[13] or in the phospho-mutant S384D were mostly found in their

acylated form as deoxy-(dihydro)-ceramide (chapter 2, Figure 5D). This suggests that the HSAN I mutations have an inhibitory effect on the activity of ceramide synthase (CerS). Free sphingoid bases but not the acylated forms, were shown to inhibit PKC[14, 15]. Therefore, free deoxy-sphingoid bases which are generated by the HSAN I mutants might induce a different signaling pathway via the inhibition of PKC and consequent downstream signaling events.

Figure 2 shows a structural model with the positions of all reported SPTLC2 HSAN I mutations and the here characterized phospho-mutations in *S. multivorum* (PDB: 3A2B). According to this structure, one can speculate that the proximity to the PLP-binding motif (around Lys379) and thus the interference with the binding pocket for the amino acid substrate might influence the binding of the canonical substrate L-serine. In that sense, Thr409, Gly382 (corresponding HSAN I mutations: T409M, G382V) are pointing away from the binding pocket and have probably no impact on the amino acid substrate binding. These mutants did neither generate dSLs in cell-free conditions, whereas Ser384 and Ala182, which are pointing towards the binding pocket, show robust dSL formation also in the absence of living cells. However, Ile504 (HSAN I mutation: I504F) is located far outside of the PLP binding region but showed nevertheless a slight activity with alanine in isolated proteins. As S384D and S384E show a difference when analyzed in cell-free conditions our results point out that not only the position but also the nature of the amino acid change are important. A bulky residue like phenylalanine in combination with the right position might lead to changed substrate specificity and thus to dSL generation in isolated proteins.

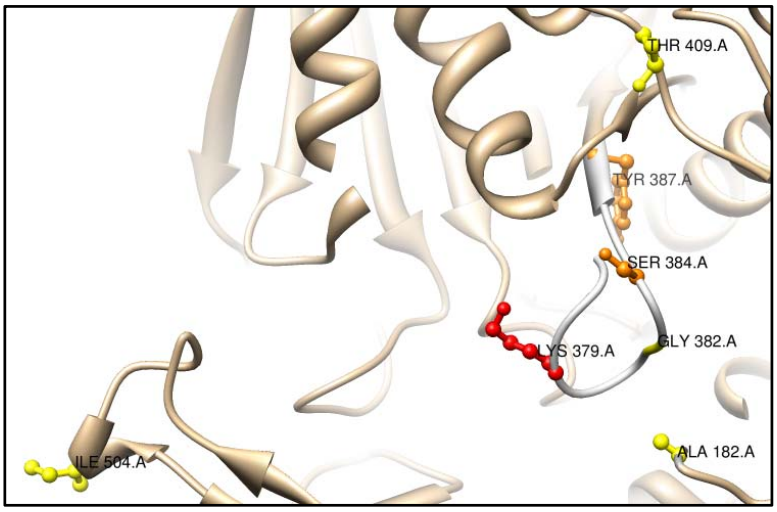

FIGURE 2: **Structural modeling of SPTLC2-HSAN I-causing mutations in *Sphingobacterium multivorum***
The sequence of the mammalian SPTLC2 subunit was modeled into the protein structure of *S. multivorum* (PDB:3A2B) using SWISS-MODEL (http://swissmodel.expasy.org). The results are illustrated using USCF Chimera 1.6.2. Both phosphosites (Ser384 and Tyr387) are shown in orange

and the Schiff-base forming Lys379 (catalytic center) is shown in red. All sites that are HSAN I-causing mutations in SPTLC2 are shown in yellow (Thr 409, T409M; Ala182, A182P; Ile504, I504F; Ser384, S384F)

HSAN I-a product of mutations in five different genes and more to come

The clinical phenotype of HSAN I can be very heterogeneous, ranging even within the same family from a very mild phenotype with primarily allodynia and late onset to very severe forms with congenital onset , progressive degeneration of sensory and autonomic neurons and severe motor involvement[16 17]. This heterogeneity argues for the role of modulating factors which might act on top of the identified mutations. Moreover, HSAN I is genetically heterogeneous. Five genes (*SPTLC1, SPTLC2, ATL1, RAB7* and *DNMTI*) have been described so far to be mutated and cause the HSAN I phenotypes. RAB7 is involved in vesicular transport; Atlastin-1 is a dynamin related GTPase that functions in the ER tubular network, and DNMT1 is involved in DNA methylation. ER stress and axonal transport are two common pathways that are shared by these genes[16]. However, there is a pool of patients with HSAN I-like symptoms but no mutations in these candidate genes. New gene sequencing methods (e.g. whole exome sequencing) will allow the identification of new disease-causing genes in these patients and might finally help to unravel a shared pathomechanism which underlies all these different mutations.

Deoxy-sphingolipids in macrophages

In chapter 3 we reported that dSLs are generated during PMA-induced THP1 differentiation into macrophages. We confirmed this observation in differentiating primary monocytes. The question of why dSLs are increased in the maturation of monocytes to macrophages and whether they play a causal role in this process is not clear. Macrophages play a key role in the context of inflammation for example in atherosclerosis or obesity. Great effort is being made to understand how an increased body fat content results in chronic inflammation which also underlies the pathology of these disorders. Lately, it has been reported that endotoxins activate sphingolipid *de novo* synthesis via LPS induced nuclear factor kappa B (NFκB) mediated up-regulation of SPTLC2 mRNA (but not SPTLC1) in RAW cells and peritoneal macrophages[18]. NFκB directly binds to the SPTLC2 promoter leading to increased expression of the SPTLC2 transcript and protein, thereby activating sphingolipid *de novo* synthesis which results in increased ceramide levels. It was shown that palmitate activates SPT activity and hence ceramide generation[19]. Holland *et al*. found that not only palmitate but also other free fatty acids (stearate, arachidate and lignocerate) can induce *de novo* ceramide generation

via interaction with the TLR4 receptor. Moreover, they found that LPS and to an even higher extent palmitate induced the transcription of enzymes involved in sphingolipid *de novo* synthesis (SPTLC2, CerS1, -2 and -6 and DES1) via the IKKβ signaling complex[20]. It is known that TLR4 signaling increases ceramide levels by activating acid sphingomyelinase[18]. Whether increased ceramide levels (*de novo* or salvage) lead to more pronounced inflammation is currently under debate. Schwartz *et al.* reported that palmitate or saturated fatty acids (SFA) increase IL-6 and IL-8 production in human THP1 cells as well as in primary monocytes[21]. The here proposed mechanism was that *de novo* generated ceramides impact on PKCζ, thereby activating MAPK which results in increased inflammation. Moreover, Schilling *et al.* reported that LPS and palmitate synergistically induce *de novo* ceramide synthesis in mouse macrophages that require TLR4 signaling via myD88 and TRIF, but this is independent of NFκB and MAP kinase activation[22]. These macrophages released TNFα and IL-1β after stimulation with LPS and this increase was enhanced with supplementation of palmitate. Notably, in mouse macrophages palmitate alone could not induce *de novo* ceramide formation and cytokine release. Schwartz *et al*. also reported differences in signaling responses in mouse and human monocytes/macrophages[21]. In contrast, Holland *et al.* reported that cytokine release upon SFA-TLR4 interaction was independent of *de novo* synthesized ceramide in mice and rats as well as in cultured macrophages[20].

In our own experiments we found that the supplementation of palmitate leads to increased SPT activity and enhanced generation of sphingolipids and dSLs in cultured cells (data not shown). Moreover, we found in several clinical studies that triglycerides are directly and significantly correlated with dSL levels in the plasma of patients with metabolic disorders[23]. It will therefore be interesting to explore whether dSLs are increased in LPS or palmitate stimulated macrophages and whether they also play a role in the described signaling processes.

Deoxy-sphingolipid *de novo* pathway in macrophages

We also reported in chapter 3 that both PMA, the stimulus for THP1 differentiation, and FB1, an inhibitor of ceramide synthase, influence the generation of deoxySO - the downstream product of deoxySA. The formed deoxySA is acylated to deoxy-dihydro-ceramide[13]. Therefore dSLs are generally found in their acylated forms - primarily conjugated to a C16, C24:1 and C24 fatty-acids [13]. We described the generation of the unsaturated downstream metabolite (m18:1 or deoxySO), suggesting that deoxy-dihydro-ceramide is a substrate for the

desaturase DES1/2. Paradoxically, deoxySO appears under conditions where FB1 was used to block the synthesis pathway at the step of CerS and hence upstream of DES. The levels of non-acylated deoxySO relative to total deoxySO bases were higher in FB1 treated THP1 cells compared to untreated cells. We propose two explanations for this phenomenon. Along with the generation of deoxySO in the presence of FB1, there is a lack of SA accumulation (chapter 3, Figure 2A). Therefore, the inhibitory potential of FB1 on CerS could be impaired. We observed SA accumulation prior to the addition of PMA for starting the differentiation (chapter 3, Supplemental Figure 1A). Thus, PMA could interfere with the FB1 related CerS inhibition. Whether there is interference and how this takes place needs to be addressed by future experiments. One may also speculate that dSLs follow a different metabolic pathway in which the desaturase is not dependent on prior acylation to a deoxy-dihydro-ceramide molecule (Figure 3). In this case we would expect that the desaturase could introduce the double-bond directly into the free deoxySA which is, however, not possible for sphinganine[24]. Hence, it has to be investigated if the majority of deoxySA/deoxySO is present as a free base or in its N-acyl form. In our experimental setup the information on the deoxy-ceramide species is lost due to the chemical hydrolysis of the N-acyls prior to the MS analysis. Future experiments have to analyze the individual deoxy-ceramide species and their metabolism and dynamics during monocyte to macrophage differentiation.

The major difference between PMA and non-PMA treated THP1cells was seen in the deoxySO levels. DeoxySO formation during differentiation was dependent on the presence of PMA. However, the addition of FB1 further enhanced deoxySO levels. FB1 and PMA are both activators of certain PKC sub-isoforms (PKCα, βII, δ, ε)[25]. Here, FB1 could play a dual role by acting as a direct activator of PKC via the diacylglycerol binding pocket[26, 27] but also causing the accumulation of SA and SO , which act as PKC inhibitors[14, 15]. However, due to unknown reasons, differentiating THP1 cells did not show any accumulation of SA (neither SO) upon FB1 treatment and would therefore lack this delayed inhibition of PKC. It will be interesting to test the effect of deoxy-sphingoid bases on the PKC subtypes, as they structurally resemble FB1. FB1 can be considered as a 1-deoxy-sphingolipid-analogue, but in contrast to deoxy-sphingoid bases, it is built on a polyketid backbone[28, 29]. The addition of FB1 was shown to also increase dSL generation in other cell lines, although the underlying mechanism is not understood[13].

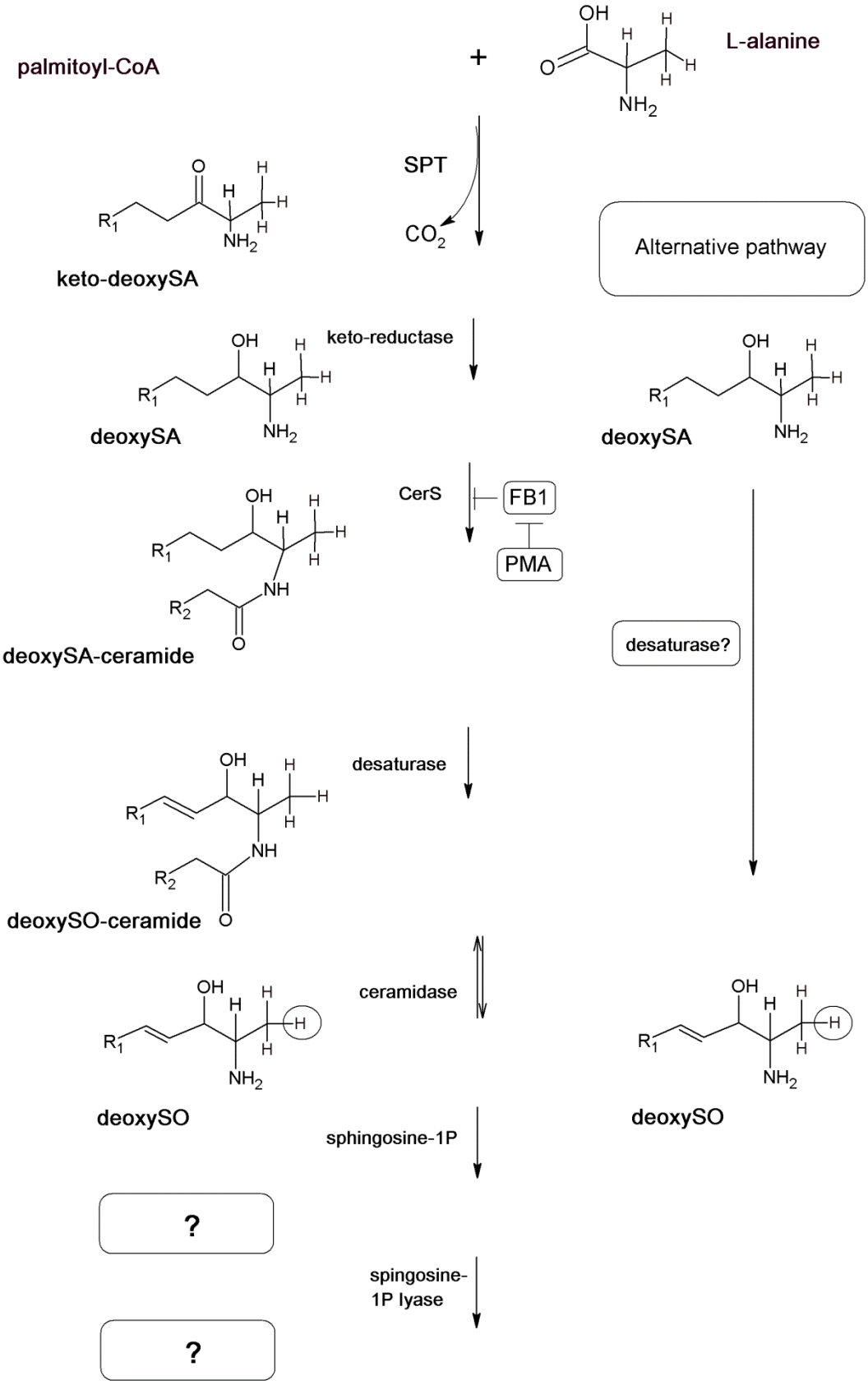

FIGURE 3: **Proposed mechanism for deoxySO generation in the presence of PMA and FB1 in THP1-derived macrophages**

Outlook

In summary this work investigated several factors that are involved in the generation and the metabolism of dSLs. Based on our results we suggest that phosphorylation of SPTLC2 at S384 leads to a shift in the amino acid substrate preference of SPT. We propose that phosphorylation acts as a molecular switch which directly affects SPT structure and results in increased dSL. However, future work needs to prove this hypothesis by identifying the responsible SPTLC2 kinase and also the regulatory stimuli that provoke SPT phosphorylation.

Comparing individual HSAN I mutations, we observed differences of SPT activity when analyzed in isolated proteins and in living cells. In contrast to wildtype SPT and the majority of HSAN I mutants, only some HSAN I mutants produced dSL in the presence of alanine in cell-free conditions. However, the expression of almost every HSAN I mutant in cells resulted in increased dSLs formation, even those variants which did not form dSLs in cell-free conditions. We therefore postulate that dSLs can be formed by different mechanisms. To further explain these differences it is important to gain better insight into the regulation of sphingolipid *de novo* synthesis and the factors which are involved in this regulation. The systematic comparison of the various HSAN I mutations in terms of the formation of supra-molecular SPT complexes with other proteins and their product spectrum might be a valuable tool to address this issue. Since we also see differences in the deoxy-ceramide species between HSAN I mutants (primarily as free sphingoid bases) and phospho-mutants (primarily N-acylated) it will be interesting to investigate a potential inhibitory effect of the HSAN I mutants on CerS in more detail. Therefore it is also essential to investigate the formed deoxy-sphingolipid species in more detail, in particular the presence and length of the conjugated N-acyl chain. Each of these dSL-metabolites could, in principle, drive a different signaling event that might explain the observed controversial responses of the dSLs, like being toxic to cultured DRGs but being generated during macrophage maturation and prolonged culture of cells.

Whether there is a physiological relevance of dSLs still needs to be determined. We found dSL generation coordinated with increased intracellular L-alanine levels and a drastic change in SPT expression pattern during the monocyte to macrophage differentiation. As dSL resemble structurally FB1, we speculated that they can play a role in signaling processes. Further experiments need to address this issue as well as the context in which the dSL signaling takes place.

We showed a close metabolic link between the sphingolipid and amino acid synthesis pathways. To gain more information about this interconnectivity, future experiments should address the regulation of the amino acid supply. As Serinc-proteins have been reported to provide a platform for the facilitated shuttling of amino acids by membrane proteins, it could be investigated if there are differences in the amino acid metabolism between HSAN I mutants and wildtype SPT.

Increased deoxy-sphingolipids are a hallmark for HSAN I and there is growing evidence that they also play a role in the pathogenesis of other neuropathies. However, besides the observation that dSLs are toxic to DRGs in culture[30], it is not known how and at which step they are involved in the underlying pathomechanism of nerve destruction. Thus, future work needs to investigate the underlying pathomechanism of dSLs in neurotoxicity. ORM proteins have been identified as regulators of SPT activity thereby potentially linking SPT with other diseases like asthma or Alzheimer's, where ORM proteins were found to play a role. It will be of interest to investigate whether dSLs also play a role in the context of these diseases.

References

1. Siow DL, Wattenberg BW. Mammalian ORMDL Proteins Mediate the Feedback Response in Ceramide Biosynthesis. Journal of Biological Chemistry 2012.
2. Rotthier A, Auer-Grumbach M, Janssens K, et al. Mutations in the SPTLC2 Subunit of Serine Palmitoyltransferase Cause Hereditary Sensory and Autonomic Neuropathy Type I. The American Journal of Human Genetics 2010;87:513-522.
3. Bejaoui K, Wu C, Scheffler MD, et al. SPTLC1 is mutated in hereditary sensory neuropathy, type 1. Nat Genet 2001;27:261-262.
4. Bi H, Gao Y, Yao S, Dong M, Headley AP, Yuan Y. Hereditary sensory and autonomic neuropathy type I in a Chinese family: British C133W mutation exists in the Chinese. Neuropathology 2007;27:429-433.
5. Dawkins JL, Hulme DJ, Brahmbhatt SB, Auer-Grumbach M, Nicholson GA. Mutations in SPTLC1, encoding serine palmitoyltransferase, long chain base subunit-1, cause hereditary sensory neuropathy type I. Nat Genet 2001;27:309-312.
6. Rotthier A, Penno A, Rautenstrauss B, et al. Characterization of two mutations in the SPTLC1 subunit of serine palmitoyltransferase associated with hereditary sensory and autonomic neuropathy type I. Human Mutation 2011;32:E2211-E2225.
7. Olsen JV, Blagoev B, Gnad F, et al. Global, In Vivo, and Site-Specific Phosphorylation Dynamics in Signaling Networks. Cell 2006;127:635-648.
8. Inuzuka M, Hayakawa M, Ingi T. Serinc, an Activity-regulated Protein Family, Incorporates Serine into Membrane Lipid Synthesis. Journal of Biological Chemistry 2005;280:35776-35783.
9. Neklesa TK, Davis RW. A Genome-Wide Screen for Regulators of TORC1 in Response to Amino Acid Starvation Reveals a Conserved Npr2/3 Complex. PLoS Genet 2009;5:e1000515.
10. Liu M, Huang C, Polu SR, Schneiter R, Chang A. Regulation of sphingolipid synthesis through Orm1 and Orm2 in yeast. Journal of Cell Science 2012;125:2428-2435.
11. Shimobayashi M, Oppliger W, Moes S, Jenö P, Hall MN. TORC1-regulated protein kinase Npr1 phosphorylates Orm to stimulate complex sphingolipid synthesis. Molecular Biology of the Cell 2013.
12. Garofalo K, Penno A, Schmidt BP, et al. Oral l-serine supplementation reduces production of neurotoxic deoxysphingolipids in mice and humans with hereditary sensory autonomic neuropathy type 1. The Journal of Clinical Investigation 2011;121:4735-4745.
13. Zitomer NC, Mitchell T, Voss KA, et al. Ceramide Synthase Inhibition by Fumonisin B1 Causes Accumulation of 1-Deoxysphinganine. Journal of Biological Chemistry 2009;284:4786-4795.
14. Gopee NV, He Q, Sharma RP. Fumonisin B1-induced apoptosis is associated with delayed inhibition of protein kinase C, nuclear factor-κB and tumor necrosis factor α in LLC-PK1 cells. Chemico-Biological Interactions 2003;146:131-145.
15. Gopee NV, Sharma RP. Sphingoid bases and their phosphates: transient activation and delayed repression of protein kinase C isoforms and their possible involvement in fumonisin B1 cytotoxicity. Toxicology 2003;187:239-250.
16. Rotthier A, Baets J, Timmerman V, Janssens K. Mechanisms of disease in hereditary sensory and autonomic neuropathies. Nat Rev Neurol 2012;8:73-85.
17. Rotthier A, Baets J, Vriendt ED, et al. Genes for hereditary sensory and autonomic neuropathies: a genotype–phenotype correlation. Brain 2009;132:2699-2711.
18. Chang Z-Q, Lee S-Y, Kim H-J, et al. Endotoxin activates de novo sphingolipid biosynthesis via nuclear factor kappa B-mediated upregulation of Sptlc2. Prostaglandins & Other Lipid Mediators 2011;94:44-52.
19. Smith ER, Jones PL, Boss JM, Merrill AH. Changing J774A.1 Cells to New Medium Perturbs Multiple Signaling Pathways, Including the Modulation of Protein Kinase C by Endogenous Sphingoid Bases. Journal of Biological Chemistry 1997;272:5640-5646.
20. Holland WL, Bikman BT, Wang L-P, et al. Lipid-induced insulin resistance mediated by the proinflammatory receptor TLR4 requires saturated fatty acid–induced ceramide biosynthesis in mice. The Journal of Clinical Investigation 2011;121:1858-1870.
21. Schwartz EA, Zhang W-Y, Karnik SK, et al. Nutrient Modification of the Innate Immune Response: A Novel Mechanism by Which Saturated Fatty Acids Greatly Amplify Monocyte Inflammation. Arteriosclerosis, Thrombosis, and Vascular Biology 2010;30:802-808.
22. Schilling JD, Machkovech HM, He L, et al. Palmitate and LPS trigger synergistic ceramide production in primary macrophages. Journal of Biological Chemistry 2012.
23. Othman A, Rütti M, Ernst D, et al. Plasma deoxysphingolipids: a novel class of biomarkers for the metabolic syndrome? Diabetologia 2012;55:421-431.
24. Michel C, van Echten-Deckert G. Conversion of dihydroceramide to ceramide occurs at the cytosolic face of the endoplasmic reticulum. FEBS Letters 1997;416:153-155.

25. Kontny E, Ziolkowska M, Maśliński W. Production of pro-inflammatory cytokines in human monocytes: not a cascade but the dependence on protein kinase C pathway. Immunology Letters 1999;67:263-267.
26. Gopee NV, Sharma RP. Selective and transient activation of protein kinase C α by fumonisin B1, a ceramide synthase inhibitor mycotoxin, in cultured porcine renal cells. Life Sciences 2004;74:1541-1559.
27. Yeung JM, Wang H-Y, Prelusky DB. Fumonisin B1Induces Protein Kinase C Translocation via Direct Interaction with Diacylglycerol Binding Site. Toxicology and Applied Pharmacology 1996;141:178-184.
28. Humpf H-U, Schmelz E-M, Meredith FI, et al. Acylation of Naturally Occurring and Synthetic 1-Deoxysphinganines by Ceramide Synthase: FORMATION OF N-PALMITOYL-AMINOPENTOL PRODUCES A TOXIC METABOLITE OF HYDROLYZED FUMONISIN, AP1, AND A NEW CATEGORY OF CERAMIDE SYNTHASE INHIBITOR. Journal of Biological Chemistry 1998;273:19060-19064.
29. Desai K, Sullards MC, Allegood J, et al. Fumonisins and fumonisin analogs as inhibitors of ceramide synthase and inducers of apoptosis. Biochimica et Biophysica Acta (BBA) - Molecular and Cell Biology of Lipids 2002;1585:188-192.
30. Penno A, Reilly MM, Houlden H, et al. Hereditary Sensory Neuropathy Type 1 Is Caused by the Accumulation of Two Neurotoxic Sphingolipids. Journal of Biological Chemistry 2010;285:11178-11187.

Publications

Hereditary sensory and autonomic neuropathy type 1 (HSANI) caused by a novel mutation in SPTLC2

Murphy SM and **Ernst D**, Wei Y, Laurà M, Liu YT, Polke J, Blake J, Winer J, Houlden H, Hornemann T and Reilly MM.
Neurology 2013 Jun 4; 80(23):2106-2111. Epub 2013 May 8.

The SPTLC3 subunit of serine palmitoyltransferase generates short chain sphingoid bases.

Hornemann T, Penno A, Rütti MF, **Ernst D**, Kivrak-Pfiffner F, Rohrer L, von Eckardstein A.
J Biol Chem. 2009 Sep 25; 284(39):26322-30. doi: 10.1074/jbc.M109.023192. Epub 2009 Aug 1.

Plasma deoxysphingolipids: a novel class of biomarkers for the metabolic syndrome?

Othman A, Rütti MF, **Ernst D**, Saely CH, Rein P, Drexel H, Porretta-Serapiglia C, Lauria G, Bianchi R, von Eckardstein A, Hornemann T.
Diabetologia 2012 Feb; 55(2):421-31. doi: 10.1007/s00125-011-2384-1. Epub 2011 Nov 29.

Grants

Forschungskredit der Universität Zürich

Project Titel: Functional Characterization of SPTLC3-a newly identified Isoform of Serine Palmitoyltransferase

Project Duration: 1.1.2009 – 31.12.2010

Conferences

2012 **Gordon Research Conference on Glycolipid & Sphingolipid Biology**
April 22-27, Lucca, Tuscany, Italy
Poster presentation

2012 **Rare and Orphan Diseases RE(ACT)**
February 29-March 2, Basel, Switzerland
Attended

2011 **6th Charleston Ceramide Conference (CCC)**

March 16-20, Villars-sur-Ollon, Switzerland
Poster presentation

2011 **IX Sphingolipid Club**
September 28-Oct 1, Favignana, Sicily
Oral presentation

2010 **Gordon Research Conference on Glycolipid & Sphingolipid Biology**
February 7-12, Ventura, California, United States
Poster presentation

2010 **HSAN I Symposium**
February 18-19, Boston, United States
Attended

2009 **International Conference on the Bioscience of Lipids (ICBL)**
September 1-5, Regensburg, Germany
Poster presentation

Acknowledgements

First of all I would like to thank Prof. von Eckardstein for giving me the opportunity to work in his Institute that allowed me to combine an interesting topic with the benefit of having a clinical environment which I enjoyed a lot. Thank you for your interest, the support of our research activities and your availability throughout the project.

I am very grateful to my direct supervisor Dr. Thorsten Hornemann for this ambitious and great PhD topic, his contagious enthusiasm, creative input and open-door philosophy that helped me to keep a lively interest in the project all over these years. Many thanks for all the advice and for providing a great environment that I loved to work in. I am much obliged for the possibility to have visited several conferences that helped me to broaden my knowledge and to discuss with experts in the sphingolipid field.

I am thankful to my committee members, Prof. Howard Riezman, Prof. Thierry Hennet and Dr. Sabrina Sonda for their interest, helpful suggestions and the availability throughout my project. I highly appreciate that you took the time for the meetings and contributed your expertise to the project.

Many thanks also to the Proteomics group from the Functional Genomic Center Zürich especially to Peter Gehrig and Claudia Fortes for advising me on experimental designs, for their kind help and shared hands-on experience during the experiments.

Furthermore, I would like to thank many people that I have come across during my PhD time in Zürich that made this stay a wonderful time.
First of all I like to thank all the former and current members of the Hornemann-lab for sharing exciting sphingolipid-adventures. This especially includes Alaa Othman, Heiko Bode, Irina Alecu, Assem Zhakupova, Iryna Sutter, Yu Wei, Markus Rütti, Anke Penno, Mari Bertea and Annelies von Rotthier. I truly enjoyed not only having fruitful scientific discussions but also just being with you in-and-outside the lab. Additional thanks to Heiko Bode for a fantastic bench to bench communication and to Irina Alecu for proof-reading parts of my thesis. A special thanks to Anke Penno for suggesting Zürich in the first place and for the friendship and on-going support all over these years.
Jovial thanks to all the IKC members and kitchen-attached groups whose presence were highly appreciated during coffee breaks, movie nights, parties, Raclette or Fondue events,

retreats and outside-lab activities. This includes Ratna Karuna, Silvija Radosavljevic, Rahel Sibler, Damir Perisa, Danielle Hof, Hans Reiser, Joanna Gawinecka, Reda Hasballa, Diana Odermatt, Carlos Schaffner, Christian Hiller, Tatjana Claro da Silva and Yuliya Plutino.

A million thanks to the best writing company ever, Alaa Othman and Jerome Robert for their support in the last part of my PhD. I so much enjoyed your sole presence and cheerful manner that were very helpful in these never-ending-writing hours. I deeply wish you the best for finishing-up your thesis and will provide my mental support!

A huge thank-you to my friends Katrin Orlowski, Dario Massa, Ola Hodor, Nadia Sanchez, Novella Calcinaghi, Dani Noain, Mauro Fernandez, Marta Morawska, Cristina Zunzunegui, Anna Bergström and Manish Gupta. It is a wonderful experience to go abroad and find friends like you. I so much hope we can keep in touch no matter where life is taking us.

Finally, I would like to thank Marc for his love and caring in all these years. Thank you so much for your understanding and all these delicious food-festivals that bring fiery joy and happiness to the people you love.

The biggest thanks go to my family for their trust in the first place. Thank you for your constant support and that you gave me the freedom of choice at all times in my life that made me become the person I am.

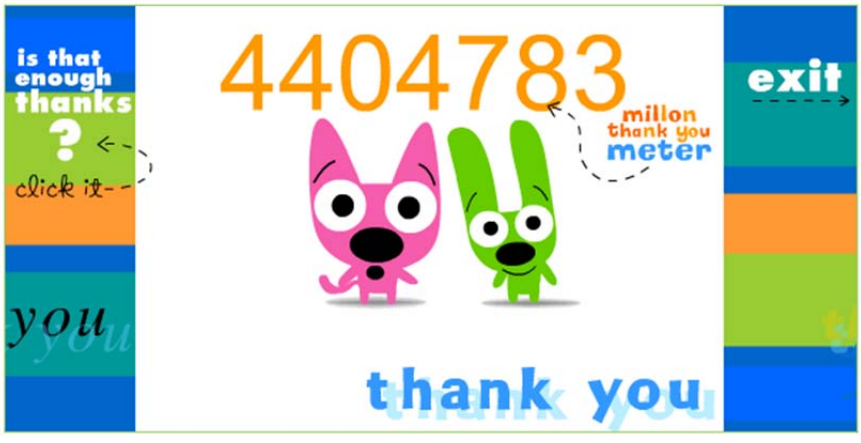

Curriculum Vitae

Personal Information:

Name:	Daniela Ernst
Born on:	03.12.1980
Nationality:	German

Academic Education:

2009-2013 **PhD studies**
Institute for Clinical Chemistry, University Hospital Zurich, Switzerland
„Regulation of Deoxy-Sphingolipids and Their Role in Disease"
Participant in PhD program Integrative Molecular Medicine (imMed)

2007-2008 **Master thesis**
Institute for Clinical Chemistry, Universitätsspital Zürich, Switzerland Institute of Cell biology and Immunology, University of Stuttgart, Germany
„Regulation of Serine Palmitoyltransferase Concerning Sphinganine and 1-Deoxy-Sphinganine Generation"

2006-2007 **Bachelor thesis**
Biotechnology and Biomolecular Science, UNSW, Australia
Institute of Biochemistry, University of Stuttgart, Germany
„Regulation of LSM genes encoding spliceosomal proteins in Saccharomyces cerevisiae"

2000-2008 **University of Stuttgart, Germany**
Bachelor and Master Studies in Technical Biology

1997 – 2000 High school „Fritz-Erler Wirtschaftsgymnasium" in Pforzheim, Germany